ROYAUME DU MAROC
Université Mohammed V - RABAT -
جامعة محمد الخامس – الرباط –
Faculté des sciences
كلية العلوم
CENTER FOR DOCTORAL STUDIES- SCIENCE AND TECHNOLOGY

N° d'ordre : 3940

THÈSE

en vue de l'obtention du : **DOCTORAT**

Centre de Recherche : Sciences et Technologies
Structure de Recherche: Laboratoire de Matière Condensée et Sciences Interdisciplinaires
Discipline : Science Physique
Spécialité : Énergies Renouvelables

Présentée et Soutenue le : *06 / 07 / 2024*

par :

Fatima-Azahraa BOURHIM

Techno-Economic Decision Support Model for the Optimal Design of Wind Turbine Production Chains based Wind Potential and Grid Electrical Characteristics

Devant le JURY :

Hamid EZ-ZAHRAOUY	PES	Faculté des Sciences, Université Mohammed V-Rabat	Président/Rapporteur
Mohammed BENAISSA	PES	Faculté des Sciences, Université Mohammed V-Rabat	Examinateur/Rapporteur
Driss ZEJLI	PES	Ecole Nationale des Sciences Appliquées, Université Ibn Tofaïl-Kénitra	Examinateur/Rapporteur
Mohammed DAOUDI	PA	Faculté des Sciences, Université Mohammed V-Rabat	Invité
Ahmed OUAMMI	PH	Ecole Supérieur de Technologie, Montréal	Co-Directeur de Thèse
Rachid BENCHRIFA	PES	Faculté des Sciences, Université Mohammed V-Rabat	Directeur de Thèse

Année Universitaire : 2023 – 24

Dedications

I dedicate this thesis to

My dear parents

No dedication can be eloquent enough to express what you deserve for all the sacrifices you have given me since birth, during my childhood, and even in adulthood.

Your prayers and blessings have been of great help in my studies.

Nothing in the world is worth the effort of day and night for my education and well-being.

This work was the fruit of your sacrifice for my education and training.

My dear sister

Thank you for always being by my side, by your presence, by your love, to give taste and meaning to our family life. May this work testify to you my sincere affections.

My dear brothers and their wife's

For your presence in all our moments of life, by your moral support and your sweet surprises. I wish you a future full of joy, happiness, success, and serenity.

My friends

You are for me brothers, sisters, and friends on whom I can count. My world without you will be without taste; I dedicate you this work and I wish you a life full of health and happiness.

And to you, dear readers.

Acknowledgements

This thesis was conducted at **the Laboratory of Condensed Matter and Interdisciplinary Science (LaMCScI)** of the Faculty of Sciences, Mohammed V- Rabat University, Morocco, under the direction of Mr. **Hamid EZ-ZAHRAOUY**, higher education Professor . Thus, I wish to express my sincere thanks and deep appreciation to this Laboratory for their accompaniment, assistance, and availability of professors, giving me the opportunity to develop my scientific knowledge.

I want to thank my supervisor Mr. **Rachid BENCHRIFA,** higher education Professor at the Faculty of Sciences, Mohammed V- Rabat University, to have accepted to welcome me within this research project as well for his help, his availability, invaluable guidance, and his advices and support that have been of great help to the accomplishment of this thesis.

I would also like to thank my co-supervisor Mr. **Ahmed OUAMMI**, authorized Professor at Superior Technology School, Montreal, for his help, availability, guidance, inspiring discussions and advices that have been of great help to the completion of this thesis.

I want to thank Mr. **Hamid EZ-ZAHRAOUY,** higher education Professor at the Faculty of Sciences, Mohammed V- Rabat University, to accept being the Rapporteur and President of the jury members of this thesis and for his patience in revising my papers and thesis.

I acknowledge Mr. **Mohammed BENAISSA,** higher education Professor at the Faculty of Sciences, Mohammed V- Rabat University, for reporting and examining this thesis.

I also thank Mr. **Driss ZEJLI** higher education Professor at National School of Applied Sciences, Ibn Tofaïl University-Kénitra, for accepting to report and examine this thesis.

I would like to express my sincere gratitude to Mr. **Mohammed DAOUDI**, assistant Professor at the Faculty of Sciences, Mohammed V- Rabat University, for accepting to assist to the defense of this thesis and participate in the judgment of its quality.

Résumé

Cette thèse présente un modèle d'aide à la décision technico-économique pour déterminer la conception optimale des turbines éoliennes (WTs) futures, et cela, en fonction du potentiel éolien du site sélectionné et les caractéristiques électriques du réseau de distribution radial (RDN) connecté. Trois paramètres techniques de WT ont été déterminés: le diamètre du rotor, la hauteur de la tour et la puissance nominale. Le modèle a été développé à l'aide de la modélisation complète de WT et une stratégie d'optimisation technico-économique soumise à des contraintes spécifiques. Cette stratégie permet d'optimiser les paramètres de conception de WT pour déterminer la valeur actuelle nette maximale des revenus de l'énergie éolienne. Deux scénarios d'optimisation ont été évalués, la conception optimale de WT est déterminée sur la base du potentiel éolien disponible sur le site dans le premier scénario; cependant, le deuxième scénario considère le potentiel éolien et la capacité du RDN. Un réseau de neurones artificiels a été utilisé dans ce deuxième scénario pour prédire efficacement le potentiel du vent du site sélectionné et maintenir la stabilité du réseau. Une évaluation du coût de l'énergie produite a été effectuée en parallèle. Le modèle d'aide à la décision proposé fournit des résultats de conception significatifs.

Mots-clés : Conception de turbine éolienne, optimisation, valeur actuelle nette (VAN), réseau de neurones artificiels (ANN), réseau de distribution radial (RDN).

Résumé Détaillé

Cette thèse présente un modèle d'aide à la décision technico-économique pour déterminer le dimensionnement optimal des turbines éoliennes (WTs) futures en fonction du potentiel éolien disponible sur un site sélectionné et les caractéristiques électriques du réseau de distribution radiale connecté (RDN). Trois paramètres techniques de WT ont été déterminés : le diamètre du rotor, la hauteur de la tour et la puissance nominale. Le modèle d'aide à la décision a été développé en utilisant une modélisation complète de WT et un cadre d'optimisation techno-économique soumis à des contraintes spécifiques. Ce cadre consiste en un problème d'optimisation dont l'objectif est la maximisation de la valeur actualisée nette (VAN) des revenus de l'énergie éolienne. Deux principaux scénarios d'optimisation ont été évalués pour atteindre l'objectif de cette étude. L'optimisation du premier scénario est basée uniquement sur le potentiel éolien soumis aux variables de conception géométrique de WT, y compris le diamètre du rotor et la hauteur de la tour en raison de leurs impacts directs d'optimisation de dimensionnement sur l'énergie, le coût de production et la VAN. Les contraintes prises en compte étaient la restriction de puissance nominale de WT et le rapport maximal autorisé entre le diamètre du rotor et la hauteur du moyeu de la tour. Dans le deuxième scénario, l'optimisation est basée sur le potentiel éolien du site étudié et la capacité du réseau RDN soumis aux mêmes variables de conception géométrique de WT du premier scénario, aux variables de conception RDN et aux contraintes RDN pour maintenir la stabilité du réseau électrique. En outre, comme la caractéristique intermittente de l'énergie éolienne est liée à la variabilité de la vitesse du vent, un réseau de neurones artificiels (ANN) a été utilisé dans ce scénario pour prévoir efficacement les vitesses horaires du vent d'un site sélectionné pour une bonne estimation de l'énergie éolienne générée par les WTs.

Le modèle d'aide à la décision technico-économique développé a été vérifié et validé à l'aide d'un modèle existant dans la littérature, démontrant son efficacité et son applicabilité. La sélection optimale de la conception de WT tient compte de la puissance nominale, du diamètre du rotor et de la hauteur du moyeu de la tour, ce qui conduit à la VAN maximale. Une analyse du coût nivelé de la production d'énergie (LCOE) a été effectuée en parallèle. En utilisant trois sites éoliens différents (Dakhla, Casablanca et Tanger), le modèle d'aide à la décision a été testé dans le premier scénario. Les résultats

ont montré que la conception optimale des technologies des WTs est donnée par les conditions limites citées, conduisant à la VAN maximale avec un faible LCOE et une plus grande exploitation du potentiel éolien disponible à Dakhla et Tanger. Cependant, il a été constaté que Casablanca n'était pas un site rentable pour les projets éoliens avec une VAN négative. Dans le deuxième scénario, l'efficacité du modèle proposé dans la détermination de la conception optimale de WT pour différents nœuds de bus dans un RDN a été validée en utilisant deux systèmes RDN différents, à savoir IEEE 9 et IEEE 33 Bus RDN. Les résultats démontrent que la détermination de la conception de WT n'est pas liée à la puissance du potentiel éolien, mais principalement à la capacité du réseau RDN connecté. Les emplacements adéquats parmi les nœuds de bus évalués pour l'installation de WT ont été déterminés en fonction de la valeur VAN maximale présentée par chaque conception de WT dans chaque nœud de bus. Le modèle d'aide à la décision technico-économique fournit des résultats de conception significatifs, agissant comme un soutien aux décideurs dans le secteur de l'énergie éolienne.

Abstract

This thesis presents a techno-economic decision support model to determine the optimal design of future wind turbines (WTs), based on the wind potential available at a selected site and the electrical characteristics of the connected Radial Distribution Network (RDN). Three technical parameters of the WT were determined: rotor diameter, tower height, and nominal power. The decision support model was developed using comprehensive WT modeling and a techno-economic optimization strategy subject to specific constraints. This strategy optimizes the WT design parameters to determine the maximum net present value (NPV) of wind energy revenues. Two main optimization scenarios were assessed: the optimal WT design was determined based on the wind potential available on the site in the first scenario; however, the second scenario considered the wind potential and capacity of the RDN. An Artificial Neural Network (ANN) was used in this second scenario to effectively forecast the wind potential of the selected site and maintain the stability of the grid. Parallel evaluation of the produced energy cost (LCOE) was performed. The proposed decision support model provided significant design results.

Keywords: Wind turbine design, optimization, net present value (NPV), artificial neural network (ANN), radial distribution network (RDN).

List of figures

List of Tables

Nomenclature

NPV : Net Present Value
RDN : Radial Distribution Network
WT : Wind Turbine
WTDO: Wind Turbines Design Optimization
WFLO : Wind Farm Layout Optimization
WF : Wind Farm
ANN : Artificial Neural Network
R : The regression coefficient
MSE : Mean Square Error
LCOE : Levelized Cost of Energy
COE : Cost of Energy
$f_i^l(v_i)$: Weibull probability density function
v_i : Wind speed of the ith class
k^l : Weibull shape parameter
C^l : Weibull scale parameter
k^l_{Hg} : Extrapolated Weibull shape parameter at height H_g
C^l_{Hg} : Extrapolated Weibull scale parameter at height H_g
$f^l_{i,h}$: The discretized Weibull function with WT tower height
$v_{average}$: The mean wind speed
a(z) : ANN activation function
w : Weight associated with the ANN input
b : Bias associated with the ANN neurons
R : Regression coefficient
MSE : Mean Square Error
$\mathcal{N}$: The number of wind speed samples
$v_{mes,i}$: The measured wind speed
$v_{pred,i}$: The predicted wind speed
$\overline{v_{mes,i}}$: The actual mean measured wind speed
$\overline{v_{pred,i}}$: The actual mean predicted wind speed
$AEP^l_{t,g}$: The yearly generated energy
g : WT technology index
l : The location of site or bus nodes
ρ : The air density
A_g : The WT Rotor swept surface
$C_{p,i,g}$: The total efficiency of the WT technology g
D_g : The Rotor diameter (m) of WT technology g
H_g : Tower height of WT technology g
$\mu_{gear,i,g}$: The WT gearbox efficiency
$\mu_{gen,i,g}$: The WT generator efficiency
P_i : Wind power
$E_{c,i}$: Kinetic energy
$P_{r,i,g}$: The Rotor power captured
$\dot{m}$: The air mass flow
$C_{pr,i,g}$: The rotor power coefficient of the WT technology g
$C_{pr,g,max}$: The rotor maximum power coefficient
$v_{op,g}$: The optimal wind speed
χ : The Wind speed operating range parameter
$v_{n,g}$: The nominal Wind speed of WT
$\lambda_{max,g}$: The maximum speed rate
NB_g : The number of blades
c_d/c_l : The ratio between drag and lift coefficients
ω_g : The angular rotation speed of the Rotor
$N_{rpm,g}$: The Rotor rotation speed (rpm)
$\psi_{gear,g}$: The gearbox efficiency factor
$\psi_{gen,g}$: The generator efficiency factor
$P_{n,g}$: The WT nominal power
$P_{op,g}$: The WT optimal power
$P_{gear,i,g}$: The WT gearbox generated power
$P_{n,gen,g}$: The WT generator nominal power

$F_{s,g}$: The factor of service of the gearbox

α : The generated WT energy losses

$AEP_{t,g,real}^{l}$: The real yearly generated energy

NPV_{g}^{l} : Net present value of a WT technology ‘g’ in a location ‘l’

$I_{t,g}^{l}$: The Investment made in year t

$C_{benif,t,g}^{Net,l}$: The total net Wind energy generation benefices

$C_{benif,t,g}^{l}$: The total benefits

$C_{OM,t}^{l}$: The Operation and Maintenance costs in year t

$C_{Sal,t,g}^{benif,l}$: The Incomes from electrical energy sales

$C_{Inc,t,g}^{benif,l}$: The Incomes from incentives for green energy production

C_{S} : The purchase tariff of electricity

C_{In} : Sales cost due to incentives for green energy production

$D_{t,g}^{l}$: The annual depreciation expense

$T_{t,g}^{l}$: Tax levy

n : The WT lifetime

r : The Discount rate

η, ξ : The investment and incomes percentages factors

$C_{T,g}^{l}$: The Transportation cost

$C_{AI,g}^{l}$: The Assembly and Installation cost

$C_{EI,g}^{l}$: The Electrical Interface cost

$C_{EP,g}^{l}$: The Engineering and Permits cost

$C_{RCW,g}^{l}$: The Roads and Civil Work cost

$C_{F,g}^{l}$: The Foundation cost

$C_{WT,g}^{l}$: The WT cost

$LCOE_{g}^{l}$: Levelized Cost of Energy generated by a WT technology ‘g’ in a location ‘l’

$P_{WT,g}^{l}$: The WT generated active power

P_{Load}^{l} : The load active power

P_{Loss}^{l} : The power losses in the branches lines of the radial distribution system

V_{l} , V_{j} : The Voltage magnitudes at bus l and j

G_{lj} : The real part of admittance matrix

B_{lj} : The imaginary part of admittance matrix

δ_{l}, δ_{j} : Voltage angles at buses *l* and *j*

J : The number of buses

Table of Contents

General Introduction

Population growth and industrial activity have led to high energy demand and consumption. This demand is mostly met by fossil fuel combustion. The reserves of these raw materials are limited, and they are responsible for greenhouse gas emissions that impact the climate. The effects of climate change are increasingly harming the world. The temperature of Earth is increasing. Fossil fuel costs rise every day, especially after the Ukrainian-Russian crisis [1]. In recent years, the world has been united to address climate and energy issues by making more efforts to reduce their energy dependence and decarbonization, thereby accelerating their transition to green energies. Renewable energy is the recommended alternative source of energy to meet electrical needs as a free and safe source. By the end of 2022, renewables accounted for 40% of the global installed power capacity, with an increase of 1.9% compared to 2021 [2]. The Africa renewable installed power capacity share is 23.6% where Morocco presented 33.6% of its global installed capacity. The world has added almost 295 GW of renewables in 2022, where the wind energy record is 75 GW compared to 2021.

Wind energy is one of the most competitive renewable energy sources and has been studied and integrated into power systems [1]. The penetration of this source as a distributed generator in the distribution network of a power system poses many challenges related to: the generation uncertainty, voltage stability, power losses, and the quality of the distributed power [3]. Voltage stability may extend to the transmission system and cause a power cut in the entire system [4]. Inappropriate wind turbine (WT) size and placement may increase the system loss [5]. Furthermore, inappropriate design of WTs may not profit from the maximum available wind energy at the studied site and may lead to high costs. To address these issues for optimal operation and maintaining the stability of the power system, it is necessary to develop a decision support model to optimally size WTs according to the available wind potential and connected radial distribution network (RDN) constraints that enhance their economic benefits to increase the competitiveness of this sector [1], [6]. This represents the motivation of the present work, and its originality is contained in a no existing WT design in the market proposition.

This thesis aims to propose a techno-economic decision support model based on a techno-economic optimization problem that provides adequate technical design parameters for future WTs, including the rotor diameter D_g, tower height H_g, and its nominal power. The WT design determined corresponds to the available wind potential at the site of interest and to electrical characteristics of the distribution network, having as objective function; the Net Present Value (*NPV*) of Wind energy economic revenues maximization. The proposed WT designs in this thesis were not selected from the available WT technology datasheets in the market, such as the studies performed in this context, where the optimal design proposed among the evaluated ones was that which presented the minimum cost of energy, low power loss reduction, or maximum NPV. However, in this thesis, these three WT technical parameters are determined through a techno-economic optimization problem resolution, which constitutes the novelty of this work. In addition, the most profitable sites and the adequate placements among all the evaluated RDN bus nodes for the installation of the WT technology were determined, as they presented the maximum value of the *NPV*.

The proposed techno-economic decision support model acts as a support for decision makers to optimally size WTs as a function of the wind potential at their site of interest and the connected RDN characteristics, avoiding sizing issues and power system instability problems. Furthermore, it constitutes an inspiration for other research projects on WT design optimization to come out at the end with an applicable model in the industry.

This thesis is organized into five chapters:

In the 1st chapter, a state-of-the-art analysis of WT design optimization from invention to mature market design optimization is introduced in several sections, which illustrate the original development of WT technology, an overview of the WT grid connection challenges, and a literature review of previous WT design optimization studies showing the originality of our work. The optimization of WT technology design studies took two main paths: either optimization of WT design parameters or its layout in the entire wind farm with or without considering the RDN characteristics in the case of wind energy connection, which is presented in the last sections of this chapter.

In the 2nd chapter, the source of wind, a description of its natural movements on the Earth's surface, and the approaches used for its quantification are presented. Wind is an

essential element used by WT to produce electricity. Thus, a presentation of WT technology components and the principal process for wind-electricity transformation is described in several sections.

The 3rd chapter focuses on modeling the proposed techno-economic decision support model. The model includes WT technology for generating electricity and economic analysis modeling, mainly *NPV* and *LCOE*. In addition, the WT design optimization strategy is presented. Two different optimization scenarios are presented to study the objective of this work, which consists of determining the optimal WT design based on the available wind potential of a selected site and the RDN constraints that is economically profitable.

In the 4th chapter, the results obtained from the first optimization scenario of this study are provided and discussed. This optimization scenario consisted of using the developed decision support model to determine the optimal WT design parameters based only on the available wind potential. Furthermore, the details of the techno-economic optimization approach are provided.

In the 5th chapter, the results of the second optimization scenario that assesses the decision support model based on wind site characteristics and RDN system constraints are presented. Two RDN systems with different power loads and electrical requirements were used in this evaluation. In this chapter, specific WT design parameters are proposed for each bus node in the evaluated RDN in response to the grid requirements.

Chapter 1 Wind Turbine Design Optimization State of Art

1.1 Introduction

The commercialized design of Wind Turbine (WT) technology is a result of the long development history summarized in this chapter. In addition, the continuous annual growth of wind energy generation and its penetration into power system networks reveal many challenges that affect the reliability of the grid, presented in the second section of this chapter. The Decision support systems that optimize Wind Farm (WF) design are increasingly required to facilitate and strengthen the exploitation of wind sources [6]. Therefore, decision support models are needed to effectively design future WTs production chains for a mature market. Many studies have been conducted in this context. In general, the decision support models provided for WFs design optimization are classified in two categories, either the WTs Design Optimization (WTDO) or the Wind Farm Layout Optimization (WFLO). The WFLO consists of optimizing the WTs in the entire WF by optimizing the layout of the WTs [6]. However, WTDO consists of optimizing a single WT parameter. Based on a state-of-the-art analysis of previous studies, the WF design optimization under the objective of WTDO or WFLO was performed with and without considering the electrical constraints of the connected Radial Distribution Network (RDN), as presented and discussed in the last sections of this chapter.

1.2 Wind Turbine Invention History

The earliest mentions of the use of wind power come from the East [7]. The WT technology design was inspired from the ancient windmills design. Reference to the windmill refers to the seventh century, as mentioned by Ali al-Tabari (A.D. 834-927) [7]. Furthermore, a Persian technician named Abu Lu'lu'a announced to Caliph Omar his ability to construct windmills before A.D. 644 [7] [8]. This incidence may demonstrate the possibility of existence of windmill in the Islamic world in the middle of the seventh century. Thus, the invention place was in the early Muslim or even pre-Muslim times [7]. However, the first operation of windmills was in Sistan region with vertical-axis in the tenth century (see **Figure 1. 1**). This region was described by al-Mas'udi (A.D. 896-956) as the land of winds and sand [7]. The wind drives mills through the aerodynamic drag forces for water pumping and grain grinding. This invention was spread throughout Islam and beyond to the Far East.

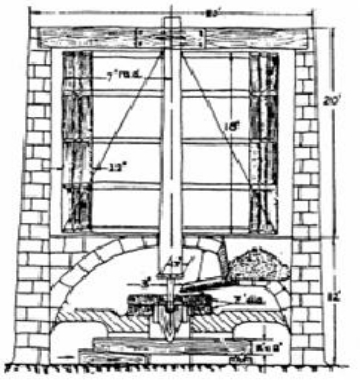

Figure 1. 1 Sistan windmill [7]

Windmills have been known in Spain since the IXth century before those in Portugal. Ibn Mucane referenced the first known windmill in Portugal where he lived around Xth century [9]. Windmill diffused in the XI century to the entire area of influence of the Mediterranean, spread by the Islamic civilization, reaching the southern half of the Iberian Peninsula conducting to a distinguishable typology of Mediterranean windmill such those built in Andalus (see **Figure 1.2**) [9].

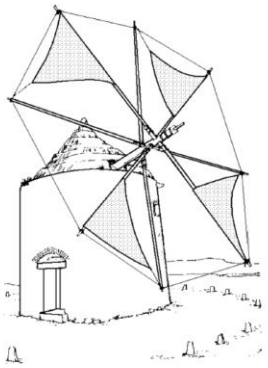

Figure 1. 2 Andalus windmills [9]

Mediterranean windmill was spread to Europe from Spain through the Caliphate of Córdoba. New windmill generation with horizontal-axis was appeared at the end of the twelfth century in Northwest Europe.

In the 19th century, windmills were replaced by electric pumps because of the increase for electricity demand[7]. Therefore, electrical WTs began to appear at the end 19th century, where Brush created a WT with a power capacity of 12 kW in Ohio 1888 (see **Figure 1. 3**) [7] [10] [11]. The next important step in the transition from windmills to WT generators

was taken by Professor Poul La Cour in Denmark [7]. He installed his first electrical WT with a power capacity of 18 kW at Askov in 1891 [11].

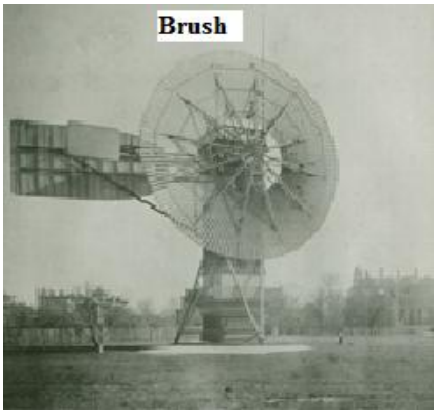

Figure 1. 3 Brush electrical wind turbine [11]

Due to the successive development of WT technology, the onshore commercial WTs in the early 2020 were nearly 70 times the size of the commercial turbines installed in the early 1980, passing from 65 kW to 4500 kW [10], [12]. The rated power capacity of most recent installed onshore WTs is in the range of 2 to 3 MW such as those installed in the first phase of Taza wind project launched in 2022 in Morocco, in a vision to satisfy 52% of installed renewable electricity in the horizon of 2030 [13]. This project has a global power capacity of 150 MW, where 87 MW constitutes the first phase installed in Taza using 27 WTs of 3.2 MW with a rotor diameter of 130 m. **Figure 1. 4** shows the design of recent generation of installed WTs.

Figure 1. 4 Recent generation of wind turbines design installed (Simens Gamesa 3.47 MW, rotor diameter 132 m) [14]

The invented WTs could be classified based on their rotational axis in two main categories, vertical axis (VAWT) and horizontal axis wind turbines (HAWT) (see **Figure 1. 5**). Several VAWT have appeared after the ancient Persian mills such as Darrieus 4.5 kW installed in France in 1930 [11], but they are currently less used . Actually, the most commonly commercialized and used WTs are HAWTs configuration with three-blade rotor upwind of the tower in which the rotor is facing the wind [12]. HAWTs operate under more powerful and stable wind speeds compared to VAWT. They have a higher aerodynamic efficiency and start autonomously providing several megawatts generating capacity.

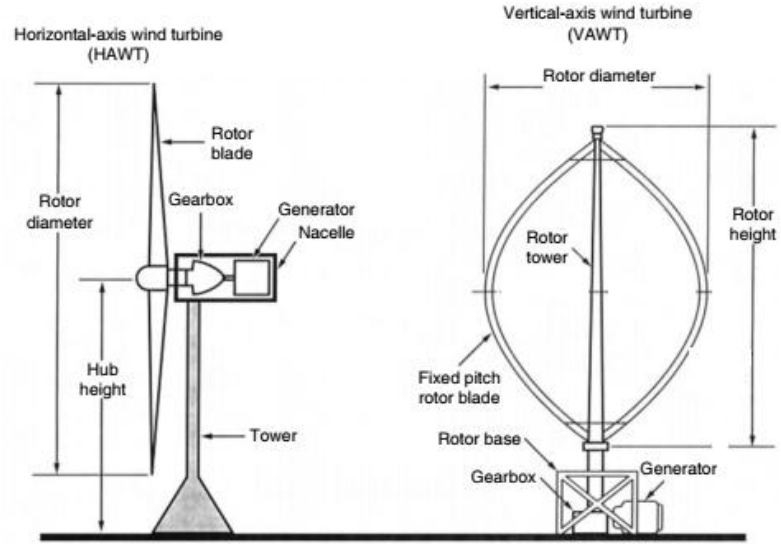

Figure 1. 5 Schematic of horizontal and vertical axis wind turbine [15]

In this thesis, only onshore WTs with horizontal axis are treated view their dominance in the market and their high application for energy generation, which compete actually the fossil fuels.

1.3 Wind Turbine Grid Connection Challenges

In the last decade, wind energy has become one of the most competitive renewable sources of energy and has been integrated into existing power systems [1] [16]. The global installed wind capacity in 2022 was 899 GW, and the onshore wind energy was 836 GW (see **Figure 1. 6**). 65.7 GW of onshore wind energy capacity was added compared to 2021 [2].

In 2022, Africa's onshore installed capacity reached 7.69 GW where South Africa, Egypt, and Morocco having the highest shares of 3.1, 1.64, and 1.56 GW respectively.

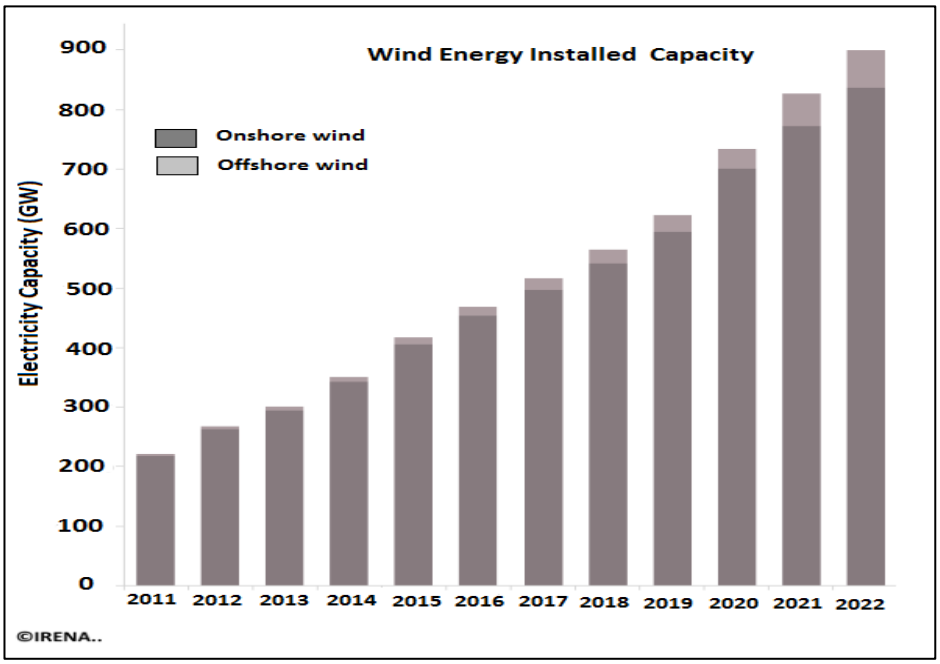

Figure 1. 6 The global installed wind capacity [17]

Small and large WT groups can be integrated into the distribution network with voltage level of 0.4 kV to 33 kV and 66 kV, respectively, in the case of onshore farms. However, many offshore WTs are integrated at voltage levels higher than 100 kV (see **Figure 1. 7**) [16].

The penetration of this source as a distributed generator in the distribution network of a power system poses many challenges that affect the operation and reliability of power systems. These challenges are related to the generation uncertainty, voltage stability, power losses, and quality of the distributed power [1], [16]. Thus, all Wind energy producers should adhere to specific available grid codes that include network technical specifications, imposed by electrical transmission companies for efficient operation of the electrical grid [16]. Grid codes include frequency and voltage variation requirements, reactive power, and power-factor regulation capabilities. In the present study, we focused on overcoming the generation uncertainty, frequency, and voltage stability challenges to improve the quality of the wind power generated and distributed to the grid. The details of these challenges are presented in the following paragraphs.

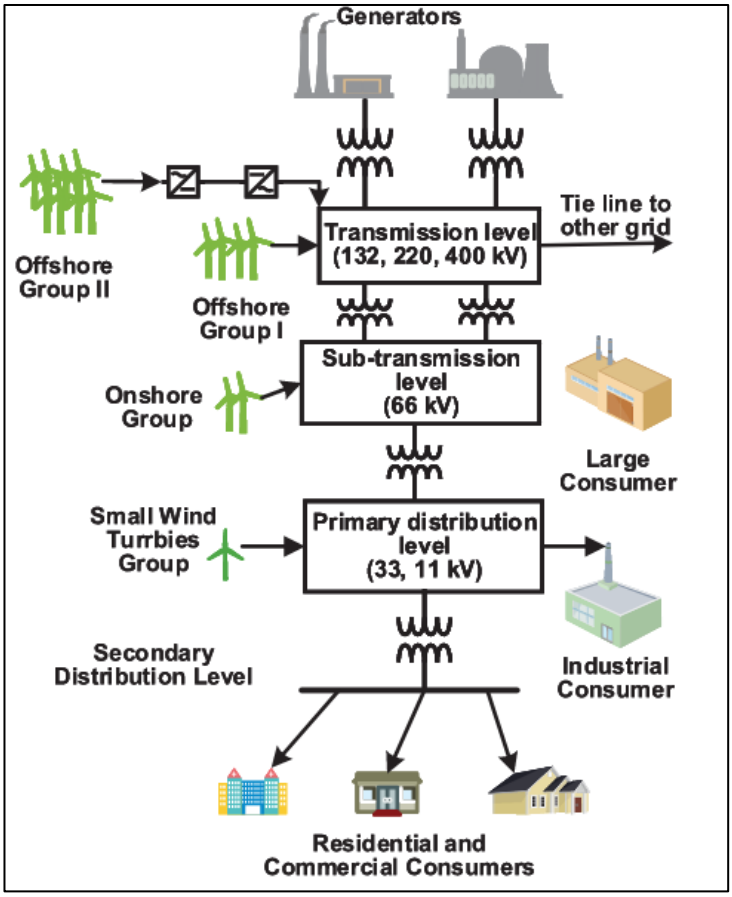

Figure 1. 7 Wind turbine integration into power system [16]

➔ **Output power prediction**

Before integration, grid operators were interested in understanding the details of the generation, as wind energy is an intermittent source related to the stochastic behavior of wind speed. Therefore, the prediction of WT output generation helps manage the network and reduce the production cost, as the absence of prediction requires the presence of large quantities of spinning reserves [16]. Spinning reserves refers to available amount of power generation capacity that exceeds power load, used to respond to sudden load changes or loss of generator [18]. Integration of energy storage systems is a mechanism used to maintain power supply and demand balance, but it has a high initial and operational cost. Intelligent prediction approaches, such as artificial intelligence, have demonstrated efficiency and accuracy in dealing with nonlinear time series owing to their adaptive nature and flexibility. These techniques are based on

historical data to forecast future power generation such as wind power. This method was used in our study to address the wind energy generation uncertainty challenge.

➔ **Voltage or Reactive power support**

The WT can maintain the stability of voltage within the point of common coupling (PCC) voltage limits in the grid by controlling reactive power production [16]. The WT generators used for electricity generation are mostly induction generators. These generator types consume reactive power for excitation to begin producing electricity. Therefore, they cannot support a grid with reactive power like the synchronous machines. Researchers have focused on improving this function of WTs. WTs can provide a network with voltage support through power electronic voltage converters, which are part of the control circuit. This converter was allowed to overload during the transient fault to avoid an increase in voltage values of the DC link connection above the permissible limit [19].

There is another way to control the voltage in power systems while integrating WTs, which consists of operating these turbines at a fixed power factor, where the reactive power is provided according to the active power generated by these WTs. This second approach is used in our study, where no reactive power is expected to be generated conducting to power factor equal to 1. Furthermore, the voltage limits at the PCC were considered.

➔ **Frequency stability support**

The stability of the frequency of electrical networks penetrated by wind energy involves managing the balance between generation and demand [16]. This challenge was addressed in our work by providing a specific amount of wind power according to the load demand.

1.4 Wind Turbine Design Optimization without Radial Distribution Network Analysis

Several studies have been carried out to optimize the design of WFs, focusing on WTs Design Optimization (WTDO) and Wind Farm Layout Optimization (WFLO) without assessing network connection challenges. As mentioned before, the WFLO consists of

optimizing the WTs in the entire WF by optimizing the layout of the WTs [6]. However, WTDO consists of optimizing the WT design parameters.

1.4.1 Wind Farm Layout Optimization

At WFLO level, a novel optimized WF control strategy with multiple WT tower heights selection for a real WFLO was used in [20]. They proved the flexibility of multiple WT tower heights installation, reduction of the Cost of Energy (COE) produced, and the efficiency of WF was enhanced. Abdulrahman and Wood [21] optimized the layout of WFs for onshore and offshore conditions including different commercial turbines using a Matlab genetic algorithm. Results showed that the maximization of the capacity factor acted as a midpoint between the two design extremes of maximizing power output and minimizing the COE. Using a gradient-based algorithm and an adjoin method for the gradient calculations, the WFLOs in both flat and complex terrains were presented by Antonini *et al.* [22]. This permitted the use of computational fluid dynamics models to accurately simulate wake effects and terrain-induced flow characteristics. By optimal siting turbines over complex terrains exploiting turbine and terrain induced flow features, the outputted energy was improved. Charhouni *et al.* [23] performed an offshore WFLO to optimally design the WF area that maximizes the extraction of wind power with low cost. That was achieved through optimal WTs placement determination in the WF using a genetic algorithm and by assessing the impact of commercial WTs on WF objectives. They observed that WF design using big WTs presented the best design layout.

These WFLO studies had the objective of maximizing the efficiency of WFs with low cost of energy (COE), evaluating sometimes the commercial WTs effect in objectives achievement, but there wasn't any improvement in the design of these existing technologies according to wind potential on the site of installation and RDN constraints.

1.4.2 Wind Turbine Design Optimization

At WTDO level, the WT technical parameters were optimized such as blades, tower height (H_g), rotor diameter (D_g), and nominal power ($P_{n,g}$).

1.4.2.1 Wind Turbine Blade Design Optimization

WT blade design optimization had constituted the only interest of some researchers to maximize the efficiency of WT. WT blade geometry design was optimized by Tahani *et al.* [24] for maximum available power extraction with an influence investigation of geometrical parameters including chord and twist distributions and also airfoils on the performance of the turbine in 1 % and 8 % turbulence intensities. A design optimization study of Small scale WT blades and their aerodynamic parameters performance was performed by Balijepalli *et al.* [25] for a Solar updraft tower, increasing the maximum power output extraction from wind. A curved WT blade design was optimized by Sessarego *et al.* [26] using neural networks and an aero-elastic simulator with synthetic inflow turbulence conducting to increase the power production by 1 % and slight increase of mean thrust on the rotor of 0.02 % compared to the straight one. The flexibility of WTs blades was investigated by Cognet *et al.* [27] through WT material optimization to maximize the overall turbine efficiency for any required geometry of classical horizontal axis turbines; resulting in 5 % and 20 % lighter than the current rigid blades

These WT blade design optimization studies focused on maximizing the efficiency of WT for maximum wind power extraction. No RDN constraints and economic assessment was done at this stage.

1.4.2.2 Wind Turbine Tower and Blade Design Optimization

Optimization of WT tower and blade simultaneously is another research objective studied to minimize the COE [6] [1]. WTDO at low wind speed areas was performed by Yang *et al.* [28] providing the blade length and tower height 'H_g' tradeoff that minimize the *COE*. Results showed that H_g enhancement had more significant effect than rotor diameter 'D_g' on *COE* minimization. Ashuri *et al.* [29] presented also a WT blade and tower design optimization study under fatigue, stresses, and deflections constraints that reduced the Levelized Cost of Energy (*LCOE*) by 2.3 % for a representative Dutch site. A multi-objective optimization method of WTs design at the system level using a coupled blade-tower model and sorting genetic algorithm was presented in Zhu *et al.* [30] to find the best tradeoff solutions between the energy output maximization and WT mass minimization. Good results were achieved. Wass [31] determined the optimal WT H_g to D_g ratio that

minimizes the COE through an optimization study of a simulated WT design using an Excel based optimization program. An aspect ratio closer to 0.5 nearing 200 m in diameter was estimated for future large scale WTs. In the same objective of COE minimization, Song et al. [32] and Mellal and Pecht [33] carried out the design optimization of WTs considering the altitude. In addition to rotor radius and tower height evaluation, the WT nominal power was limited and maximized with respect to wind potential variation with the altitude. Results of the both studies showed an increase in the COE with the increase of altitude. The best WT design parameters were found within the design limits in [33]. A multidisciplinary design optimization technique was used in [34] to investigate the economic attractiveness and technical feasibility of optimized up-scaling WTs with a power capacities of 5, 10, and 20 MW. WT tower and rotor were the design variables studied to minimize the levelized cost of energy. Results showed that the evaluated WTs were technically feasible but their costs were expensive [1].

Considering the above mentioned studies, it can be concluded that the main objective in WT tower and blade optimizations was the *COE* reduction. These studies did not evaluate also the integration of WTs in the distribution network; while the optimal design parameters were provided.

1.4.2.3 Wind Turbine Tower or Rotor Diameter Optimization

Optimization of single WT design parameters such as tower or rotor diameter constituted the only interest of some researchers [1]. WT tower height was optimized for the optimization of WFs in [35] and [36], to maximize the WFs energy output and reduce their cost. The optimal design of a steel conical turbine tower for offshore applications was studied by [37], considering tower thickness and bolt type as design variables. Optimization of WT rotor diameter was performed in [38] using a co-design optimization study minimizing the cost of energy. The main objective was novel designs development for the future generation of turbines designed for mature markets based on a WT baseline design with a power capacity of 5 MW and a rotor diameter of 206 m. Results indicated an increase in rotor diameter to 220 m, reducing the cost of energy by 1.3% without affecting loads at the tower base. In [39], the rotor diameter was one of design variables studied to optimize the aerodynamic geometry design of a small-scale WT (1 kW) blade enhancing

the output power. The resulted new WT design showed more output power at lower wind speed value than the tested turbine.

Enhancing the output power and reducing the COE are the principal optimization objectives studied at this stage. Provided WT design data not suggested based on the available wind potential at a selected site and there were no evaluation of RDN constraints

1.4.3 Wind Farm Layout and Wind Turbine Design Optimizations

- WFLO and WTDO at the same time constituted another research axis studied to improve the overall WF design performance [6]. A framework for WFLO and WT technical parameters optimization mainly D_g and H_g was involved in [40] to accelerate the design analysis and optimization of WF using real WF terrain and conditions. The framework provided contained a set of analytical wake models and wake superposition schemes that considered the partial influence of one turbine on another, resulting in increased annual energy production, reduced cost and land usage. The optimal size and height of WT plus the WF layout selection, in addition to the strategic onshore or offshore allocation of WFs were studied by [41] to reduce the wind-powered hydrogen supply system cost using a new optimization model. Coupled turbine design parameters (H_g, D_g, $P_{n,g}$, tower diameter, tower shell thickness, and implicit blade chord-and-twist distributions) and layout optimization demonstrated better results in WFs optimization than separate optimization procedure, and by including two different turbine designs in the same WF, the *COE* was minimized [42].

These studies did not evaluate the economic revenues of a project with such optimized coupled approach of WTDO and WFLO and its feasibility that attracts the investors. The only interest was *COE* minimization like the previous studies.

- The economic incomes evaluation of coupled WFLO and WTDO was treated by maximizing the *NPV* in [43] using a proposed environmental decision support system for the sustainable design of WFs with complex orography. WFLO was performed based site selection over a regional territory and WTDO is conducted by selecting the optimal technology design among a set of thirteen evaluated technologies. For maximization of welfare of the electricity sector and to guide the agent's decision-making, [44] defined also

the optimal combination of WFL and WTD to be installed through an optimization methodology where one of its objectives studied was the *NPV*.

The objective of the design provided in the both mentioned studies is to maximize the WT net revenues (*NPV*) without assessing the grid connection issues of the studied WFs. In this thesis, we focused only on WTDO evaluating the grid connection challenge, using a more powerful economic analysis of the optimized WTs design (LCOE and NPV).

1.5 Wind Turbine Design Optimization with Radial Distribution Network Analysis

1.5.1 Power Flow Optimization in Radial Distribution Network

Optimal power flow in RDN while integrating wind energy presents an important challenge to overcome [1]. The optimal dispatches of active and reactive powers in an active distribution network were optimized simultaneously using a developed economic dispatch model that considers the spatial temporal correlation of wind power output [45]. The model provided enhanced the operation efficiency of the system by maintaining the stability of system voltage level and loss, reducing the operational cost. Using a metaheuristic method called the Aquila Optimizer, a stochastic optimal power flow was presented in [46] to obtain the best scheduled power from WFs integrated into the power system minimizing the total operational costs.

In these studies, WTDO was not studied for the treated WTs integrated into the power system. They investigate the optimal power flow in RDN while connecting WTs to minimize the operational cost.

1.5.2 Wind Turbine Design and Placement Optimizations in Radial Distribution Network

- WTDO and its optimal location in the RDN, in addition to the optimal power flow in the power system constituted another research interest to enhance the efficiency of the power system [1]. For the stability of the power system voltage and power loss reduction, the optimal location and size of the WT were found using the Grid Search Algorithm and Salp Swarm Algorithm in [4] and [5] respectively. Different penetration levels of WT active

power and different power factors were evaluated in [4]. For an energy loss reduction of 66%, three WTs in a 69 bus tested system were integrated [5]. considering the WTs reactive power capacity, wind speed, and demand curves and minimizing also the power losses in AC distribution network, the optimal placement and sizing of WTs were studied in [47] using a developed optimization model and by restricting the maximum number of installed WTs in the tested RDN to three. Furthermore, an ANN was used for short-term forecasting, to address the uncertainties in wind power generation [47].

In these studies, the optimal location and size of WTs in the distribution network were corresponded to the bus node that had presented the minimum power loss value. In addition, there was no evaluation of the economic benefits of WT installation in the RDN.

- WT design and location optimization in the RDN with economic evaluation was rarely realized by researchers. Minimization of the total energy loss and maximization of *NPV* economic indicator associated with the WT investment over the planning horizon are the main objective functions studied in [48] using a multi-objective optimization method to determine the optimal number, size, and placement of WTs among different WTs selected and candidate buses. [3] proposed a decision framework to optimal plan wind power plants in a distribution network with technology selection for various bus locations maximizing also the *NPV*.

In these studies, the optimal WT size was selected among evaluated technologies from the market, and the best bus locations for WTs installation were based on the wind profile. A not commercialized WT design is proposed in this thesis and the best bus location is selected from an economic analysis of *NPV*.

1.6 Conclusion

In this chapter, a state of art analysis of WT historical development and previous WTDO studies are presented. On one hand, the main objective shared between the optimization studies performed without RDN evaluation was the energy generation efficiency enhancement to reduce the COE. The optimal WT design determination was selected in general among tested commercialized technologies according to the maximum NPV or minimum COE generated [6]. There was no study that gives a decision support model to optimally size the WT based on the wind potential available on the studied site. In contrast, the first research objective of this thesis is to provide a techno-economic decision support model that gives the suitable WT design parameters (D_g, H_g, and nominal power) for onshore applications based on the wind potential of the selected site, maximizing the NPV of wind system revenues assessing in parallel the generated *LCOE*.

On the other hand, at WTDO with RDN electrical characteristics evaluation, we conclude that the optimal WT size and location in the RDN were given either for power loss reduction, *NPV* maximization, or both. Furthermore, the optimal WT design provided was often based on the tested commercialized technologies or on the design corresponded to the bus location presenting minimum power loss value [1]. No study had assessed simultaneously the available wind profile of the evaluated site and the RDN characteristics while determining the optimal WT design evaluating in its objective, the economic benefits of the design provided. This constitutes the second research interest of this thesis. The techno-economic decision support model developed in the first step of this thesis is employed with RDN constraints to determine the same optimal WT design parameters (D_g, H_g, and nominal power) and candidate RDN bus locations for the installation of WT.

The proposed WTs design parameters in this report are not selected from the technologies datasheets available in the market like the mentioned studies in this chapter but they are proposed in this work. That constitutes the originality and one of the novelties realized in this work.

Chapter 2 Wind Potential Origin, Quantification, Wind Turbine Components and Operation Process Presentation

2.1 Introduction

The profitability of a wind turbine (WT) in terms of power generation initially depends on a good definition of the wind speed. First, the objective of this chapter is to introduce the origin of the wind source and its movements on Earth's surface. The efficient methods for wind quantification are presented in a second section. This chapter also provides a description of the different components of WT technology through which the wind speed potential is exploited to produce electrical energy. To this end, a detailed description of the operation process of the WT blade airfoil, which is mainly responsible for the rotor rotation, is presented. Furthermore, the WT output must be monitored and controlled because the wind speed varies randomly. Thus, a power control strategy was presented. Different types of generators are used with WTs, which provide different power properties. Therefore, WT generators were defined. Brakes are important devices integrated into the WT structure to control the rotational speed of the wind rotor. This rotor can be operated by following different rotational speeds to capture the maximum possible wind power, as described in the last section of this chapter.

2.2 Wind Origin

Wind is the mean parameter required by wind turbines to generate electricity. Understanding the construction of this natural element and its movements at earth's surface is necessary to improve the installation of WTs and their operational efficiency. Wind results from the circulation of airflow produced by temperature variations. This variation is due to the unequal repartition of solar radiation over Earth's surface, as described in **Figure 2. 1**[49] [50].

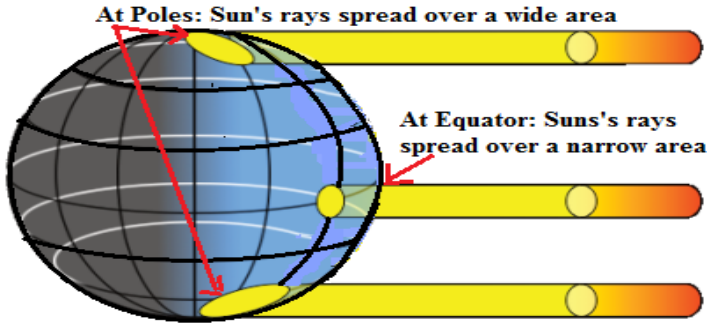

Figure 2. 1 Solar radiation repartition over the Earth's surface [50]

1.74 kWh of solar energy is absorbed every day by the earth, and 2% of this energy is converted into wind [51]. Temperature differences lead to differences in pressure. Air circulates from a region of high pressure to a region of low pressure. The higher the pressure gradient, the more powerful the wind speed generated. There are two main types of winds: global and local.

2.2.1 Wind at Global Scale

2.2.1.1 Definition

At the global earth surface and because of its sphericity, the sun's rays are perpendicular to the equator and parallel to the poles, as shown in **Figure 2. 1** [49] [50]. Sun's rays spread over a more large area at poles conducting to less heat of this surface than at the equator. Furthermore, the ice, snow, and cloud cover at poles creates a higher albedo, reflecting more solar radiation than they absorb compared to the equator [50]. Therefore, the air is warmed at the equator and cold at the poles, resulting in surplus heat energy in tropical regions and a deficit in Polar Regions, as shown in **Figure 2. 2** [52] [50]**.**

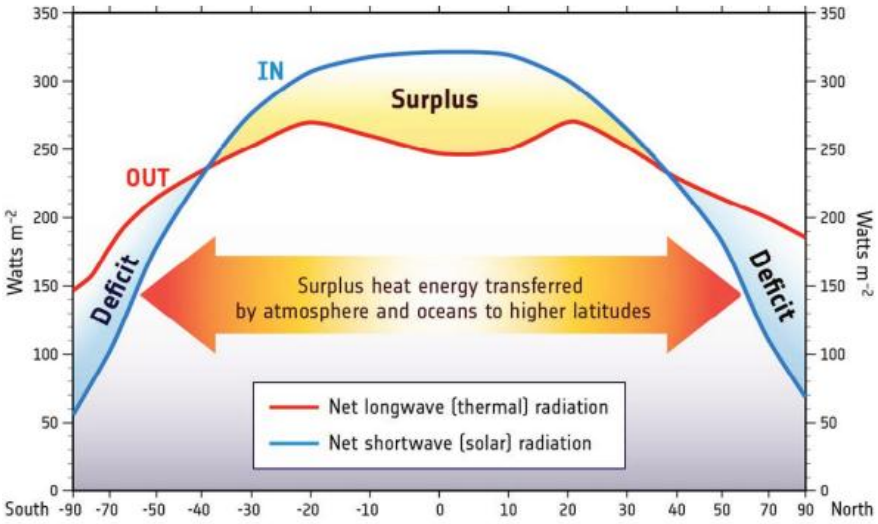

Figure 2. 2 The balance between heat gain and heat loss as a function of latitude [50]

This surplus heat energy is transferred toward the poles by natural convection, which moderates the climate. Therefore, the tropics and poles are protected from being heated up or frozen because of the excess heat or deficit [52] [50].

The air pressure at the poles is greater than that at the equator. Thus, warm air moves from the equator towards the poles to be cooled and reaches buoyant equilibrium with the surrounding air [49]. The expansion of air creates a low pressure [51]. Unlike the cold pole, where the air descends towards the equator to be warmed and equalizes the pressure [49], [51]. These cycles are repeated on the global Earth surface. Wind movements are influenced by the rotation of the earth, providing a force called the Coriolis force, which deflects the direction of the wind [49].

2.2.1.2 Coriolis Force

This force was named after the French mathematician Gaspard-Gustave de Coriolis (1792–1843) [51]. Under this force effect, the wind is always diverted to the right in the Northern Hemisphere from the point of origin, and to the lift in the Southern Hemisphere, as described in **Figure 2. 3** [50].

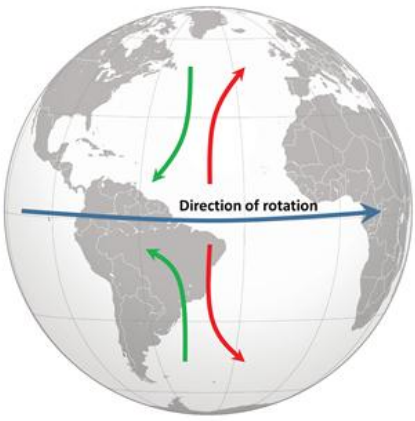

Figure 2. 3 Wind Direction under Coriolis Effect. Objects moving from the equator towards the poles (red arrows). Movement from high latitudes to low latitudes (green arrows) [50]

As mentioned previously, air moves from the equator to the poles. However, air circulation is stopped at 30° latitude north and south before arriving at the poles because the warmed equatorial air meets a high-pressure area of cooler air [51] [53]. This involves the apparition of three different wind cells classified into three hemispheres describing the wind circulation over the Earth's surface: Polar, Ferrel, and Hadley cells. In Polar and

Hadley cells, the wind blows towards the equator [50]. However, it blows towards the poles in the Ferrel cell, as shown in **Figure 2. 4**.

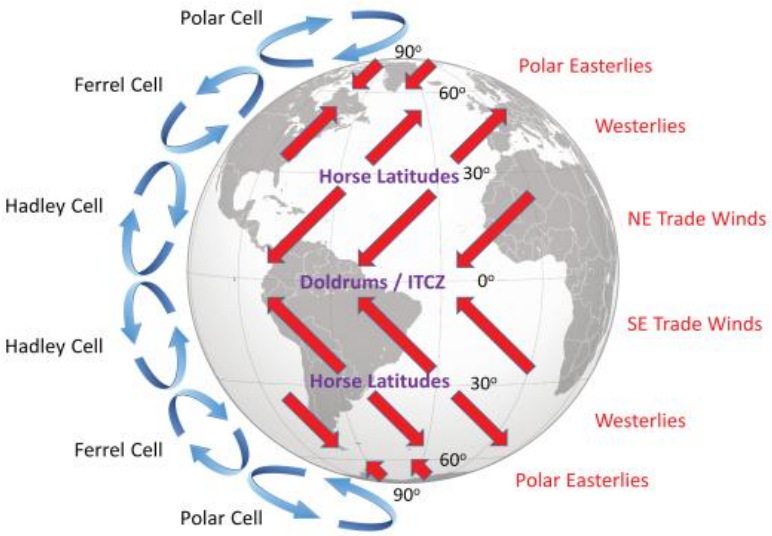

Figure 2. 4 Atmospheric Convection Cells and Prevailing Wind Patterns [50]

The circulate wind inside these cells deviates under the Coriolis Effect towards the west or east, defining the worldwide prevailing wind patterns, namely, Easterlies, Westerlies, and Trade winds, as described in **Figure 2. 4** [50] . In the polar hemispheres between 60° and 90°, we found that easterly winds blow from east to west and are often weak and irregular. Westerly winds are dominant and blow across the mid- or horse latitudes between 30° and 60° of the earth and circulate from west to east. Trade winds are found in the tropics towards the equator at latitudes of 0° and 30°, and they circulate from the northeast in the Northern Hemisphere and from the southeast in the Southern Hemisphere.

2.2.2 Wind at Local Scale

Wind movements are influenced by other factors such as local geographical and topographical conditions that define the local prevailing winds and their directions, such as sea/land and mountain/valley breezes [51].

2.2.2.1 Sea and Land Breezes

Sea breeze occurs during the daytime, when seawater warms more slowly than on the land surface. Therefore, the warmed air beyond the land with less density rises, and the high pressure of sea air moves behind it into a lower pressure, resulting in onshore wind [51]. The opposite of this path occurs at night, resulting in offshore wind. This process characterizes the land breeze. The both processes are shown in **Figure 2. 5** [50]

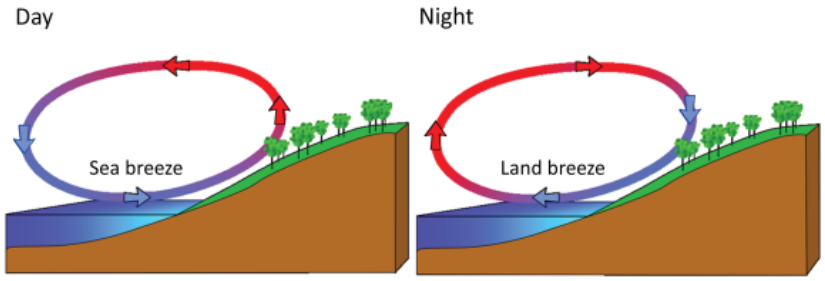

Figure 2. 5 Land and Sea Breezes [50]

2.2.2.2 Mountain and Valley Breezes

Mountains have a significant effect on wind direction [51]. During the day, the mountain slope air is heated by the sun and ascends the mountain slopes, generating a valley breeze [54]. At night, mountain breezes are created where mountain slopes are cooled and cool dense air descends into the valley. These breezes occur mostly in calm and clear weather conditions.

2.3 Wind Quantification

Wind speed variation exhibits stochastic behavior that impacts the energy generated by WTs. Therefore, it is necessary to quantify this variation over time [49]. There are many efficient statistical methods used to model and describe the variation in wind speed, such as Rayleigh and Weibull distributions [49] [16]. These models can be used to estimate the annual wind energy generated. The Rayleigh distribution is a special case of a Weibull distribution with a shape parameter equal to two [55] [49]. The Weibull method is the most commonly used method to provide a good description of wind speed distribution [56] [6]. Therefore, this method was adopted in this thesis.

2.3.1 Weibull Distribution.

This distribution is characterized by a probability density function called the Weibull probability density function, which represents the probability of observing wind speed *v* in (m/s) [6]. This function is associated with two main parameters, namely scale C^l(m/s) and shape k^l, which permit the definition of the wind distribution at a specific location l. The Weibull function is expressed as follows [3] [1]:

$$f_i^l(v_i) = \left(\frac{k^l}{C^l}\right)\left(\frac{v_i}{C^l}\right)^{k-1} exp\left(-\frac{v_i}{C^l}\right)^k \tag{2.1}$$

The Weibull parameters (C^l(m/s) and k^l) can be determined using several methods, such as graphical [49], standard deviation, Lysen, and Moroccan methods [57], [58].

2.3.1.1 Standard Deviation Method

The standard deviation formulas for k^l and C^l determination are as follows [57], [58], [1]:

$$k^l = \left(\frac{\sigma}{v_{average}}\right)^{-1.086} \tag{2.2}$$

$$C^l = \frac{v_{average}}{\Gamma\left(1+\frac{1}{k^l}\right)} \tag{2.3}$$

$$v_{average} = \frac{1}{N}\sum_{i=1}^{N} v_i \tag{2.4}$$

$$\sigma = \sqrt{\frac{1}{N-1}\sum_{i=1}^{N}\left(v_i - v_{average}\right)^2} \tag{2.5}$$

Where, Γ is the gamma function, $v_{average}$ is the mean wind speed, σ is the standard deviation of wind speed, and *N* is the number of wind speed samples [1].

2.3.1.2 Graphical Method

Based on the double natural logarithm of the cumulative distribution probability $F^l(v_i)$ of the Weibull probability density function, given by the following function [49]:

$$F^l(v_i) = 1 - exp\left[-\left(\frac{v_i}{C^l}\right)^{k^l}\right] \tag{2.6}$$

$$ln[-\ln(1 - F^l(v_i)] = k^l \ln(v_i) - k^l \ln(C^l) \tag{2.7}$$

The cumulative distribution probability requires a frequency table to be manipulated as follows:

$$F^l(v_{i=1}) = f^l_{i=1}(v_{i=1}) \tag{2.8}$$

$$F^l(v_{i=N}) = f^l_{i=N}(v_{i=N}) + F^l(v_{i=N-1}) \tag{2.9}$$

The Weibull parameters can be determined through linear regression by plotting $y = ln[-\ln(1 - F^l(v_i)]$ versus $x = \ln(v_i)$, giving a straight line to the actual wind data characterized by a linear equation [58]. The slope of the line represents the Weibull shape coefficient, k^l, and the intersection point with y axis represents$(-k^l \ln(C^l))$, from which the Weibull scale factor, C^l can be found.

2.3.1.3 Lysen Method

The Lysen formulas for Weibull parameters determination are given by [58]

$$k^l = \left(\frac{\sigma}{v_{average}}\right)^{-1.086} \tag{2.10}$$

$$C^l = v_{average}(0.568 + \frac{0.433}{k^l})^{-1/k^l} \tag{2.11}$$

2.3.1.4 Moroccan Method

This method was used to evaluate the Moroccan potential [57]. Using this approach, k^l and C^l can be determined using the following equations.

$$C^l = \frac{v_{average}}{\Gamma\left(1+\frac{1}{k^l}\right)} \tag{2.12}$$

$$k^l = 1 + (0.483(v_{average} - 2))^{0.51} \tag{2.13}$$

2.3.1.5 Methods Accuracy Analysis

The regression coefficient '*R*' and Mean Square Error '*MSE*' are the error indicators used to select the most accurate method for determining the Weibull parameters that correctly fit the actual measured wind speed distribution. Good fitting results were obtained, with an *R* value close to one and an *MSE* near zero. The *R* and *MSE* equations are as follows [59] [1]:

$$MSE = \frac{1}{N}\sum_{i=1}^{N}(v_{mes,i} - v_{pred,i})^2 \tag{2.14}$$

$$R = \frac{\sum_{i=1}^{N}(v_{mes,i}-\overline{v_{mes,i}})(v_{pred,i}-\overline{v_{pred,i}})}{\sqrt{\sum_{i=1}^{N}(v_{mes,i}-\overline{v_{mes,i}})}\sqrt{\sum_{i=1}^{N}(v_{pred,i}-\overline{v_{pred,i}})}} \quad (2.15)$$

Where, N is the number of samples, $v_{mes,i}$ is the measured wind speed, $v_{pred,i}$ is the predicted wind speed, and ($\overline{v_{mes,i}}$, and $\overline{v_{pred,i}}$) are the actual mean value.

2.3.1.6 Weibull Parameters Extrapolation

The Weibull probability density function $f^{l}{}_{i}$ describing the wind speeds is adjusted automatically with the estimated WT tower height H_g given by the present techno-economic decision support model to $f^{l}{}_{i,,h}$, by extrapolating the Weibull parameters k^l and C^l calculated using the available wind speed data at an initial height H_0 to a new height H_g using the modified Mikhail formulas given in [60], [61]. The extrapolation method permits the analysis of the impact of the WT tower height H_g variation that occurred during the evaluation of the developed decision support model on the wind speed distribution, the energy generated by the WT, and the whole WT techno-economic design optimization problem presented in the next chapter. The formulas adopted for extrapolation are as follows [60], [61] :

$$C_{H_g}^{l} = C_{H_0}^{l}\left(\frac{H_g}{H_0}\right)^{p} \quad (2.16)$$

$$p = \alpha_0 \left[\frac{1-\frac{\ln(C_{H_0}^{l})}{\ln(67)}}{1-\frac{\alpha_0 \ln\left(\frac{H_0}{h_r}\right)}{\ln(67)}}\right] \quad (2.17)$$

$$\alpha_0 = \left(\frac{z_0}{h_r}\right)^{0.2} \quad (2.18)$$

$$k_{Hg}^{l} = k_{H0}^{l}\left[\frac{1-\frac{\alpha_0 \ln\left(\frac{H_0}{h_r}\right)}{\ln(67)}}{1-\frac{\alpha_0 \ln\left(\frac{H_g}{h_r}\right)}{\ln(67)}}\right] \quad (2.19)$$

Where, p is the power law exponent, h_r is the reference height equal to 10 m given by [61] , α_0 is the surface roughness exponent, z_0 is the surface roughness length of the site, H_g is the estimated height by the present decision support model, H_0 is the initial height of the measured wind speeds, C^{l}_{Hg} and k^{l}_{Hg} are the extrapolated Weibull parameters at the new height H_g, and, C^{l}_{H0} and k^{l}_{H0} are the Weibull parameters calculated at H_0.

The extrapolated Weibull distribution function $f^{J}_{i,,h}$ is included in our techno-economic decision support model presented in the next chapter to address WT design and location problems.

2.3.2 ANN Wind Speed Prediction

Wind energy is an intermittent source related to the variability of wind speed. The integration of this energy into the power system affects its stability. Therefore, as mentioned in the first chapter, wind energy prediction is required by grid operators to manage their networks and reduce production costs. Furthermore, the wind power captured by a WT is dependent on cubic wind speed; thus, a few variations in wind speed have a significant influence on the generated wind energy [1]. Therefore, as the effectiveness of wind speed prediction increases, the energy generated by WTs becomes more accurate. The Artificial Neural Network (ANN) is an artificial intelligence approach used to predict future stochastic behaviors, such as wind speed, based on previously observed wind speed data [1]. More precisely, ANN is used in deep learning as a subset of machine learning in artificial intelligence. Machine learning consists of making a machine learn automatically to perform specific actions based on specific data, following one of these techniques: supervised or unsupervised techniques [62]. In supervised learning, there are inputs and awaited output data. However, there is no specific data structure for unsupervised learning. An ANN saves the entered data in its memory in a process similar to that of a human neural biological network. ANN tends to reduce the error between the entered and predicted data using an optimization algorithm [47]. This method has proven to be effective in providing good prediction results [62].

As the integration of wind energy to the grid constitutes the interest of the second optimization scenario evaluated in this thesis, the ANN is employed in this case to deal with the wind energy generation uncertainty challenge imposed on the grid. A feed-forward neural network model with a supervised learning technique trained using the Levenberg-Marquardt back-propagation optimization algorithm is used to forecast the future hourly wind speed at a studied site (Essaouira City) for a time horizon of one year. The ANN structure comprises four main components: an input layer linked to the sources of information, a hidden layer composed of several neurons, a target that contains the

previous data of the desired output parameter, and an output layer containing the information sent from the ANN, as shown in **Figure 2. 6** [59]. The input data are divided into two parts: one part is used to train the ANN, and the remaining data are used during a time period called testing. Note that an ANN model can contain several hidden layers, with different numbers of neurons in each layer. The hidden layers outputs are hidden for users and are used only for the output layers [63].

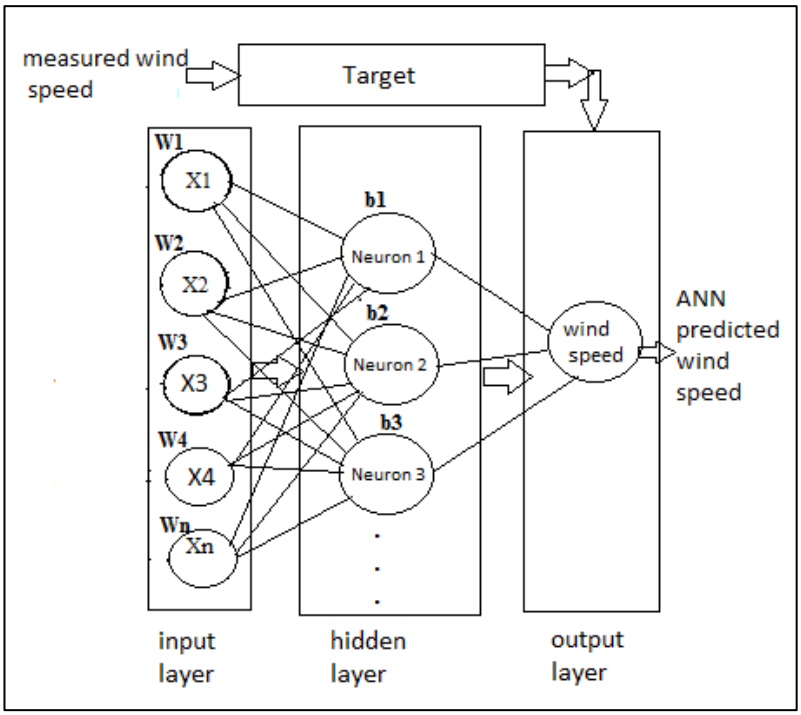

Figure 2. 6 Simplified ANN model architecture [1].

In the feed-forward neural network every input 'x' is combined with a weight 'w' and their sum is added to a parameter called bias 'b' to generate a single value 'z' for a nonlinear mathematical function 'a(z)' called 'Sigmoid' contained in the bottom of each neuron in the hidden layer [1] [59] [47]. This function is used as a nonlinear activation function in the hidden layer, and another linear fitting function called 'fitnet' is used in the output layer to fit the neural network output. z and a(z) are expressed as follows [64] [59]:

$$z = \sum wx + b \tag{2.20}$$

$$a(z) = \frac{1}{1+e^{-z}} \tag{2.21}$$

The main parameters in the ANN model are the weights and bias calculated at the training time and change at the testing time through the optimization algorithm (Levenberg-Marquardt back-propagation) to reduce the error between the predicted and measured wind speed data [59]. This prediction approach addresses the uncertainty of the generated wind energy and improves the effectiveness of our proposed techno-economic decision support model for determining the future design of WTs. The regression coefficient 'R' and Mean Square Error 'MSE' are also the error indicators used at this stage to evaluate the performance of the ANN involved in forecasting wind speed at the location cited.

2.4 Wind Turbine Components and Operation Process

The major horizontal-axis wind turbine components are the rotor, nacelle, and tower, as shown in **Figure 2.7**:

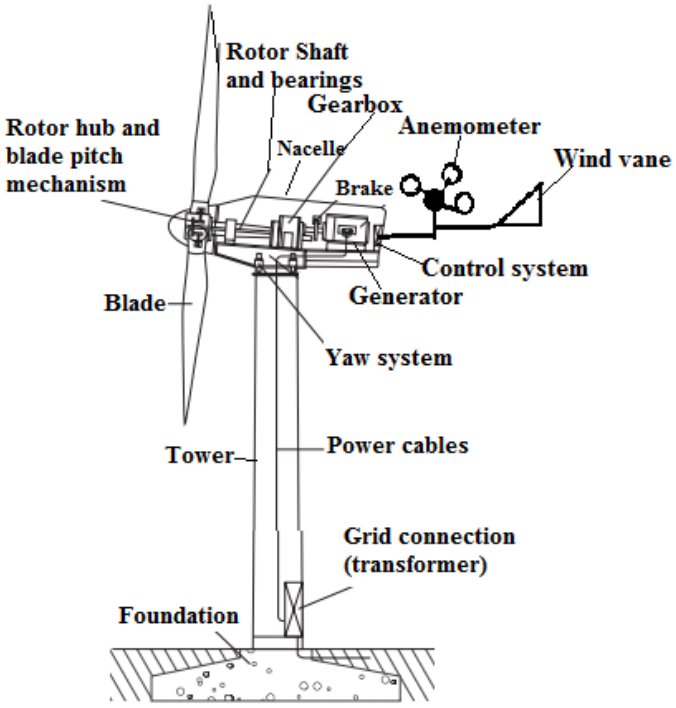

Figure 2. 7 Horizontal axis wind turbine components [65]

- The rotor is composed of two units: blades and a hub. It's the initial component in a WT machine that captures the kinetic energy of wind through the airfoil-shaped blades integrated into the hub [66]. Blades rotate under the influence of the wind,

converting its kinetic energy into rotational mechanical power at the rotor hub level, which drives a low speed shaft.

- The gearbox is connected to the rotor through a low speed shaft, and its principal role is to increase the rotational speed of the low speed shaft to drive the generator through a high speed shaft placed between the gearbox and generator [66].
- The generator is connected to the gearbox through a high speed shaft, which drives it to start generating electricity.
- Nacelle is a box placed on top of the tower and contains a part of the low speed shaft, gearbox, generator, and any associated equipment needed to control and operate the wind machine [67] [66]. This box protects these electronic components [67].
- The tower supports the rotor and nacelle weight and permits to reach more powerful and stable wind speeds according to its height [67]. Single monopoles and three- or four-leg lattice towers are the most commonly employed structures.

There are other components of the wind turbine such a:

- Orientation devices to keep the rotor facing the wind, such as the tail and drive motor. Small wind machines with rotors smaller than 50 square meters use a tail device. However, yaw systems, including drive motors and wind direction sensors (wind vanes), are used on tower by larger machines [67].
- Foundation to fix the WT to the ground, providing high resistance against high wind speeds.
- Brakes used to maintain the safety of WT against high wind by stopping blades rotation or in the case of system maintenance.
- Anemometer measures wind speed and informs the control system when the wind is blowing sufficiently strong to start producing electricity efficiently.
- The controller essentially monitors the rotor speed of the wind machine to start and stop by releasing the mechanical break at the correct time function of the wind speed [67]. This permits the protection of the machine and its effective operation. The controller also monitors the output generated by the WT to assess whether the voltage, current, and frequency are within the typical operating conditions [67]. Otherwise, the turbine is stopped by creating a fault condition.

2.5 Wind Turbine Blades Airfoil

The horizontal-axis wind turbine rotor is composed of airfoil blades with a shape similar to airplane wings [67]. These blades have a flat form on one side and a curved form on the other side for maximum airflow. The airflow is faster on the curved part than on the flat side, causing a high air pressure on this later. This pressure difference on both blade sides generates aerodynamic forces that rotate the rotor, namely drag and lift forces. Drag and lift are the forces applied to the airfoil (blade) moving through the wind, which are determined experimentally according to the attack angle 'α' [67]. This angle is the angle between the chord line of the airfoil and the relative wind, as described in the **Figure 2. 8**.

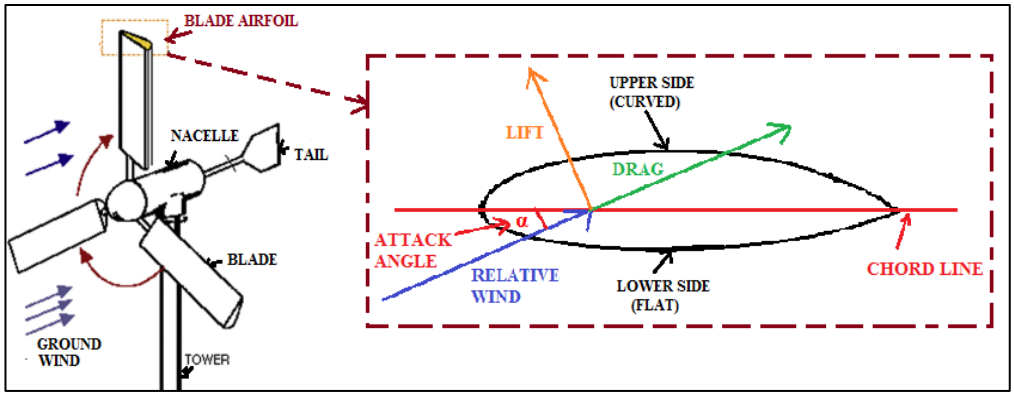

Figure 2. 8 Applied aerodynamic forces on wind turbine blade [67]

The relative wind named also the apparent wind, is composed of the vector sum of the wind across the ground and the wind owing to the movement of the rotor blade, as described in the **Figure 2. 9**.

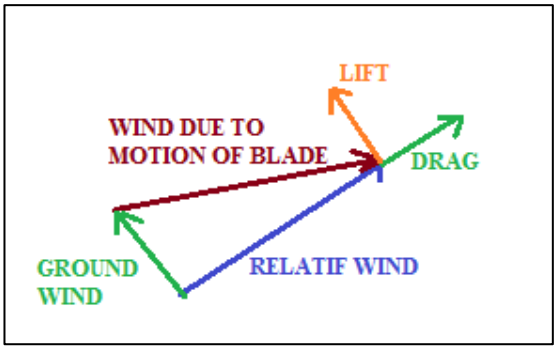

Figure 2. 9 Relative wind applied to wind turbine blade [67]

The angle of attack controls the quantity of lift that contributes to rotor rotation about the horizontal axis, as described in the next section [67]. The horizontal-axis WTs are mostly equipped with three blades. This architecture proved its efficiency in maintaining rotor blades across clear and stable wind compared to more blade numbers, which conduct only to wind turbulence, decreasing the efficiency of the WT technology and increasing its cost. Furthermore, the three-blade architecture provides stability for the rotor at all points during the rotation, in contrast to the WT with fewer blades, which involves instability rotation points causing loads and fatigue on the rotor [67]. Blades can be located upwind or downwind of the tower; however, in recent installed WTs they are generally upwind.

2.6 Wind Turbine Power Control

The power generated by the WTs according to the registered wind speed generally follows the power curve shown in **Figure 2. 10** [68]. At a cut-in wind speed generally between 3 and 4 m/s, the WT starts generating power and increases with the wind speed. It reaches its rated power at the rated wind speed value, which can range from 12 m/s to 15 m/s. After a specific wind speed value, called the cut-out wind speed, the turbine is not allowed to generate more power to prevent its safety. Between the rated and cut-out speeds, the machine should be regulated to generate the same rated power specified by its constructor. If no regulation is applied, the generated power continues to increase as the wind speed increases, as indicated by the dotted line in the **Figure 2. 10**. This accelerates the rotor speed of the WT reaching the runaway state [68]. Therefore, the WT output power must be regulated at a constant level at speeds higher than the rated wind speed, controlling the rotor rotational speed. Two methods are generally used in wind power regulation: pitch and stall controls.

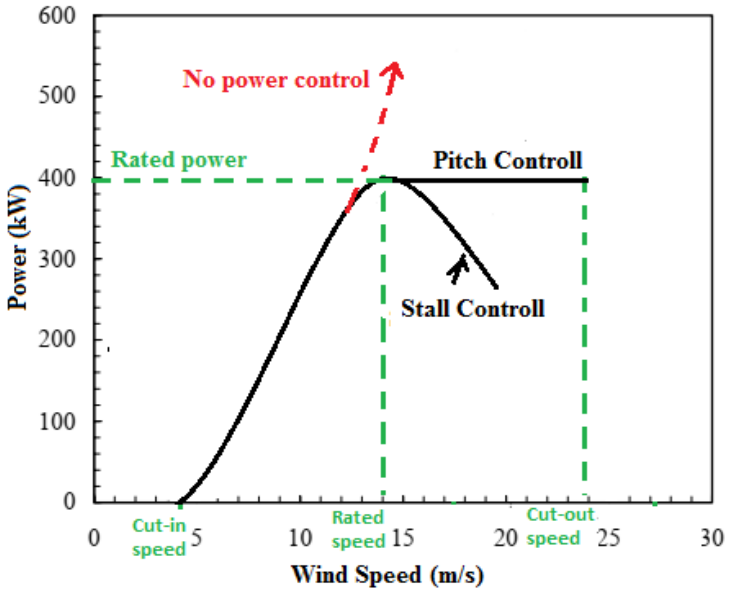

Figure 2. 10 Wind turbine power curve with power regulation methods [68]

In pitch control, WT blades are rotated about their longitudinal axis function wind speed variation, thereby changing their associated attack angle [68]. This movement is governed by the moving components integrated into the blade. The WTs equipped with this mechanism adjust the attack angle to an optimum value to operate the WT at its maximum efficiency between the cut-in and rated wind speeds. At speeds higher than the rated value, this angle is minimized to reduce the efficiency of the WT rotor minimizing the input wind power to control the power output, as described in **(Figure 2. 11 (b))** [68] [65]. A WT with pitch control is expensive because of its high construction sensitivity to wind. Furthermore, the WT can be equipped with fixed or variable pitch controllers depending on the attack angle if it is fixed or variable [67]. Variable attack angle allows the blades to rotate around their longitudinal axes to control the speed of rotor and power output. However, the blades cannot rotate around their axes at all wind speeds during operation in fixed-pitch wind machines.

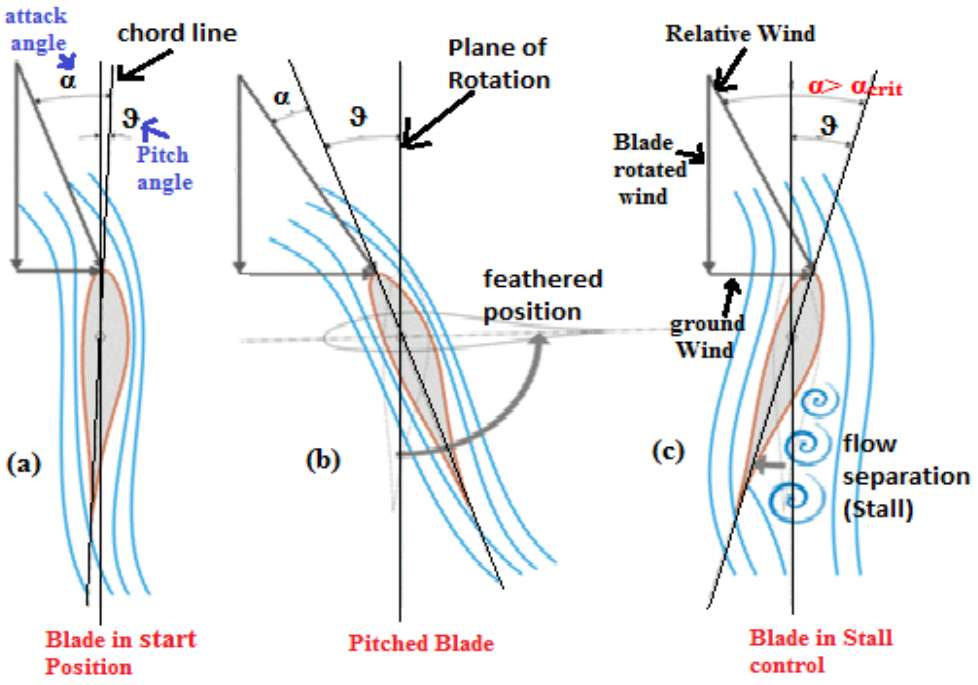

Figure 2. 11 the rotor input power control by pitching the blade towards feather or towards stall [65]

In the stall control mechanism, the aerodynamic profile of the WT blades is designed specifically to increase the attack angle up to the so-called critical aerodynamic angle when the wind velocity exceeds the rated limit **(** see **Figure 2. 11 (c))** [68] [65]. This results in turbulent air flow on the upper side of the blade limiting the lift force and leading to blade stall in a power regulation process. No pitching mechanism or control system is required for the blades to be twisted in this control type, but an almost sophisticated design is required to avoid vibration problem. WTs with stall control are not efficient at high wind speeds because the output power decreases below its rated value, as described in **Figure 2. 10** [68].

Two other types of power regulations are used in modern turbines. The first is the active stall control that combines the pitch and stall control options [68]. The second type is furl or yaw control, which is employed only for stall turbines. It consists of pushing the rotor partly away from the wind direction at higher wind speeds.

2.7 Wind Turbine Brakes

Brakes are important devices for controlling the rotor speed of WTs under high-wind conditions, normal start and stop, or maintenance and repair requirements [67]. Aerodynamic and mechanical brakes are commonly used in WTs [68]. Furthermore, two braking systems are typically employed with WTs to ensure safety. One works as a primary brake, and the other as a backup option that operates if the primary brake fails.

Aerodynamic brakes are employed as the primary system in most WTs [68]. This depends on the power control method used with the WTs, that is, either pitch or stall. In both controls, the entire blade is turned along its longitudinal axis, limiting the lift force to reduce or stop rotor rotation, as discussed in section 2.6 [68]. Stall control cannot completely stop the blades; however, it reduces the rotor speed. Mechanical brakes placed on the high-speed shafts of systems with gearboxes are employed as backup systems to completely stop the rotor in stall-controlled turbines and during turbine maintenance [67] [68].

2.8 Wind Turbine Generator Types

Several types of generators have been used in wind turbine technologies. Small scale turbines used for battery charging use DC generators of few Watts to kilo Watts with a charge current controller; these turbines disappeared in the early 1950 [67] [68]. However, large-scale turbines use three-phase AC synchronous or asynchronous generators, because they are generally connected to the grid [68].

2.8.1 Asynchronous Generators

Asynchronous generators, known as induction generators, are the most dominant type of generators in the wind industry [68] [16]. They are inexpensive and require simple controls to manage the voltage and frequency of electricity produced to match grid requirements [67]. They are also efficient in operating under variable conditions such as wind speed variations [68]. The gearbox increases the wind rotor speed up to the operating speed of the generator. Therefore, these generator types control the rotor speed to a nearly constant rotational speed, and the wind rotor does not operate at its peak efficiency [67]. These

generators consume reactive power for excitation to start producing electricity. Therefore, they must be connected to the grid at all times to attire the power, associated voltage, and frequency from the utility [67].

An induction generator is composed of a stator and a rotor (see **Figure 2. 12**). The rotor has a cylindrical laminated core named squirrel-cage rotors that consist of slots for conductor bars (aluminum or copper) placement, which are short-circuited by aluminum end rings [68]. Wound rotors have also been used in induction generators. The stator contains several wound coils connected to the grid. Induction machines can operate in both motor and generator modes [67] [68].

- ➔ At starting induction generator behave as motor: external excitation current is required to start work. A rotating magnetic flux at a uniform speed, called synchronous speed, is developed at the stator when the stator windings are fed with a three-phase grid supply [68]. This flux reaches the stationary rotor and cuts the conductors. A strong electromagnetic force is induced in the rotor due to the relative speed between the rotating flux and the stationary rotor conductors. This induced a very strong current in the short-circuited rotor bars, which tended to reduce the relative velocity. To this end, the rotor starts rotating in the same direction as the flux; however, it always has a slightly lower rotational speed than the synchronous speed. Therefore, the rotor speeds of these generators is not synchronized [67]. The synchronous speed of an induction motor depends on the number of poles. It decreases when number of poles increase [68]

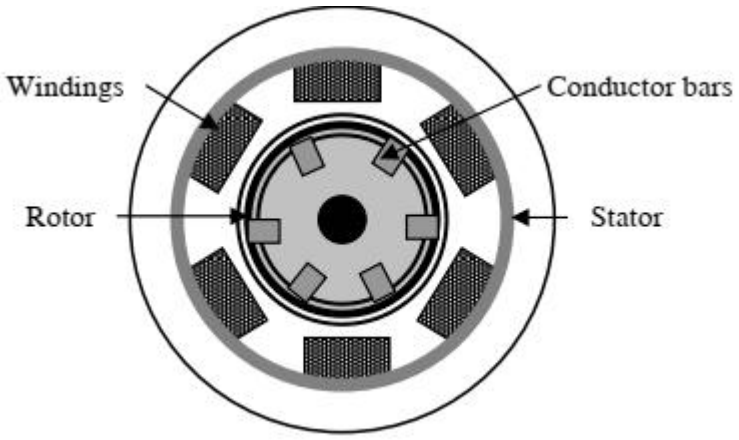

Figure 2. 12 Induction generator [68]

➔ In the generator operation mode, the rotation of the WT causes the generator rotor to rotate at speed higher than synchronous speed, and current flows this time from the system to the grid. The generator is disconnected from the grid during calm periods when no wind is available or when wind speeds are lower than the cut-in speed of the WT [68]. At the cut-in speed, the system is gradually connected by thyristors to the grid to receive excitation and then function as a generator.

2.8.2 Synchronous Generators

The synchronous generator has a similar configuration to an induction generator, composed of a rotor and a coils-wound stator. Both components have identical poles number [68]. In contrast to an asynchronous generator, the rotor and magnetic field rotate at the same speed in a synchronous generator [68]. The rotors of these generators types can be equipped with permanent magnets or electromagnets. Electromagnets are the most commonly used with WTs synchronous generators, which require exciters or a direct current to be fed to the rotor windings for magnetization. This current can be extracted from the grid. The internal field developed by the rotor is captured by the stator windings, which induce a sinusoidal voltage in the coils that varies with time due to WT rotation. A balanced three-phase supply is generated, treated, and injected into the grid.

The permanent magnet synchronous generator was developed to be coupled directly to the rotor hub of large-scale horizontal axis WTs without using the gearbox unit (see **Figure 2. 13**) [69]. This structure of WTs is called a direct-drive WTs. The rotational speed of the rotor of the WT is equal to the rotor generator speed. A converter is used with this generator structure to convert the varying mechanical speed to a consistent frequency of the power grid [6].

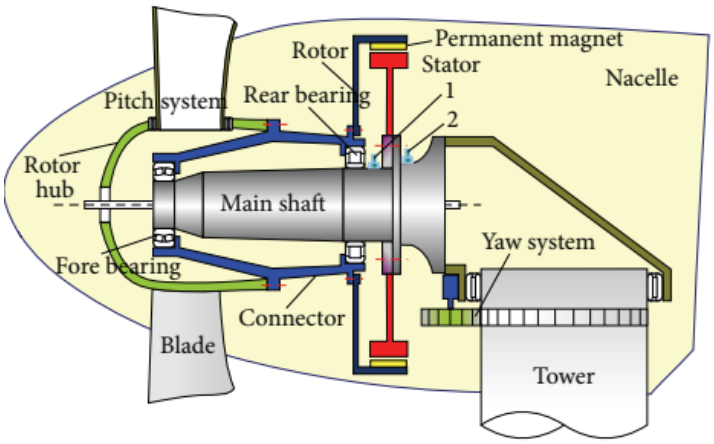

Figure 2. 13 Direct drive wind turbine with permanent magnet synchronous generator

2.9 Fixed and Variable Speed Wind Turbines

Wind turbine can be designed to operate at fixed or variable speed. The rotor of the fixed-speed turbine turns at a constant speed N_1 (rpm) and cannot generate maximum power from the available wind speed potential. In contrast, the variable speed option operates the WT at its optimum level at different wind speeds for maximum power generation, rotating the rotor at different speeds, such as N_1 and N_2, as shown in **Figure 2.14** [68].

A fixed-speed WT derived at a constant speed is attached to an induction generator [68]. As mentioned previously, this generator is first electrically excited through the stator winding connected to the grid and provides the network with power at the required frequency 50 Hz or 60 Hz. Capacitors are used specially with weak networks to avoid voltage variations due to the extracted excitation power.

However, variable-speed WT is attached either to synchronous generators or a doubly fed induction generators [68]. Synchronous generators provide variable voltage and frequency outputs according to changes in wind speed. Hence, an electronic converter is used to convert the AC generated by the synchronous generator into DC and then invert it back to AC at standard grid frequencies (50 Hz or 60 Hz) before feeding it to the grid. In case of doubly fed induction generator, the stator winding of the WT is directly connected to the grid. However, the rotor winding is fed through a converter that can vary the electrical

frequency as desired by the grid. Thus, the electrical frequency is differentiated from the mechanical frequency, which makes variable speed operation possible.

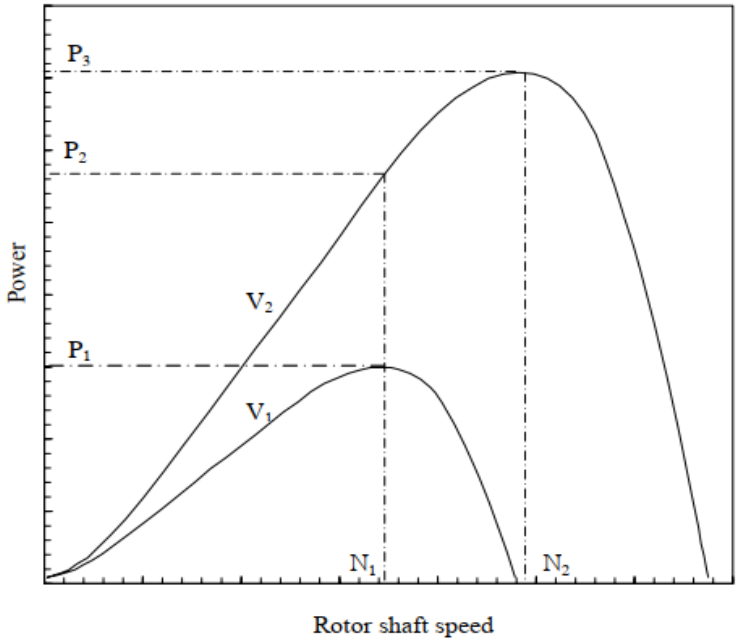

Figure 2. 14 Wind turbine power function rotor speed at two different wind [68]

Variable-speed turbines are complex in construction, expensive compared to fixed one, and cannot respond to grid code requirements without power treatment [68] [16]. However, they can smooth 75% of the voltage fluctuations produced by the fixed-speed turbines. As mentioned in the previous chapter, the WTs designs determined by our proposed techno-economic decision support model in this thesis do not support the grid with a reactive power capacity. They operate at a unit power factor in the process of voltage stability. Therefore, these WTs are assumed to operate at a constant speed attached to the induction generator type with a pitch power control mechanism.

2.10 Conclusion

In a conclusion, this chapter provides an introduction to the understanding of wind energy from wind sources to electrical energy generation. The origin of wind, its movements on the Earth's surface, ANN wind prediction, and the methods used for its modeling are presented in details in sections 2 and 3. In section 4, wind turbine components that exploit the wind to produce electrical energy are defined. The remaining sections are focused on providing an overview of the blade airfoil and its rotation process that drives the WT rotor shaft, a description of the different generator types used in WTs presenting the characteristics of each type, the mechanisms used to regulate the power output within the desired limits, brake devices used to prevent the operation of wind machines, and finally, the methods used to operate the WT at its peak efficiency. Based on these knowledge's, our proposed techno-economic decision support model is modeled to determine the optimal WT design, as presented in the next chapter.

Chapter 3 Techno-economic Decision Support Model for Optimal Wind Turbine Design Determination Modeling

3.1 Introduction

In this chapter, the developed techno-economic decision support model for the optimal design of future wind turbines (WTs) is presented in detail. A decision support system is generally based on optimization problem resolution to determine the optimal solution for a given issue. WT investment projects are challenged by the cost of wind technology. Therefore, the optimization of WT design is a key to reduce its associated cost of energy. The design optimization of the technology with its economic attractiveness constitutes a solution for the development of the wind energy sector and its applications [1]. However, economic attraction is not limited to the low cost of energy (COE) but mostly to the Net Present Value (NPV) of the economic benefits associated with the WT designs involved. This constitutes the interest of our proposed decision support model, which consists of maximizing the NPV revenues of optimized WT designs with an analysis of the LCOE produced. The development of the techno-economic decision support model starts with WT technology and its economic analysis modeling to the optimization problem construction; to determine the optimal WT design parameters, mainly the rotor diameter (D_g), tower height (H_g), and WT nominal power ($P_{n,g}$). The proposed decision support model does not consider the characteristics of the plant, such as the possibility to react better to fluctuations of the wind due to the system inertia and the availability of strategies to start and to stop according to the wind pattern [6]. The computation of the WT rotor power coefficient by aerodynamic methods requires a large amount of data, involving the geometry of the blade. In this study, an analytical relation that was fitted to experimental data was used. The Weibull distribution used to model the wind was assumed to change only with the hub height H_g of the WT in this thesis [1], [6]. To this end, Weibull parameters were extrapolated to follow the height H_g variation during the evaluation of the decision support model.

3.2 Wind Turbine Technology Generation Modeling

In this thesis, the wind turbine (WT) technology model is assumed to be composed of three main components: rotor, gearbox, and generator. The Annual Energy Produced $AEP_{t,g}^{l}$ by a WT technology ‘g’ in a selected location ‘l’ (l=1…M) is given by the following formula [1], [3], [6], [56]:

$$AEP_{t,g}^{l}(kWh/year) = \frac{8760}{1000}\,\frac{\rho}{2} A_g \sum_{i=1}^{N} v_i^3\; f_{i,h}^{l}\; C_{p,i,g} \tag{3.1}$$

Where, ρ (kg/m3) is the air density, A_g(m^2) is the surface swept by the rotor of WT technology 'g', $\mathcal{N}$ is the number of wind speed samples, v_i is the wind speeds of the ith class, $f_{i,h}^{l}$ is the discretized Weibull function with WT tower height for the selected site 'l', and $C_{p,i,g}$ is the total efficiency of the WT.

$C_{p,i,g}$, depends on the efficiency of the mentioned WT components given as follows:

$$C_{p,i,g} \;=\; C_{pr,i,g}\;\mu_{gear,i,g}\;\mu_{gen,i,g} \tag{3.2}$$

Where, $C_{pr,i,g}$ is the rotor power coefficient, $\mu_{gear,i,g}$ is the gearbox efficiency, and $\mu_{gen,i,g}$ is the generator efficiency. The details of these parameters are given in the following subsections.

3.2.1 Rotor Power Coefficient

Wind contains power P_i, which depends on its kinetic energy $E_{c,i}$. Wind power P_i is a derivative of the wind kinetic energy $E_{c,i}$. The rotor of wind turbine technology 'g' can capture the available wind power in a location 'l' converting it to mechanical energy form. However, the rotor of a wind turbine cannot exploit all the available wind potential. Therefore, P_i is a theoretical power limited by the rotor power coefficient $C_{p,r,i}$. The WT rotor power coefficient and its captured power $P_{r,i,g}$ are given by the following equations [3], [6]:

$$P_i = \frac{dE_{c,i}}{dt} = \frac{1}{2}\dot{m}\; {v_i}^2 \tag{3.3}$$

$$\dot{m} = \rho\; A_g\; v_i \tag{3.4}$$

$$P_i = \frac{1}{2}\rho\; A_g {v_i}^3 \tag{3.5}$$

$$P_{r,i,g} = \frac{1}{2}\rho\; C_{pr,i,g} A_g\; v_i^3 \tag{3.6}$$

$$A_g = \frac{\pi\; D_g^2}{4} \tag{3.7}$$

$$C_{pr,i,g} = C_{pr,g,max}\; exp\left[-\frac{(ln\, v_i - ln\, v_{op,g})^2}{2(ln\, \chi)^2}\right] \tag{3.8}$$

$$v_{op,g} = \frac{v_{n,g}}{exp[3(ln\,\chi)^2]} \tag{3.9}$$

Where, $\dot{m}$ is the mass flow of air (kg/s), D_g is the rotor diameter (m), $C_{pr,g,max}$ is the rotor maximum power coefficient, $v_{op,g}$ is the optimal wind speed, χ is the operating range parameter of the wind speed, and $v_{n,g}$ is the nominal wind speed of wind turbine technology.

The maximum rotor power coefficient $C_{pr,g,max}$ is derived using Betz's law. This law determines that a WT will never be able to convert more than 59.3 % of the kinetic energy contained in the wind into mechanical energy [70] [6]. Thus, $C_{pr,g,max}$ is given by the following expression [1], [6]:

$$C_{pr,g,max} = 0.593\left[\frac{\lambda_{max,g}(NB_g)^{0.67}}{1.48+((NB_g)^{0.67}-0.04)\lambda_{max,g}+0.0025(\lambda_{max,g})^2} - \frac{1.92(\lambda_{max})^2\,NB_g}{1+2\lambda_{max,g}\,N_{Bg}} \cdot \frac{C_d}{C_l}\right] \tag{3.10}$$

$$\lambda_{max,g} = \frac{\omega_g\,D_g}{2v_{op,g}} \tag{3.11}$$

$$\omega_g = \frac{2\pi N_{rpm,g}}{60} \tag{3.12}$$

Where, NB_g is the number of WT blades, $\lambda_{max,g}$ maximum speed rate, ω_g is the rotor angular rotation speed, $N_{rpm,g}$ is the rotor rotation speed (rpm), and c_d/c_l is the ratio between drag and lift coefficients related to their aerodynamic forces assumed to be a constant value in this study.

3.2.2 Gearbox Efficiency

As mentioned previously, gearbox is an essential unit in the WT used to increase the rotational speed of the rotor shaft and drive the generator to produce electrical energy. At this stage, the gearbox efficiency $\mu_{gear,i,g}$ is modeled for annual energy estimation as follows [1], [6]:

$$\mu_{gear,i,g} = 1 - \left[\left(1-\psi_{gear,g}\right)\left(\frac{P_{n,g}}{4P_{r,i,g}} + \frac{3}{4}\right)\right] \tag{3.13}$$

$$\psi_{gear,g} = 0.89(P_{n,g})^{0.012} \tag{3.14}$$

$$P_{n,g} = P_{op,g}\,.\,exp(4.5(ln\,\chi)^2) \tag{3.15}$$

$$P_{op,g} = \frac{1}{2}\rho C_{pr,g,max}\, A_g (v_{op,g})^3 \tag{3.16}$$

Where, $P_{n,g}$ is the WT nominal power, $\psi_{gear,g}$ is the efficiency factor of the gearbox, and $P_{op,g}$ is the optimal power corresponding to $C_{pr,g,max}$ for the optimal wind speed $v_{op,g}$.

3.2.3 Generator Efficiency

The WT generator efficiency is computed as follows [1], [6]:

$$\mu_{gen,i,g} = 1 - \left[\left(1 - \psi_{gen,g}\right)\left(5\left(\frac{P_{gear,i,g}}{P_{n,gen,g}}\right)^2 + 1\right)\left(\frac{P_{n,gen,g}}{6P_{gear,i,g}}\right)\right] \tag{3.17}$$

$$\psi_{gen,g} = 0.87(P_{n,g})^{0.014} \tag{3.18}$$

$$P_{n,gen,g} = P_{n,g}\psi_{gen,g}\psi_{gear,g}\, F_{s,g} \tag{3.19}$$

$$P_{gear,i,g} = \mu_{gear,i,g}\, P_{r,i,g} \tag{3.20}$$

Where, $\psi_{gen,g}$ is the generator efficiency factor, $P_{n,gen,g}$ nominal power of the generator [56], $P_{gear,i,g}$ generated power by the gearbox, and $F_{s,g}$ is the factor of service of the gearbox named also working coefficient takes values depending on the WT regulation type: stall-constant-speed (SCS); pitch-constant-speed (PCS) or pitch-variable-speed (PVS) [56].

$$F_s = \begin{cases} 1.75\ if\ PCS \\ 1.25\ if\ PVS \\ 2\ if\ SCS \end{cases} \tag{3.21}$$

Discounting the losses 'α' that occur during energy generation, the real annual energy generated by the WT becomes [1]:

$$AEP^l_{t,g,real} = AEP^l_{t,g} - \alpha\, AEP^l_{t,g} \tag{3.22}$$

3.3 Wind Turbine Economic Analysis Modeling

3.3.1 Net Present Value Model

Net Present Value (*NPV*) is a sophisticated economic indicator used to evaluate the profitability of an investment associated with a given project over its lifetime, considering

all future cash flows in and out of the project at a given discount rate [6]. An *NPV* greater than or equal to one indicates that the project is profitable, and vice versa, which supports investors' decision making to invest in the wind energy field. We provide a *NPV* equation developed from [3] and [71], expressed as follows [1], [6]:

$$NPV_g^l = \sum_{t=1}^{n} \frac{C_{benif,t,g}^{Net,l}}{(1+r)^t} - I_{t=0,g}^l \tag{3.23}$$

$$C_{benif,t,g}^{Net,l} = C_{benif,t,g}^l - C_{OM,t}^l - T_{t,g}^l - D_{t,g}^l \tag{3.24}$$

Where, $I_{t,g}^l$ is the WT investment made in year t (\$),$C_{benif,t,g}^l$is the total economic benefits, $C_{OM,t}^l$ is the WT operation and maintenance cost in year t (\$), $D_{t,g}^l$ is the annual depreciation expense (\$), $T_{t,g}^l$, is Tax levy (\$), n is the WT lifetime, r is the Discount rate, and $C_{benif,t,g}^{Net,l}$ are the total net wind energy generation benefices (\$) removing all the expenses related to tax payment, the costs of operation and maintenance of WT, and the recovered investment ($D_{t,g}^l$).

3.3.1.1 Investment Model

The investment cost model $I_{t,g}^l$ of an optimized WT design technology 'g' at a location 'l' adopted in this thesis was a modified model of the National Renewable Energy Laboratory study [72], where the WT cost model ($C_{WT,g}^l$) was the result of our study, which is discussed and presented in the next chapter. $I_{t,g}^l$includes the following costs [1], [6]:

$$I_{t,g}^l = C_{T,g}^l + C_{AI,g}^l + C_{EI,g}^l + C_{EP,g}^l + C_{RCW,g}^l + C_{F,g}^l + C_{WT,g}^l \tag{3.25}$$

Where, $C_{T,g}^l$ is the WT Transportation cost, $C_{AI,g}^l$is the WT Assembly and Installation cost, $C_{EI,g}^l$ is the Electrical Interface cost, $C_{EP,g}^l$ is the Engineering and Permits cost, $C_{RCW,g}^l$ is the Roads and Civil Work cost, $C_{F,g}^l$ is the Foundation cost, and $C_{WT,g}^l$is the WT cost.

- The WT Transportation cost is expressed as follows:

$$C_{T,g}^l(\$) = P_{n,g} C_{TF,g}^l \tag{3.26}$$

$$C_{TF,g}^l(\$/\text{kW}) = (1.581 * 10^{-5})(P_{n,g})^2 - 0.0375\, P_{n,g} + 54.7 \tag{3.27}$$

Where, $C_{TF,g}^l$is the Transportation cost factor.

- The WT Assembly and Installation cost is expressed as follows:

$$C_{AI,g}^{l}(\$) = 1.965(H_g D_g)^{1.1736} \quad (3.28)$$

- The WT Electrical Interface cost is expressed as follows:

$$C_{EI,g}^{l}(\$) = P_{n,g} C_{EIF,g}^{l} \quad (3.29)$$

$$C_{EIF,g}^{l}(\$/kW) = (3.49 * 10^{-6})(P_{n,g})^2 - 0.0221\, P_{n,g} + 109.7 \quad (3.30)$$

Where, $C_{EIF,g}^{l}$is the Electrical Interface cost factor.

- The WT Engineering and Permits cost is expressed as follows:

$$C_{EP,g}^{l}(\$) = P_{n,g} C_{EPF,g}^{l} \quad (3.31)$$

$$C_{EPF,g}^{l}(\$/kW) = (9.94 * 10^{-4}) P_{n,g} + 20.31 \quad (3.32)$$

Where, $C_{EPF,g}^{l}$is the engineering and permits cost factor.

- The WT Roads and Civil Work cost is expressed as follows:

$$C_{RCW,g}^{l}(\$) = P_{n,g} C_{RCWF,g}^{l} \quad (3.33)$$

$$C_{RCWF,g}^{l}(\$/kW) = (2.17 * 10^{-6})(P_{n,g})^2 - 0.0145\, P_{n,g} + 69.54 \quad (3.34)$$

Where, $C_{RCWF,g}^{l}$is the roads and civil work cost factor.

- The WT Fondation cost is expressed as follows:

$$C_{F,g}^{l}(\$) = 303.24(H_g A_g)^{0.4037} \quad (3.35)$$

- The WT cost model is expressed as follows:

Note that the adopted WT cost model $C_{WT,g}^{l}$is the result of our study performed in [6], given by:

$$C_{WT,g}^{l}(\$) = C_{WTF,g}^{l} P_{n,g} \quad (3.36)$$

$$C_{WTF,g}^{l}(\$/kW) = 5002.5\ (P_{n,g})^{-0.189} \quad (3.37)$$

Where, $C_{WTF,g}^{l}$is the WT cost factor.

3.3.1.2 Total Wind Energy Generation Economic Benefits Model

The total wind energy generation benefits $C^{l}_{benif,t,g}$per year t are measured using two different income parameters [1], [3], [6]: $C^{benif,l}_{Sal,t,g}$ and $C^{benif,l}_{Inc,t,g}$, which are the income from electrical energy sales and incentives for green energy production, respectively. Defined as follows:

$$C^{l}_{benif,t,g}(\$) = C^{benif,l}_{Sal,t,g} + C^{benif,l}_{Inc,t,g} \tag{3.38}$$

$$C^{benif,l}_{Sal,t,g}(\$) = C_S \, AEP^{l}_{t,g,real} \tag{3.39}$$

$$C^{benif,l}_{Inc,t,g}(\$) = C_{In} \, AEP^{l}_{t,g,real} \tag{3.40}$$

Where, $C_S(\$/\text{kWh})$ is the purchase tariff of electricity, and $C_{In}(\$/\text{kWh})$ are sales cost due to incentives for green energy production.

3.3.1.3 Wind Turbine Operation and Maintenance Cost Model

The operation-maintenance cost $C^{l}_{OM,t}$ is an important factor that require automated fault detection systems in WTs [73]. The $C^{l}_{OM,t}$ of the WT made in year *t* is estimated as a percentage of the investment cost and the benefits from annual energy production sales $C^{benif,l}_{Sal,t,g}$ following this expression [3] [1], [6]:

$$C^{l}_{OM,t}(\$) = \eta \, I^{l}_{t,g} + \xi \, C^{benif,l}_{Sal,t,g} \tag{3.41}$$

Where, η and ξ are the investment and sales income factors, respectively.

3.3.1.4 Depreciation Model

Depreciation is a method used to estimate the real value of the investment $I^{l}_{t,g}$ at the end of wind turbine lifetime 'n' [71]. In this thesis, the real value was cited at zero to completely recover the $I^{l}_{t,g}$over WT lifetime. The depreciation model is as follows [1], [6]:

$$D^{l}_{t,g}(\$/\text{year}) = \frac{I^{l}_{t=0,g}}{n} \tag{3.42}$$

3.3.1.5 Tax Model

The economic benefits registered from wind electricity sales are associated with tax payment [71]. In this study, the tax system applied in the country of the evaluated sites is the Value-Added-Tax [6]. It is applicable when a service is performed, goods are delivered, or in case of the imports. The applicable tax rate was cited as 14% and was applied to electrical energy [74]. The taxes can be estimated using the following expression:

$$T_{t,g}^{l}(\$) = 0.14(C_{benif,t,g}^{l} - C_{OM,t}^{l}) \tag{3.43}$$

3.3.2 Levelized Cost of Energy Model

The Levelized Cost of Energy (*LCOE)* can be defined as the present value of the price of the produced electrical energy, considering the economic life of the plant, typically 20 years for wind generators, and the costs incurred in the construction, and operation-maintenance [71]. After an in-depth study of the *LCOE*, we obtained the following equation [71] [75]:

$$LCOE_{g}^{l}(\$/kWh) = \frac{\sum_{t=0}^{n} \frac{(I_{t,g}^{l} + C_{OM,t}^{l} - PTC_{t} - D_{t,g}^{l} + T_{t,g}^{l})}{(1+r)^{t}}}{\sum_{t=1}^{n} AEP_{t,g,real}^{l}} \tag{3.44}$$

Where, $I_{t,g}^{l}$ present the Investment made in year t (\$), $C_{OM,t}^{l}$ is Operation and Maintenance costs in year t (\$), PTC_t is the Production Tax Credit (\$), $D_{t,g}^{l}$is the annual depreciation expense (\$), $T_{t,g,}^{l}$ is Tax levy (\$), $AEP_{t,g,real}^{l}$is the Real Electrical generation in year t (kWh), *n* is the WT lifetime and *r* is the Discount rate.

Wind energy production gradually decreases over its lifetime, perhaps because of falling availability, aerodynamic performance, or conversion efficiency. WTs were found to lose 1.6 $\pm$0.2 % of their output per year, increasing the levelized cost of electricity by 9 % [76]. PTC_t is a tax incentive adopted by several countries to support wind investment [77]. PTC_t provides wind investor with annual tax credit based on the amount of electricity produced (kWh) [77]. Based on this and adapting the previous formula to the economic procedure applied in the country of the evaluated sites, the PTC_t was not available, so the *LCOE* equation becomes [74]:

$$LCOE_g^l = \frac{\sum_{t=0}^{n} \frac{(I_{t,g}^l + C_{OM,t}^l - D_{t,g}^l + T_{t,g}^l)}{(1+r)^t}}{\sum_{t=1}^{n} (AEP_{t-1,g,real}^l - 0.016\, AEP_{t-1,g,real}^l)} \quad (3.45)$$

3.4 Wind Turbine Design Techno-economic Optimization Problem

Optimization problems are important, particularly in engineering design and decision-making, which consists of determining a feasible solution that corresponds to the extreme value of an objective function [78], [6]. A techno-economic optimization problem was developed and presented in this thesis. The objective of this optimization problem is to maximize the economic benefits of WT-generated energy, using the NPV_g^l indicator to determine the optimal technical design parameters of future WT technologies based on the available wind potential at a selected site and the radial distribution network characteristics. To this end, two different optimization scenarios were assessed. Three essential WT technical design parameters were determined through the resolution of the optimization problem: rotor diameter D_g, tower height H_g, and rated power $P_{n,g}$ of the machinery. Our optimization study used Weibull distribution parameters that describe wind speeds updated with the resulting tower height, H_g. Optimization problems are generally based on three components: design variables, constraints, and an objective function, which are described in detail in the following subsections.

3.4.1 Objective Function

The objective function is an optimized element that is either maximized or minimized [21]. As mentioned previously, the optimized function in this thesis is the NPV_g^l maximization of all economic incomes from WT energy output. The NPV_g^l model presented previously is used.

$$Max\left(NPV_g^l\right) = Max\left\{\sum_{t=1}^{n} \frac{C_{benif,t,g}^{Net,l}}{(1+r)^t} - I_{t=0,g}^l\right\} \quad (3.46)$$

The technical parameters of the WT were determined based on the wind potential in the first optimization scenario, and then in the second optimization scenario, the WT parameters were determined based on the wind potential and connected grid characteristics.

The studied objective function was maximized using different design variables and constraints in both scenarios.

3.4.2 Scenario 1 Design Variables and Constraints

In this scenario, the design variables and constraints used in the optimization are as follows [6]:

3.4.2.1 Design Variables

Present the variable input parameters of the optimization problem, adjusted sometimes within lower and upper limits in order to achieve the optimum solution [23] [21]. In this scenario, the selected design variables were: tower height H_g and rotor diameter D_g, because of their direct influence on the energy production, the studied objective function NPV_g^l, and on the energy cost $LCOE_g^l$ [6]. The developed optimization model requires other input parameters, such as the operating range of the wind speed *(χ),* nominal wind speed of the wind technology ($v_{n,g}$), and rotor rotational speed ($N_{rpm,g}$). To this end, an analysis of the technical characteristics of 23 existing technologies in the market was carried out [14]. Based on this analysis, an average value was adopted for these parameters mainly, $N_{rpm,g}$=18.15 rpm and v_n=13.2 m/s. However, χ was selected based on a previous study [79].

3.4.2.2 Constraints

Constraints are all restrictions to which the optimization should be subject [23], [21]. During the optimization of the WT design in this thesis, all the developed decision support model equations presented before including the WT generation models were considered as constraints. Two other constraints are defined in this scenario [80].

- One geometrical constraint, represented in the ground clearance between the blade tip and ground, where a safety clearance of 15 m should be respected (equation 3.47). This is performed through WT scale parameters, mainly D_g and H_g, which have a powerful influence on techno-economic optimization of WTs.

$$\frac{D_g}{2} + 15 \leq H_g \tag{3.47}$$

- The second constraint was the restriction of maximum output power for a WT technology ‘g’; view its direct impact on the WT cost [6].

$$P_{n,g} \leq M \tag{3.48}$$

Where, M is the maximum power value allowed for the WT technology.

- In addition, the lower- and upper-bound limits of the design variables constitute a simple form of constraint [21]. From the analysis previously mentioned in the design variables subsection of this scenario [14], the most commonly installed power capacity was in the range of 2 MW. Therefore, in the next calculations for this optimization scenario, the M power value and rotor diameter limits are as follows:

$$1\ MW \leq M \leq 2.5\ MW \tag{3.49}$$

$$40\ m \leq D_g \leq 130\ m \tag{3.50}$$

3.4.3 Scenario 2 Design Variables and Constraints

Radial distribution network design variables and constraints were considered in this second optimization scenario, while defining the optimal wind turbine design parameters at a specific site with a specific wind potential [1].

3.4.3.1 Design Variables

Similar to the previous optimization scenario, the WT geometrical parameters, mainly $D_g$and H_g, were cited as design variables in this second scenario. In addition to one design variable of the connected RDN, principally the voltage magnitude V_j at different bus nodes j=1,..,J [1]. Moreover, there are other RDN input parameters required in the optimization problem, such as the real and imaginary parts of the admittance matrix G_{lj} and B_{lj} of the jth row and lth column, and the voltage angle δ_j at different bus nodes j. G_{lj} and B_{lj} are related to the resistance and reactance of grid electrical lines, respectively.

3.4.3.2 Constraints

Two types of constraints were employed in this scenario [1].

- The first constraint type was similar to the previous optimization scenario related to the geometrical design variables of the WT (D_g and H_g). In this second scenario, the WT-rated power $P_{n,g}$ is not restricted, as in scenario 1, to find the best WT design parameters according to the existing potential and RDN constraints. Therefore, we performed another study on the available onshore WT technologies in the market regarding their power capacities and their corresponding diameters to define new WT geometrical parameters-bound limits. This study gathered more large-scale power, where the WTs power capacity studied was between 50 kW and 6000 kW [14]. Results of this study are illustrated in the last chapter of this thesis. The new rotor diameter D_g variation limits determined, and the possible associated tower height, H_g, are estimated as follows [1]:

$$40\ m \leq D_g \leq 200\ m \tag{3.51}$$

$$\frac{D_g}{2} + 15 \leq H_g \tag{3.52}$$

- The second constraint type is related to the RDN electrical characteristics modeled through the power flow equation (3.53), used in our techno-economic decision-support model to optimally design WTs connected to the RDN. According to this expression, the active power flow generated by the WT was controlled while feeding the load [48], [81].

$$P_{WT,g}^{l} - P_{Load}^{l} - P_{Loss}^{l} = 0 \tag{3.53}$$

$$\text{Where: } P_{WT,g}^{l} = P_{n,g} \tag{3.54}$$

$$P_{Loss}^{l} = V_l \sum_{j=1}^{J} V_j \left[G_{lj} \cos\left(\delta_l - \delta_j\right) + B_{lj} \sin\left(\delta_l - \delta_j\right) \right] \tag{3.55}$$

Where, $P_{WT,g}^{l}$ is the WT generated active power, P_{Load}^{l} is the load active power, P_{Loss}^{l} is the power flow or lost from bus node *l* of the RDN [81], V_l and V_j are the voltage magnitudes at buses *l* and *j*, respectively, G_{lj} and B_{lj} are the real and imaginary parts of the admittance matrix of the jth row and lth column, respectively, δ_l and δ_j are the voltage angles at buses *l* and *j*, respectively, and *J* is the number of buses.

- In addition, the voltage magnitude in the RDN is cited to vary within 5% of the initial value in all the RDN bus nodes, presenting another form of RDN electrical constraint.

$$V_l/V_j(p.u) = 1 \pm 0.05 \tag{3.56}$$

Therefore, our techno-economic decision support model maintains the stability of the power system voltage by controlling the voltage variation at the point of common connection while searching for the best design for the WT technology at this connection point or bus node of the RDN. Thus, one of the most important wind energy grid connection challenges was addressed in this thesis.

3.5 Conclusion

The techno-economic decision support model proposed for the optimal design of future wind turbines is presented in this chapter. This model was based on a techno-economic optimization problem resolution to provide adequate technical parameters for the WTs; based on the available wind potential through the Weibull distribution and the electrical characteristics of the radial distribution network that can make such a project economically profitable. To this end, the optimized objective function in the optimization problem evaluated was the net present value (NPV) of the generated wind energy benefit maximization. The levelized cost of energy (LCOE) is another important parameter in the economic assessment of wind projects. Thus, it was analyzed in parallel with our decision support model for the determined WT designs. To ensure the effectiveness of the proposed techno-economic decision support model in providing good WT designs, the model is validated and verified in the next chapter.

Chapter 4 Decision Support Model for Optimal Design of Wind Technologies Based Techno–Economic Approach

4.1 Introduction

In this chapter, the results of the proposed techno-economic decision support model applied to the first optimization scenario case study mentioned in the previous chapter are presented and analyzed. In this scenario, the decision support model determines the optimal design parameters of wind turbine (WT) technology based on the available wind potential at a selected site. Optimization in this scenario was subject to the Net Present Value (NPV_g^l) maximization of the net incomes from wind energy generation, under the constraints on WT nominal power restriction and the maximum ratio permitted between the rotor diameter and tower height [6]. The effectiveness of the proposed techno-economic decision support model in determining future optimal WT design parameters based on the available wind potential for a specific site was first validated through comparison with a previously existing model. It was then verified by selecting three different Moroccan wind sites: Dakhla, Casablanca, and Tanger. The optimal WT design selection considers: the nominal power $P_{n,g}$, rotor diameter D_g, and tower hub height H_g, which led to the maximum NPV_g^l in each site. In addition, a parallel analysis of the Levelized Cost of Energy production ($LCOE_g^l$) was performed.

4.2 Techno-economic Decision Support Model Validation

In this section, the performance of the proposed techno-economic decision support model for the optimal design determination of future WTs is validated in two steps [6]:

- The adopted decision support model is described in general through the NPV_g^l and $LCOE_g^l$ models. These economic models include all of the WT models cited previously because they are based mainly on the investment cost $I_{t,g}^l$ and the real energy produced $AEP_{t,g,real}^l$. Wind energy generally follows the mathematical model given in this study. However, the investment model $I_{t,g}^l$ has been defined differently in the literature. This allowed us to verify the performance of the proposed $I_{t,g}^l$ model in this thesis. $I_{t,g}^l$ model was validated using a previous model in the literature [3], which were tested for different values of rotor diameter. The validation test showed compatibility between the both models, conducting nearly to the same progression of the $I_{t,g}^l$, $LCOE_g^l$ and the NPV_g^l

function rotor diameter. The results are shown in **Figures 4. 1**, **4. 2**, and **4. 3** [6]. Therefore, we conclude that the developed techno-economic decision-support model is effective and works correctly.

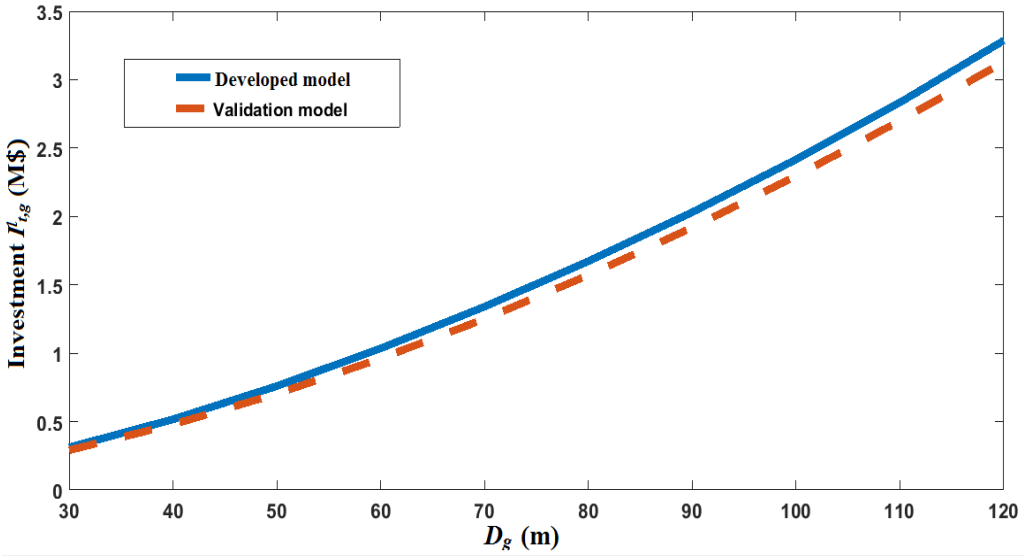

Figure 4. 1 Investment cost model validation [6]

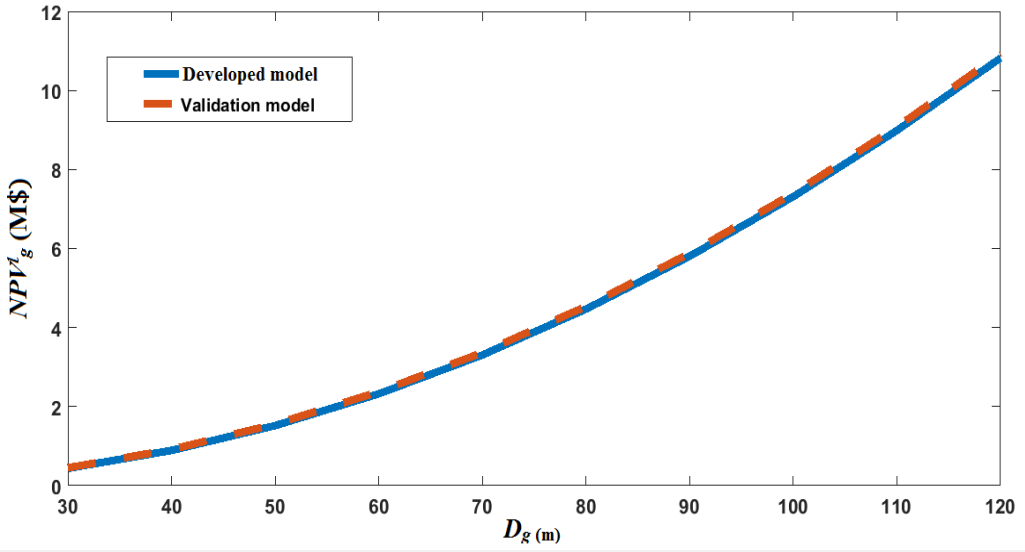

Figure 4. 2 NPV model validation [6]

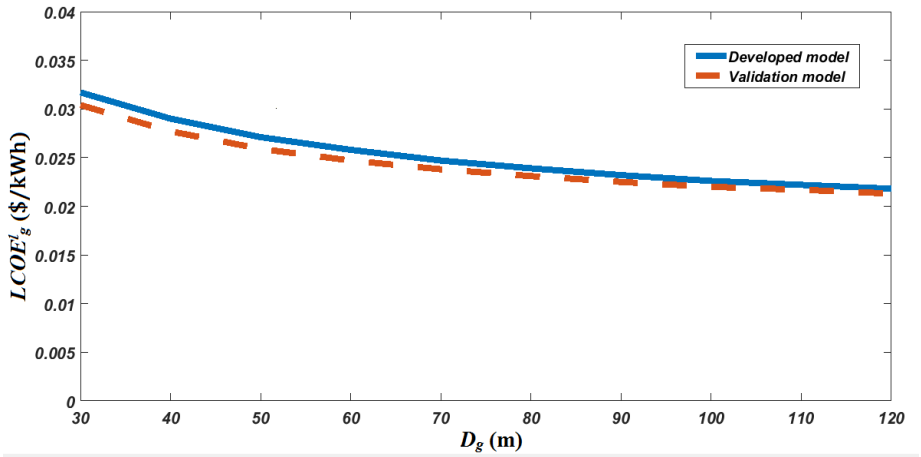

Figure 4. 3 LCOE model validation [6]

- In the second step, the constrained optimization problem presented in the previous chapter was resolved and validated using three widely used optimization algorithms in the optimization of WT design, to ensure the efficiency of the design results obtained in this thesis [6]. The algorithms employed were the Genetic algorithm (GA), Fmincon, and Particle Swarm Optimization (PSO). All the tested algorithms yielded the same WT design with nearly identical results for the optimized objective function (NPV_g^l), as shown in **Figure 4. 4**. Therefore, the presented techno-economic optimization problem can be resolved using one of these algorithms.

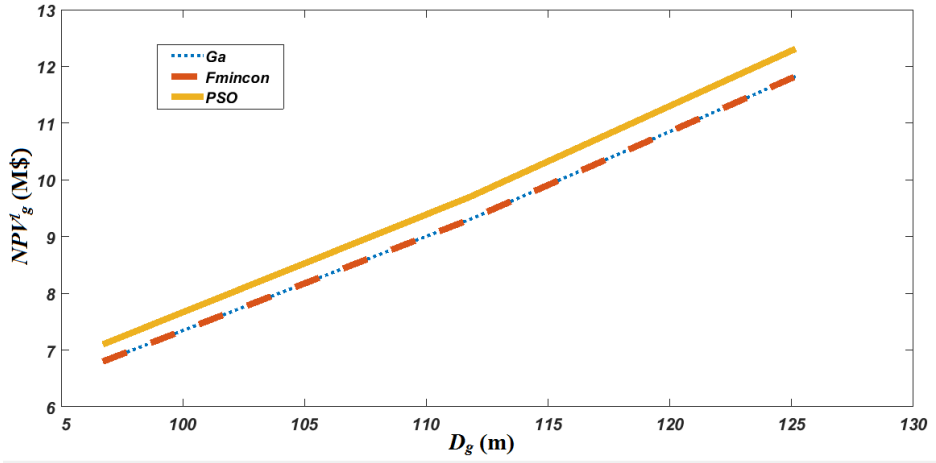

Figure 4. 4 Optimization problem validation [6]

In this study, a genetic algorithm was selected to resolve the techno-economic optimization problem described in the previous chapter.

4.3 Wind Turbine Investment Evaluation

As presented in the previous section, the investment cost model $I_{t,g}^{l}$ is validated, demonstrating its effectiveness and applicability in our study. This cost model is defined based on a developed WT cost model $C_{WT,g}^{l}$ and other cost parameters given in chapter three. In this section, the details of the resulting WT cost model $C_{WT,g}^{l}$ and an evaluation of the investment cost of wind projects are presented and discussed in the following subsections.

4.3.1 Wind Turbine Cost Assessment

The most expensive component of investment in wind projects is the cost of WT technology [6]**.** Thus, we performed a bibliographic study of this cost variation with power according to available data in the literature and the market. In this study, 48 WTs with different capacities were assembled from [71], [72], and [68], [82], [83], [84], [85], [86], [87], [88], [89], [90], [91]. Then, we fitted a curve by power regression combined with a model that estimates the cost of WT technology for any rated power in ($/kW) with an accepted determination coefficient R^2 = 0.59, as presented in **Figure 4. 5**.

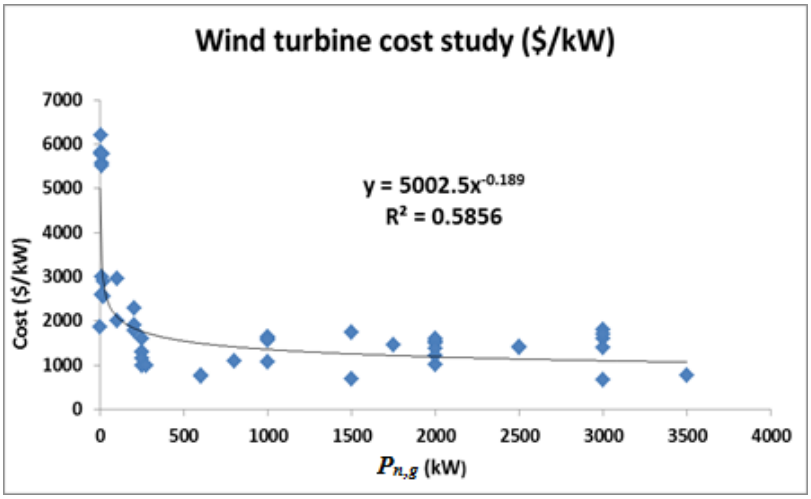

Figure 4. 5 Wind Turbine cost function nominal power [6]

We can observe that the greater the power capacity of the WT technology, the higher its cost becomes shipper [6]. From 2 MW to 3.5 MW of WT power with nearly a step of 250 kW intervals, a few decreases were observed in its associated cost. The resulting WT cost model is presented in the previous chapter as $C_{WTF,g}^{l}$ in the investment model subsection, using the following expression:

$$C_{WTF,g}^{l}(\$/kW) = 5002.5\ (P_{n,g})^{-0.189} \tag{4.1}$$

This generated model is required for investment cost evaluation and verification of the overall developed decision support model.

4.3.2 Investment Cost Study

Investment is the first cost determined before starting any kind of project and is an important sign in decision making [6]. As presented in the previous chapter, the investment cost $I_{t,g}^{l}$ of wind projects depends on several costs, such as transportation and WT costs. These cost parameters were modeled function WT design parameters researched by the decision support model of this thesis, specifically: rotor diameter (D_g), tower height (H_g), and WT nominal power ($P_{n,g}$). This permits the evaluation of their impact on the investment cost $I_{t,g}^{l}$, which has a direct influence on the optimized objective function NPV_g^l.

First, the developed WT cost model $C_{WTF,g}^{l}$was validated through an evaluation of the investment cost model $I_{t,g}^{l}$ using the design parameters of an optimized WT technology of 2 MW provided by the presented techno-economic decision support model [6]. The results prove that the WT technology cost has a large share in the total cost of investment, at 82% as shown in **Figure 4. 6**. However, the costs of transportation, assembly installation, electrical interface, engineering and permits, roads and civil work, and foundation are only 18%.

Second, this section provides the evaluation results of different investment cost parameters in response to variations in the WT design parameters, as presented in **Figures 4. 7** and **4. 8** [6]. The assembly and installation cost ($C_{AI,g}^{l}$) and foundation cost ($C_{F,g}^{l}$) are described as functions of rotor diameter and tower height. Considering that these two WT design

parameters are dependent, we studied the variation in the rotor diameter for the aforementioned costs. Linear and exponential trend lines were observed for the evolution of $C_{F,g}^{l}$ and $C_{AI,g}^{l}$, respectively (**Figure 4. 7**). At 100 m of diameter, the $C_{AI,g}^{l}$cost exceeds the $C_{F,g}^{l}$ cost, which can be explained by the fact that as the rotor diameter increases, the blade length increases, and the gearbox and generator units required are larger. Therefore, for a WT rotor diameter of 100 m, collecting and installing all these components is much more expensive than foundation construction.

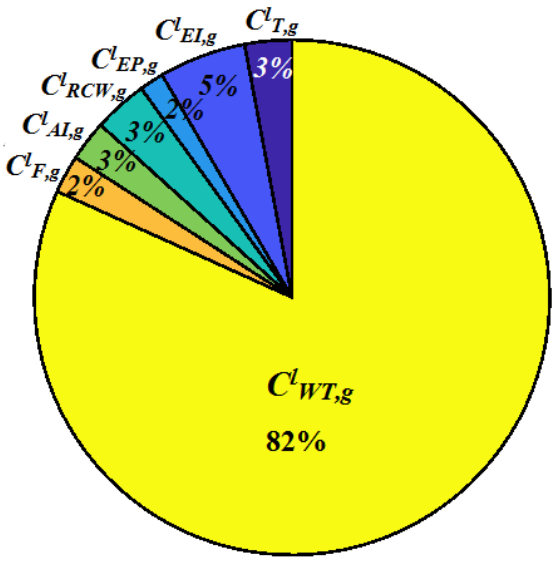

Figure 4. 6 Optimized wind turbine technology investment cost disk [6]

Figure 4. 8 shows the variation curve of the rest of the investment cost parameters that depend mainly on WT nominal power $P_{n,g}$: Roads and Civil Work ($C_{RCW,g}^{l}$), Transportation ($C_{T,g}^{l}$), Engineering, and Permits ($C_{EP,g}^{l}$), and Electrical Interface ($C_{EI,g}^{l}$) [6]. The material needed for electrical energy connection such as transformer and an important wiring, in addition to terrain and road preparation conducted to expensive cost components ($C_{EI,g}^{l}$and $C_{RCW,g}^{l}$) per kW installed, followed by transport cost ($C_{T,g}^{l}$) and the cost involved during engineering and obtaining the permission and certifications for installation ($C_{EP,g}^{l}$) costs [6]. From 2 MW of nearly WT power, $C_{T,g}^{l}$ passes above $C_{RCW,g}^{l}$cost, which can also be explained, as mentioned in the previous paragraph, by the largest transported material.

More precisely due to the long blades transported in this power range of the WT bringing on, high cost of transportation.

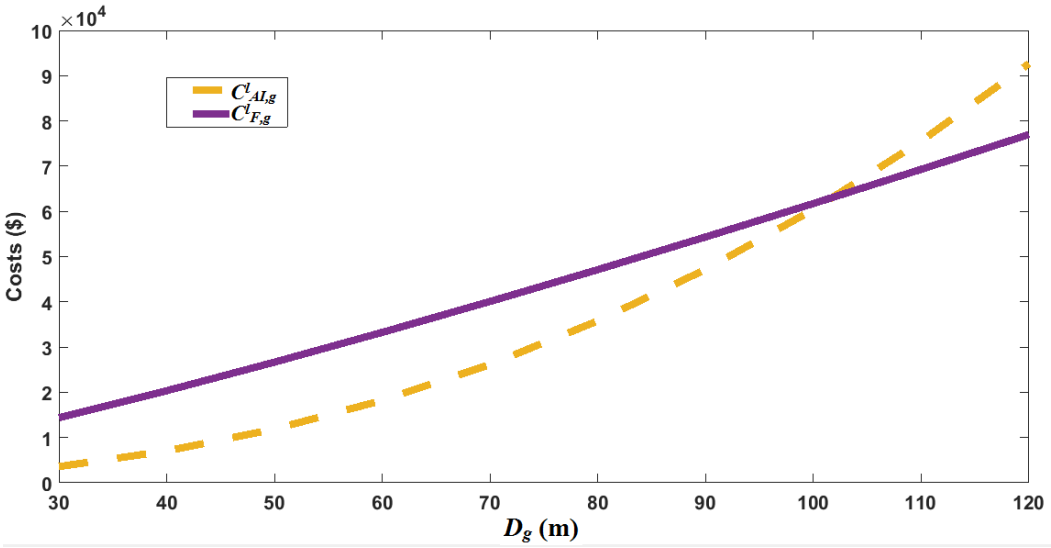

Figure 4. 7 Assembly-Installation costs and Foundations cost function rotor diameter variation [6]

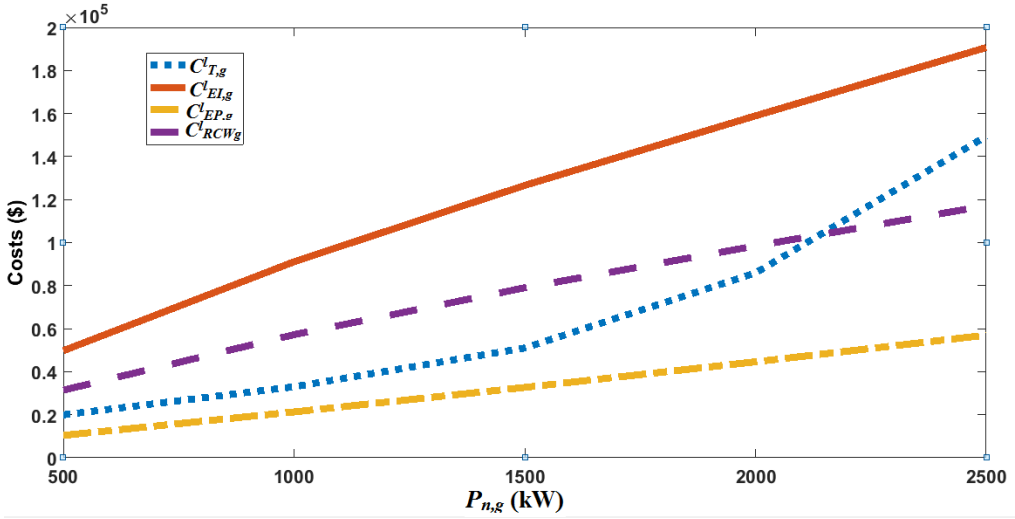

Figure 4. 8 Costs curve of Roads and Civil Work, Transportation, Engineering and Permits, and Electrical Interface function wind turbine nominal power variation [6]

4.4 Techno-economic Decision support Model Evaluation

As presented in the previous chapter, the developed techno-economic decision support model depends on the resolution of the optimization problem. This later consists of maximizing an objective function mainly; the net present value of wind energy economic

benefits $Max\left(NPV_g^l\right)$ to determine the optimal design parameters of the WT based on available wind potential and mentioned constraints in the first optimization scenario. The wind potential was described using the Weibull distribution function. This section presents the Weibull parameters of the tested sites, input parameters and constraints used in the evaluation of the techno-economic optimization problem, optimization algorithm details, and obtained WT design parameters.

4.4.1 Weibull parameters definition

As mentioned previously, the Weibull distribution function was selected for the description of wind speed distribution in this thesis. Thus, the associated Weibull parameters, mainly the shape k^l and scale C^l parameters, were calculated for the selected sites using the standard deviation, graphical, Lysen, and Moroccan methods defined in chapter 2. For the Dakhla site, annual wind distribution data measured at 10 m of height was used for this evaluation [92]. **Table 4. 1** lists the obtained Weibull parameters.

Table 4. 1 Dakhla Weibull parameters with Graphical, Standard Deviation, Moroccan, and Lysen methods

	k^l	C^l (m/s)	R	RMSE
Graphical	1.97	10.02	1	0.015
Standard Deviation	2.38	10.58	1	0.011
Moroccan	2.91	10.51	1	0.013
Lysen	2.38	10.58	1	0.011

Standard Deviation and Lysen methods results were identical presenting the minimum error value for the root means square *'RMSE'* of 0.011 and the maximum determination coefficient '*R*' equal to 1. The wind data observed in Dakhla were correctly fitted using these methods, as shown in **Figure 4. 9**.

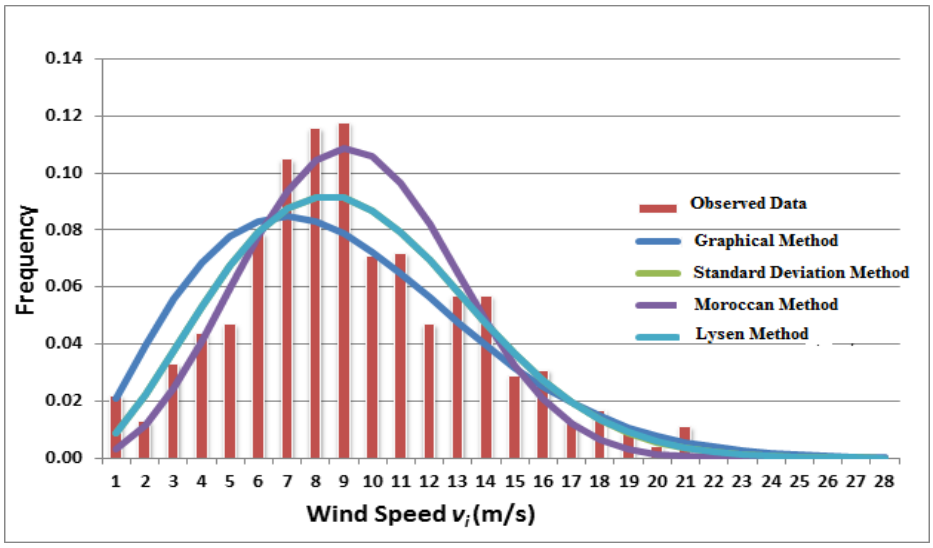

Figure 4. 9 Weibull distribution at Dakhla site measured at 10m of height

Moreover, the Standard Deviation method was demonstrated to be the best method for fitting wind speed potential in Tanger and Casablanca [56]. Therefore, the Weibull parameters obtained using this method were adopted for the subsequent numerical applications of this study.

Table 4. 2 Weibull Parameters and Average Wind Speed of The Sites Selected at 10 m [6]

Site l	k^l	C^l (m/s)	$v_{average}$ (m/s)
Casablanca	1.42	3.8	3.45
Tanger	1.62	6.012	5.38
Dakhla	2.38	10.58	9.38

In this thesis, the wind density was assumed to change only with the hub height of the WT tower H_g [6]. Therefore, this change was computed by extrapolating the Weibull parameters presented in **Table 4. 2**, measured at 10 m at the new tower heights calculated by the presented decision support model. This extrapolation was performed using the mathematical expressions presented in chapter 2. According to the average wind speed

($v_{average}$), Casablanca, Tanger, and Dakhla are characterized by low, medium, and high wind speed potentials, respectively.

4.4.2 Optimization Problem Input Parameters

In one hand, the techno-economic decision support model had considered for the evaluation of WT generated energy, the obtained Weibull parameters (k^l and C^l) in Dakhla, Casablanca, and Tanger, and all the inputs cited before principally: blades number $NB_g = 3$, the operating range of the wind speed χ=1.7, WT nominal wind speed $v_{n,g} = 13.2\ \mathrm{m/s}$, rotor rotational speed $N_{rpm,g}$=18.15 rpm, drag and left ratio C_d/C_l=1/120, air density ρ=1.225 kg/m3, and WT energy generation losses percentage α=5% [6].

On the other hand, the decision support model had considered the following inputs for the evaluation of the presented economic parameters (NPV_g^l and $LCOE_g^l$) [6]: investment η =2% and sales income ξ =1% factors adopted for the operation and maintenance cost, Discount rate r=8%, WT life time n=20 years, annual depreciation expense of the investment $D^l_{t,g}$=5%, tax payment applied to wind energy economic benefits $T^l_{t,g}$=14%, the purchase tariff of electricity in Morocco C_s=0.094 $/kWh [93], and Sales cost due to incentives for green energy production C_{In}=0.053 $/kWh. C_{In} was estimated in accordance with the Law 13-09 of renewable energies, where the renewable energy operators can sell the electricity produced to The National Electricity Office (NEO) with a sale price named feed-in tariff negotiated within the framework of a sales contract between the operator and NEO. The feed-in tariff is expected to be approximately 60% of the NEO 's Moyne Voltage (MV) electricity sales tariff [74]. For peak hours, MV = 0.088 $/kWh [13]. With, Dirham-Dollard-Euro change on 17/07/2020 (1 $ = 0.88 € = 9.58 MAD).

4.4.3 Optimization Problem Constraints

At this stage, the constraints presented in the first optimization scenario of this thesis (see chapter 3) are employed mainly, geometrical, and rated power constraints [6]:

$$\frac{D_g}{2} + 15 \leq H_g \tag{4.2}$$

$$P_{n,g} \leq 1.5/2/2.5\ M \tag{4.3}$$

$$40\ m \leq D_g \leq 130\ m \tag{4.4}$$

4.4.4 Optimization Algorithm

As the techno-economic optimization problem of the developed decision support model was proved to be resolved using any of the previous mentioned optimization algorithms, the genetic algorithm was used in this study to solve the presented optimization problem and determining the optimal WT design parameters output that maximizes the optimized objective function NPV_g^l. As a first step, the characteristics of the wind sites described by the Weibull distribution parameters (k^l and C^l), in addition to all other inputs presented in the previous subsection (**4.4.2**) and the WT design variables (D_g and H_g) were specified for the optimized objective function model. This function was then evaluated under the constraints declared by the genetic algorithm, as shown in **Figure 4. 10** [1].

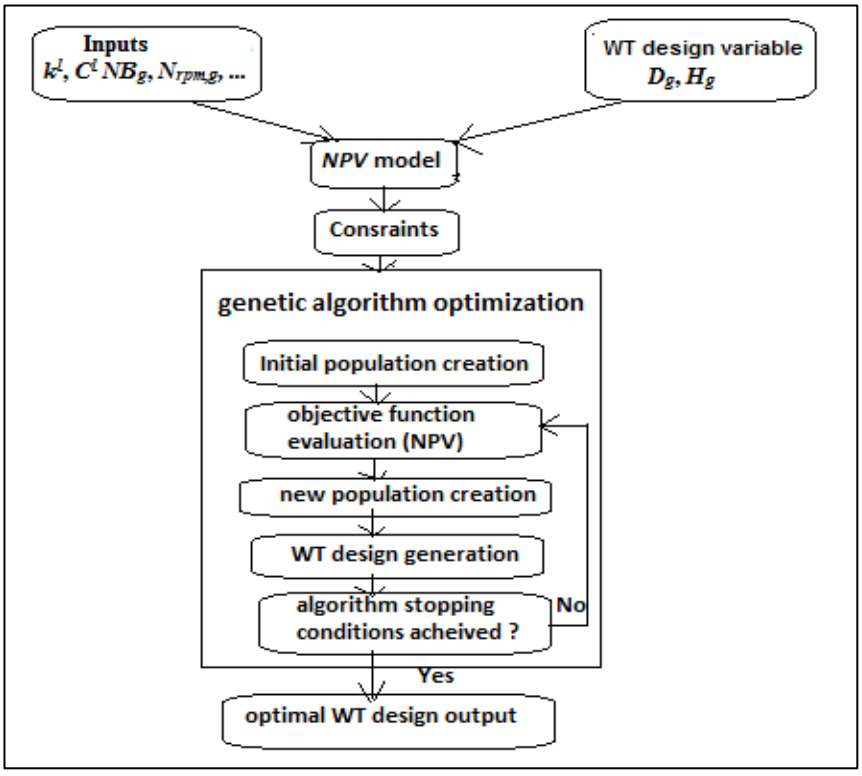

Figure 4. 10 Optimization process flowchart [1]

The genetic algorithm evaluates the NPV function using the following steps [1]:

- The algorithm begins by creating a random initial population containing several individuals.

- The objective function is evaluated for each individual of the population created.
- Create a new population based on the individual selection of the current population with the maximum objective function value (NPV). The selected individuals are called parents and are used by crossover or mutation operators of the genetic algorithm to produce children. Mutation involves making random changes to a single parent. However, the crossover operator combines the vector entries of a pair of parents. A new population was formed through the creation of children.
- WT design parameters is generated from the new population created

These steps are repeated to generate the best new population that provides the most feasible WT design solution with the maximum NPV value until one stopping criterion of the algorithm is reached, such as the maximum number of iterations or time limit [1]. The optimization process is illustrated in **Figure 4. 10**.

4.4.5 Optimal Wind Turbine Design Parameters Results

In this section, the results of the techno-economic optimization problem of the developed decision support model are presented, showing the optimal WT technology design parameters (H_g, D_g, and $P_{n,g}$) found at the studied sites [6]. According to the defined constraints in the first optimization scenario, and by limiting the upper limit of the rated power permitted at 1.5, 2, and 2.5 MW successively, three different WT technologies were identified as optimal solutions in Dakhla and Tanger. Linear propagation between the nominal power $P_{n,g}$ and the NPV_g^l was observed when the selected site had a medium and powerful wind profile. Therefore, the optimal WT design was found at the power constraint limits cited in Dakhla and Tanger, as presented in **Table 4. 3** [6].

The optimized WT design results in Dakhla and Tanger were acceptable presenting good NPV_g^l [6]. However, only one optimized WT design was provided in Casablanca despite the increase in the permitted power constraint, showing a negative value for the NPV_g^l. This can be explained by the low wind potential available in Casablanca, leading to its classification as a non-profitable site for a wind project.

Table 4. 3 Optimized Wind Turbine Technologies Design Parameters for the Selected Sites [6]

Site	constraints	Optimized WT technical parameters			Coresponding NPV_g^l (M$)
		$P_{n,g}$ (MW)	D_g (m)	H_g (m)	
Dakhla	$P_{n,g}$≤1.5MW	1.5	97	63	6.80
	$P_{n,g}$≤ 2MW	2	112	71	9.30
	$P_{n,g}$≤2.5MW	2.5	125	78	11.82
Casablanca	$P_{n,g}$≤1.5MW	0.256	40	35	-0.23
	$P_{n,g}$ ≤2MW	0.256	40	35	-0.23
	$P_{n,g}$ ≤2.5MW	0.256	40	35	-0.23
Tanger	$P_{n,g}$ ≤1.5MW	1.5	99	64	1.61
	$P_{n,g}$ ≤2MW	2	116	73	2.33
	$P_{n,g}$ ≤2.5MW	2.5	130	80	3.04

The maximization of the objective function NPV_g^l was found to be much affected by the enhancement of WT rotor diameter increasing respectively: the energy output ($AEP_{t,g,real}^l$), Tax payment ($T_{t,g}^l$), associated investment cost ($I_{t,g}^l$), depreciation amount ($D_{t,g}^l$), and operation and maintenance cost $C_{OM,t}^l$ [6]. The increase in the investment cost of optimized WT technologies in Dakhla and Tanger does not affect much the NPV_g^l results, because of the important yearly economic incomes ($C_{benif,t,g}^l$) estimated to be generated over the WT lifetime as presented in **Table 4. 4** [6]. That explains the obtained NPV_g^l results in these locations.

In addition, **Table 4. 4** demonstrates well, why the NPV_g^lcalculated was negative in Casablanca site, which can be related to the low yearly generated energy and economic incomes $C_{benif,t,g}^l$ registered in that site [6]. Furthermore, a few changes were observed in the investment cost of the proposed WT technologies with the same power capacity when changing the location between Dakhla and Tanger. As different investment cost $I_{t,g}^l$ parameters presented before depend either on the WT rotor diameter (D_g) and tower height (H_g) or on the WT nominal power ($P_{n,g}$), the cost parameters depending on power were the same in these locations because the power of the optimized WTs was closed, leading to near $I_{t,g}^l$. However, the cost parameters of the $I_{t,g}^l$ that vary with the diameter D_g and H_g mainly, foundation cost $C_{F,g}^l$ and assembly and installation cost $C_{AI,g}^l$ show more the effect of location on the $I_{t,g}^l$ generated. **Figures 4. 11** and **4. 12** present the results obtained, and it

is clear that every location has its own $C_{F,g}^{l}$and $C_{AI,g}^{l}$costs. For a 2.5 MW WTs power, which corresponds nearly to a rotor diameter of 110 m, $C_{AI,g}^{l}$ exceeds $C_{F,g}^{l}$, confirming our previous observation in the investment assessment section related to the size of the material used in this power range.

Table 4. 4 Economic Indicators Analysis of Optimized Wind Turbines [6]

Site	$P_{n,g}$ (MW)	$AEP_{t,g,real}^{l}$ (GWh/y)	$I_{t=0,g}^{l}$ (M$)	$C_{OM,t}^{l}$ (M$/y)	$C_{Sal,t,g}^{benif,l}$ (M$/y)	$C_{Inc,t,g}^{benif,l}$ (M$/y)	$C_{benif,t,g}^{l}$ (M$/y)	$T_{t,g}^{l}$ (M$/y)	$D_{t,g}^{l}$ (M$/y)
Dakhla	1.5	7.564	2.287	0.053	0.711	0.399	1.110	0.148	0.114
	2	10.211	2.910	0.068	0.960	0.539	1.499	0.200	0.145
	2.5	12.887	3.537	0.083	1.211	0.680	1.892	0.253	0.177
Casablanca	0.256	0.123	0.542	0.011	0.012	0.006	0.018	0.001	0.027
Tanger	1.5	2.869	2.291	0.049	0.270	0.151	0.421	0.052	0.115
	2	3.909	2.918	0.062	0.367	0.206	0.574	0.072	0.146
	2.5	4.917	3.517	0.075	0.462	0.260	0.722	0.091	0.176

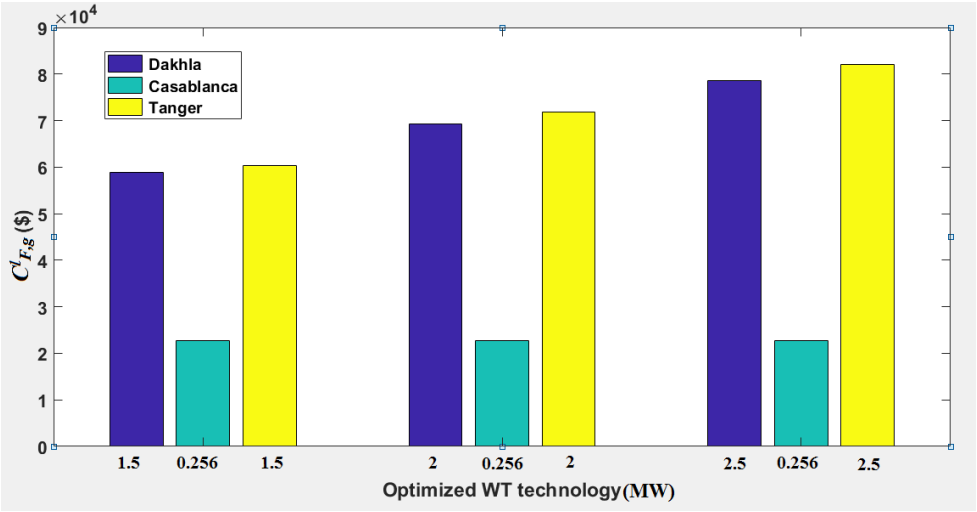

Figure 4. 11 Fondation cost ($) for the optimized wind turbiness in Dakhla, Casablanca and Tanger [6]

The levelized cost of the generated energy $(LCOE_{g}^{l})$ of each optimized WT at different sites is presented in **Table 4. 5** [6]. k_{Hg}^{l} and C_{Hg}^{l} are the extrapolated Weibull parameters in

accordance with the tower height (H_g) provided by the decision support model for the optimized WTs at each site [6]. More the design of WT technology is big, more the $LCOE_g^l$ of the energy produced decreases. In this study, rotor maximum power coefficient $C_{pr,g,max}$ and the $LCOE_g^l$ were found approximately constant because there is no widely difference between the power ranges provided for these optimized WT technologies in each site. This reinforces our study, presented in the WT cost assessment section, where the WT cost per kW installed was observed to be approximately constant in this power range.

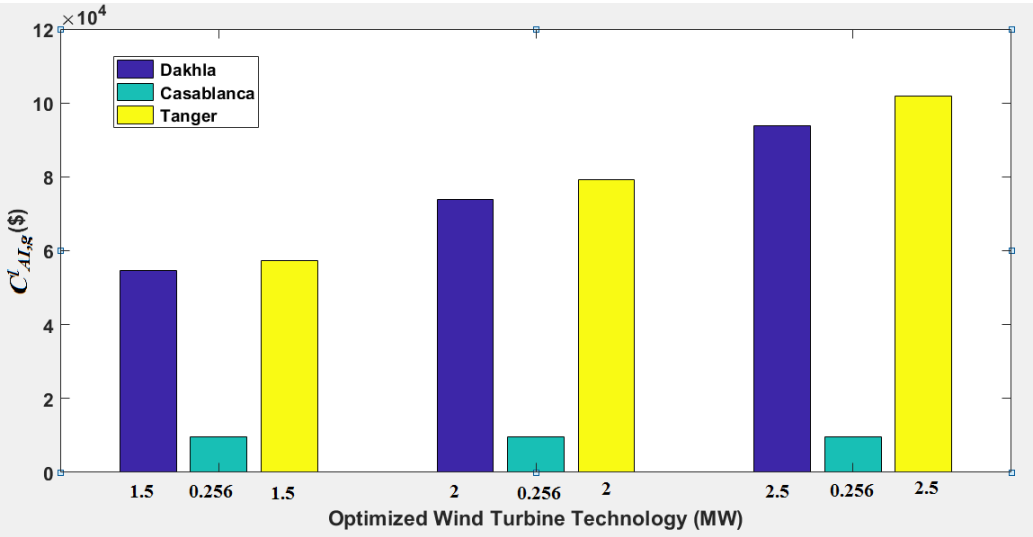

Figure 4. 12 Assembly and Installation cost ($) for the optimized wind turbiness in Dakhla, Casablanca and Tanger [6]

Table 4. 5 Rotor Maximum Power Coefficient, Generated Energy, and LCOE for the Optimized Technologies [6]

Site	$P_{n,g}$ (MW)	k^l_{Hg}	C^l_{Hg} (m/s)	$AEP^l_{t,g,real}$ (GWh/y)	$C_{pr,g,max}$	$LCOE^l_g$ ($/kWh)
Dakhla	1.5	2.534	11.832	7.564	0.512	0.023
	2	2.543	11.912	10.211	0.512	0.022
	2.5	2.552	11.978	12.887	0.510	0.022
Casablanca	0.256	1.481	4.276	0.123	0.511	0.185
Tanger	1.5	1.726	6.967	2.869	0.490	0.042
	2	1.733	7.034	3.909	0.479	0.040
	2.5	1.739	7.087	4.917	0.468	0.039

The cost of energy in Tanger was greather than Dakhla, because of the low energy generated and the design parameters required to respond to the same WT power was bigger leading to high foundation cost $C_{F,g,}^{l}$ assembly and installation cost $C_{AI,g}^{l}$, and more investment cost value $I_{t,g}^{l}$in Tanger as presented previously in **Figures 4. 11** and **4. 12**. That can be referred to the available wind potential in Tanger which is lower than Dakhla site, requiring more large scale WT design.

In the end, it appears that the design parameters of the third provided WT technology by the present techno-economic decision support model is the most suitable for the studied sites, mainly Dakhla and Tanger providing the best trade-off between NPV_{g}^{l}, $LCOE_{g}^{l}$ and the generated energy $AEP_{t,g,real}^{l}$ [6]. However, Casablanca was classified as non-profitable site for wind projects.

4.5 Conclusion

The developed techno-economic decision support model was validated and verified using the provided techno-economic optimization procedure of the first scenario, presented in the previous chapter and by selecting three different wind sites principally: Dakhla, Tanger, and Casablanca. Significant results were achieved, demonstrating the effectiveness of the proposed decision support model [6]. This model gives the adequate WT design parameters function the available wind potential in the selected site showing the profitability of a project with such design. Results showed that the optimal design of the WT is given by the limit power constraints cited, conducting to a maximum net present value NPV_g^l, more exploitation of available wind potential in Dakhla and Tanger, and presenting low cost of energy $LCOE_g^l$. However, Casablanca was found as no profitable site for wind projects presenting a negative NPV_g^l, because of the low wind potential available in that site. Moreover, the developed decision support model interact well with the variation of location, where a change was observed in the investment cost I_t. It shows that every location can have its own investment cost for the same installed power capacity, which can be related to different factors. These factors depend on the different investment cost parameters such as foundation $C_{F,g}^l$ and assembly and installation costs $C_{AI,g}^l$, which were found to vary with the location.

The provided decision support model acts as an aid for strength decision making in the wind sector, where the most suitable WT design information is provided for the site of interest presenting its economic profitability. In this chapter, the integration constraint of wind energy into the grid was not treated when determining the optimal design parameters of the WT, which constitutes the second objective of this thesis, presented in a second optimization scenario. Results are given in the next chapter.

Chapter 5 Optimal Wind Turbine Design Based Wind Potential and Radial Distribution Network Characteristics

5.1 Introduction

The electrical energy produced by wind turbines (WTs) is mostly destined to high electrical usages. Thus, WT operator has to transfer this energy to grid operators under regulations and conditions specified, because they are the main responsible for electrical energy production, transmission, and its management. In this chapter, our proposed techno-economic decision support model is evaluated using the second optimization scenario specifications presented in chapter three, which consider the grid capability in case of integration of the WT. Optimization in this scenario was also subject to the Net Present Value (NPV_g^l) maximization of the net incomes from wind energy generation. Unlike the study performed in the previous chapter, in this study, the techno-economic decision support model determines the optimal design parameters of future WT technologies not only based on available wind potential on a selected site but also it takes into account the electrical constraints of the connected radial distribution network (RDN) [1]. Furthermore, to deal with wind energy generation uncertainty challenge that impact grid stability, an Artificial Neural Network (ANN) was used in this study to effectively forecast the wind speed distribution for good estimation of the generated wind energy. The decision support model was evaluated using the wind potential of Essaouira Moroccan site and the electrical characteristics of two different RDNs mainly, IEEE 9 and IEEE 33 Bus nodes. Each RDN system is composed of several bus nodes with different power load and electrical requirements. Thus, our developed decision support model proposes a specific WT design for each evaluated bus node. Then, the optimal WT design selection considers: the nominal power $P_{n,g}$, rotor diameter D_g, and tower height H_g, which led to the maximum NPV_g^l in each bus node. That leads also to identify the best bus candidates for a WT project installation.

5.2 Weibull parameters determination

As the wind potential was described using the Weibull distribution function in the studies of this thesis [6], [1], the standard deviation method was also found in this case as best method to determine the Weibull parameters in Essaouira site [1]. It gives the best Weibull parameters (kl=2.56 and Cl=8.63 m/s) with an R and $RMSE$ equal to 1 and 0.01 respectively, that correctly describe the available measured wind speed on this site as

shown in **Figure 5. 1**. The wind distribution measured in 2015 at an initial height of H_0 = 50 m was used in this evaluation [92].

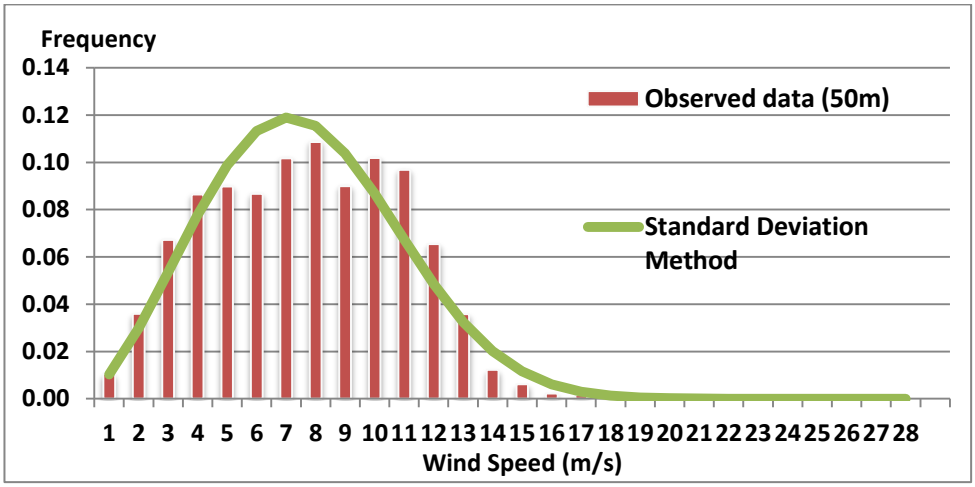

Figure 5. 1 Weibull Probability distribution at Essaouira

The standard deviation method is also used in the next section to determine the new Weibull parameters for the achieved ANN predicted wind speed data [1]. The Weibull parameters calculated using the measured and predicted data are having the same height of measurement H_0 = 50 m. Standard deviation formulas for k^l and C^l determination were given in chapter two**.**

5.3 Artificial Neural Network Wind Speed Forecasting

As presented previously in chapter two, the wind energy generation uncertainty challenge related to the variability of wind speed is addressed in this study to maintain the grid stability using the ANN artificial intelligence approach. The ANN can effectively predict future stochastic variables such as wind speed, based on previously entered data. This previous data is considered as target to reach by the ANN. ANN tends to reduce the error between the entered and predicted data [47]. In this study, Essaouira is the evaluated site for WTs installation and grid integration. Therefore, the hourly wind speed distribution in this site is forecasted by the ANN method for a time horizon of one year based on the previous wind speed data measured at an initial height of H_0 = 50 m [92]. As mentioned before, an ANN is composed of three layers: an input layer, hidden layer, and an output layer. Calendar data were the inputs used in this study including, season, month, week, day,

and hour and the anticipated output was the wind speed as illustrated in **Figure 5. 2**. The global entered data consisted of 8760 values [1]. Part of this data is used for training the ANN, and the rest is used to test the efficiency of the results involved before the ANN model performs the prediction [1].

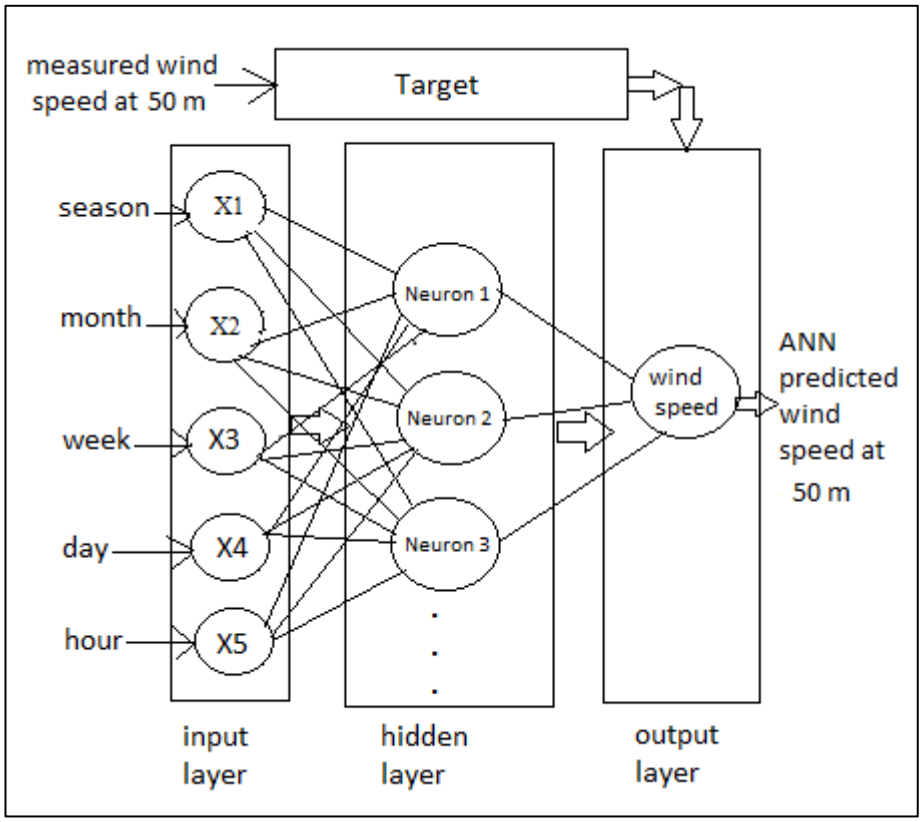

Figure 5. 2 Simplified ANN architecture [1]

The best prediction results were obtained with an ANN structure composed of three hidden layers and 22 neurons in each hidden layer, as shown in **Figure 5. 3** [1].

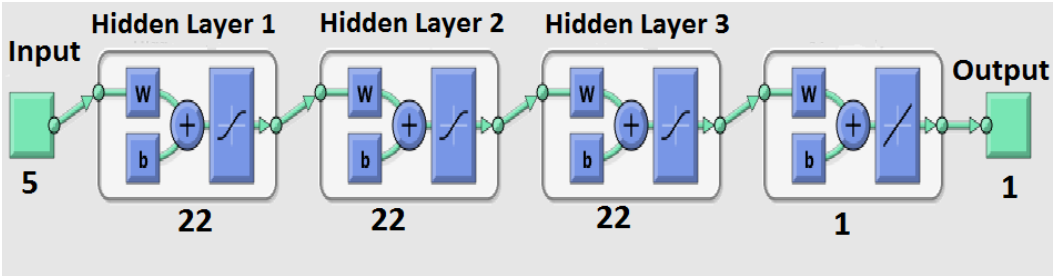

Figure 5. 3 Resulted ANN structure [1]

In addition to a resulted data partition in the learning phase of 80% in the training and 20% in the testing where the minimum errors were reached, with an R and MSE values of 0.97 and 0.57, respectively, as shown in **Figure 5. 4,** and **Figure 5. 5**.

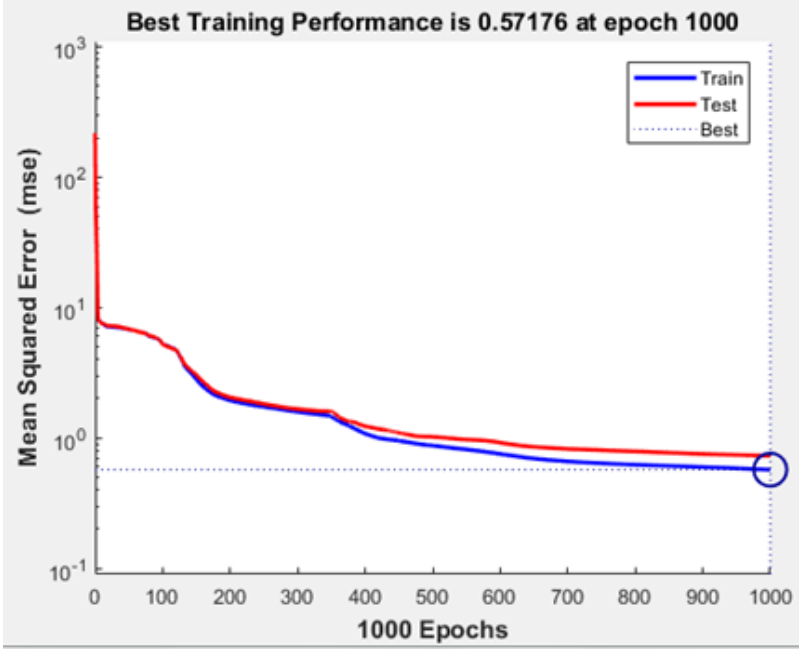

Figure 5. 4 MSE error results of the ANN model [1]

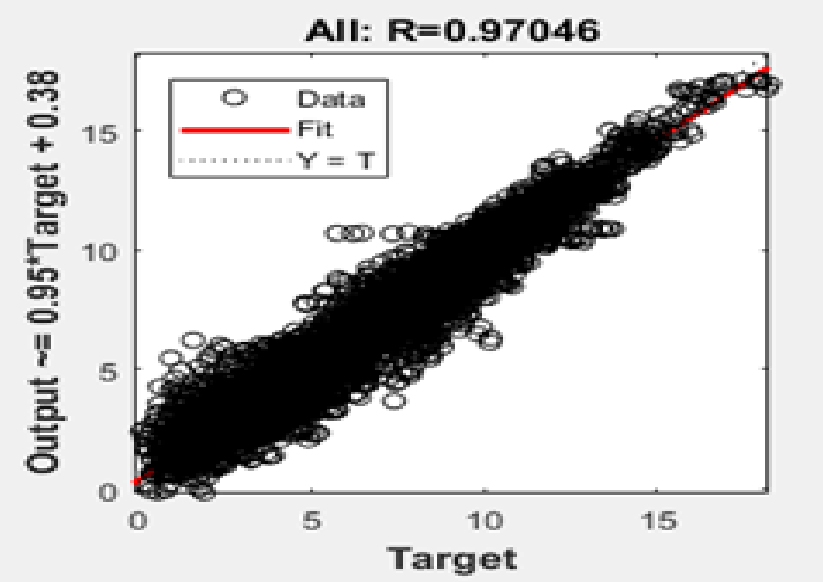

Figure 5. 5 Regression coefficient R error results of the ANN model [1]

The hourly wind speed data measured and predicted by the ANN model for the actual and future year, respectively, in Essaouira site is composed of 8760 wind speed values, as presented in **Figure 5. 6** [1].

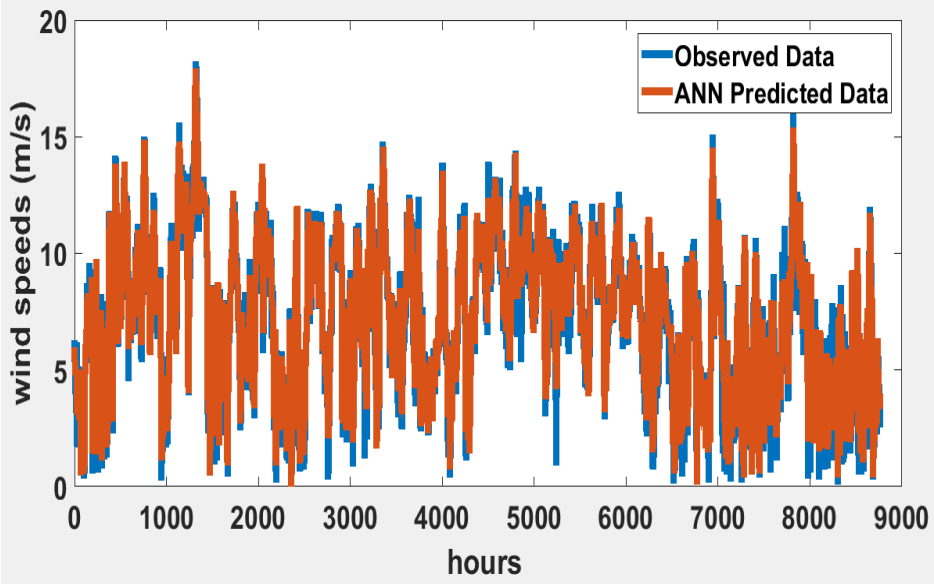

Figure 5. 6 Essaouira observed and predicted wind speeds [1]

These ANN forecasted wind speed values were used to find the new Weibull function parameters k^l and C^l, using the standard deviation method equations. As presented previously, this Weibull function is required for the WT energy generation estimation having a direct impact on the optimized objective function (NPV_g^l) [1]. Achieved results conduct nearly to the same values of measured Weibull parameters as presented **in Table 5. 1**. This demonstrates the stability of the future wind potential at Essaouira site, leading to a real estimation of the generated wind energy. This supports the validity of WT designs proposed by our decision support model in the future.

Table 5. 1 Essaouira Weibull Parameters at H_0=*50 m* [1]

	k^l	C^l (m/s)	$v_{average}$(m/s)
With measured wind speeds data	2.56	8.63	7.17
With ANN Predicted wind speeds	2.62	8.63	7.17

Using these predicted and measured Weibull parameters, and by classifying the associated wind speed data into different classes varying between 1 m/s and 29 m/s, the Weibull

probability density function presenting the wind speed frequency was calculated and fitted to the measured and predicted Weibull parameters [1]. The results are shown in **Figure 5. 7**.

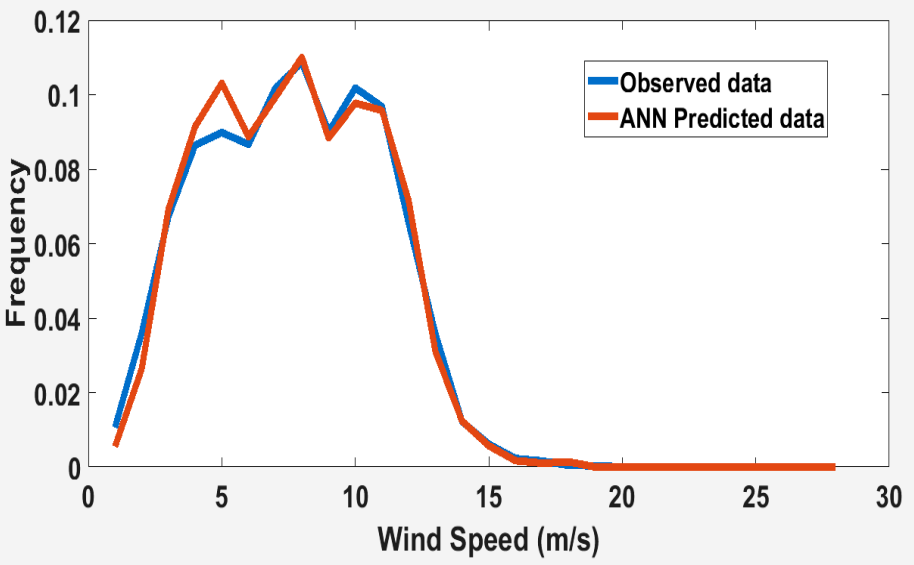

Figure 5. 7 Observed and predicted Weibull data in Essaouira city [1]

Figure 5. 7 shows the observed frequency of wind speeds and demonstrates more the stability of wind potential in Essaouira site, where the observed and predicted Weibull function data results are nearly the same. Small differences at 5 m/s and 10 m/s are observed, but generally the average wind speed is identical ($v_{average}$ = 7.17 m/s) [1]. As discussed and presented previously, wind energy is a function of the cubic wind speed, so, a few wind speed difference has an important impact on the generated wind energy. Hence, the Weibull parameters obtained using the ANN predicted wind speed data are used in the rest of the calculation in this study. These parameters are extrapolated automatically with tower height H_g values obtained by the present techno-economic decision-support model, using the extrapolation method presented in chapter 2 to overcome its influence on the wind speed profile.

5.4 Techno-economic Decision Support Model Evaluation Wind Turbine Grid Integration Case Study

As the developed techno-economic decision support model was verified validating its work performance in the previous chapter, it is adopted in this study to achieve the second objective of this thesis. Principally, at this stage, the developed techno-economic decision support model is evaluated in determining the optimal design parameters of the WT based on: available wind potential of the studied site (Essaouira), the connected radial distribution network (RDN) constraints, and all the constraints mentioned in the second optimization scenario presented in chapter 3. The objective function studied by the optimization problem was also the maximization of the net present value of the wind energy economic benefits $Max\left(NPV_g^l\right)$. Two different RDN test systems, data: IEEE 9 and IEEE 33 composing of 9 and 33 bus nodes respectively, were used in this evaluation [4], [94],[1]. Each bus node has its own electrical characteristics and its own load demand. The tested RDN systems were assumed to have the same wind characteristics as the studied site (Essaouira) and all buses are candidates for WT installation from the wind potential viewpoint [1]. Thus, specific WT technical parameters, including rotor diameter D_g, tower height H_g, and nominal power ($P_{n,g}$) are proposed for each evaluated bus node of the tested RDN systems. In this section, the input parameters and constraints used in the evaluation of the techno-economic optimization problem, the optimization algorithm details, and the optimal WT design parameters obtained at the evaluated RDN systems are presented.

5.4.1 Optimization Problem Input Parameters

Except the Weibull distribution parameters which correspond to the new evaluated wind site "Essaouira" obtained through the ANN forecasted wind speed data (k^l = 2.62 and C^l = 8.63 m/s), all the input parameters employed in our previous optimization study performed in [6] presented in the previous chapter are used also in the evaluation of the present optimization problem. These inputs are as follows [1]: the blades number $NB_g = 3$, the WT nominal wind speed $v_{n,g}$ = 13.2 m/s, wind speed operating range χ = 1.7, rotor rotational speed $N_{rpm,g}$ = 18.15 rpm, drag and left ratio C_d/C_l = 1/120, air density ρ = 1.225 kg/m3, WT energy generation losses percentage α = 5%, tax payment $T^l_{t,g}$ = 14%,, WT life time n=20 years, Discount rate r=8%, annual depreciation expense $D^l_{t,g}$ = 5% of the

investment, percentages adopted for the operation and maintenance cost η = 2% and ξ = 1%, the purchase tariff of electricity C_s = 0.094 $/kWh, and Sales cost due to incentives for green energy production C_{In} = 0.053 $/kWh.

5.4.2 Optimization Problem Constraints

The constraints of the second optimization scenario presented in chapter 3 are considered in this optimization problem. Three main constraints were employed [1].

1) The first one is related to the WT geometrical design variables, where we presented the resulted rotor diameter $D_g$variation limits. The D_g bound limits were found through power capacity assessment of the available onshore WT technologies in the market, with a larger scale power capacity (6 MW) than the study provided in chapter 3 (see **section 3.4.2**). The resulted WT power variation function rotor diameter is shown in **Figure 5. 8** [14].

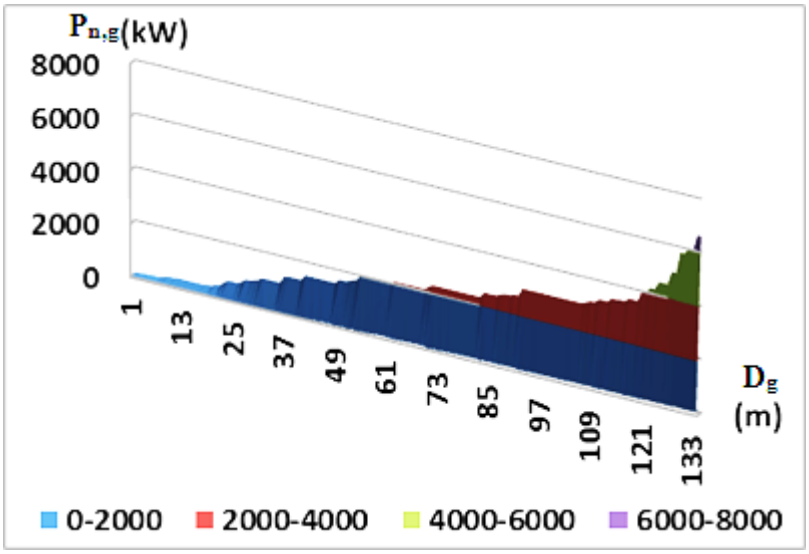

Figure 5. 8 Wind turbine power variation function rotor diameter [1]

Based on **Figure 5. 8**, the D_g bound limits were specified as follows:

$$40\ m \leq D_g \leq 200\ m \tag{5.1}$$

$$H_g \geq \frac{D_g}{2} + 15 \tag{5.2}$$

We notice that in this study, in contrast to the first optimization scenario, the WT nominal power is not limited but determined by the optimization problem according to the evaluated site and RDN characteristics.

2) The second constraint used, controls the active generated power $P_{WT,g}^{l}$ by the WT to respond to power load P_{Load}^{l} and grid requirements, using the mentioned power flow expression (see chapter 3, **section 3.4.3**) given as follows:

$$P_{WT,g}^{l} - P_{Load}^{l} - P_{Loss}^{l} = 0 \tag{5.3}$$

Where:

$$P_{WT,g}^{l} = P_{n,g} \tag{5.4}$$

$$P_{Loss}^{l} = V_l \sum_{j=1}^{J} V_j \left[G_{lj} \cos\left(\delta_l - \delta_j\right) + B_{lj} \sin\left(\delta_l - \delta_j\right) \right] \tag{5.5}$$

3) The third constraint employed, controls the voltage at different bus nodes of the tested RDN systems mainly, IEEE 9 and IEEE 33. Therefore, the voltage stability challenge in the grid due to the integration of WTs is addressed by our decision support model allowing a maximum and minimum variation of 5% over it initial value as follows [1].

$$V_l / V_j(p.u) = 1 \pm 0.05 \tag{5.6}$$

Furthermore, the grid voltage stability was also controlled in this thesis by providing the WT active power at constant power factor where no reactive power is expected to be generated.

5.4.3 Optimization Algorithm

Like the previous chapter, the genetic algorithm was also the optimization algorithm used in this study to solve the presented optimization problem and determine the optimal WT design parameters output that maximizes the optimized objective function NPV_g^l. This function is evaluated at this stage under the previous cited constraints considering: the studied design variable in the tested RDN system (V_l/ V_j), the WT design variables (rotor diameter D_g and Tower Height H_g), the Weibull parameters of Essaouira site (k^l and C^l), in

addition to all other inputs presented in subsection **5.4.1**. The updated optimization process flowchart is described in **Figure 5. 9** [1].

Following the same optimization process described in the chapter 4, the best optimal WT design parameters are provided by the optimization algorithm [1].

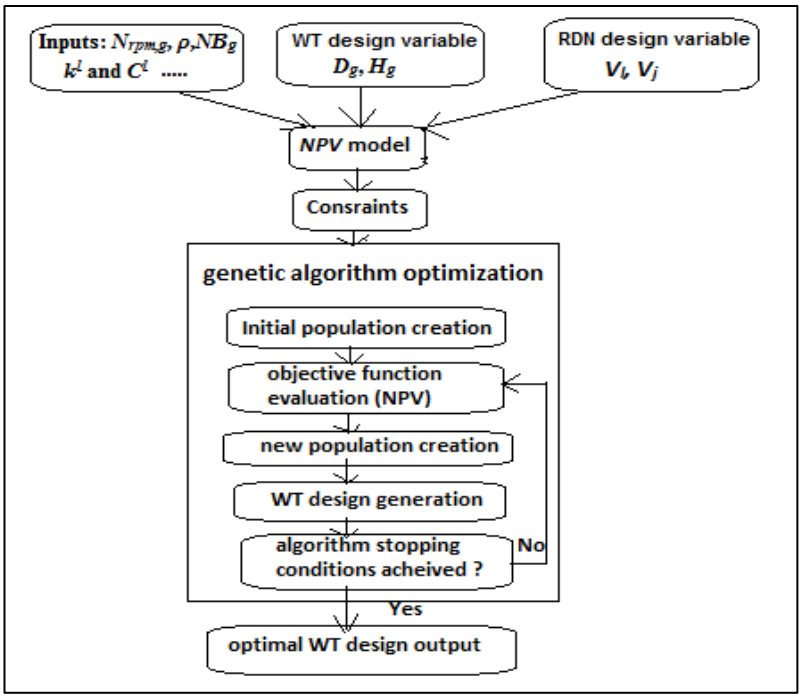

Figure 5. 9 Optimization process flowchart [1]

5.4.4 Optimal Wind Turbine Design Parameters Results

The optimal WT design parameters (H_g, D_g, and $P_{WT,g}^l$) determined for the tested RDN systems by the presented techno-economic decision support model, through the optimization procedure described previously are presented in **Table 5. 2** and **Table 5. 3** [1].

Table 5. 2 Optimal Wind Turbine Designs Parameters for the IEEE 9 Bus Radial Distribution System [1]

Buses	$P^{l}_{WT,g}$ (kW)	D_g (m)	H_g (m)
1	5128.75	200	115
2	5128.75	200	115
3	2654.17	135.39	82.70
4	2613.72	134.23	82.11
5	2140.58	120.08	75.04
6	1494.87	98.79	64.39
7	1575.97	101.63	65.82
8	1230.57	89.06	59.53
9	1804.29	109.35	69.68

Table 5. 3 Optimal Wind Turbine Designs Parameters for the IEEE 33 Bus Radial Distribution System [1]

Buses	$P^{l}_{WT,g}$ (kW)	D_g (m)	H_g (m)	Buses	$P^{l}_{WT,g}$ (kW)	D_g (m)	H_g (m)
2	1794.33	109.02	69.51	18	291.06	42.68	36.34
3	360.81	47.48	38.74	19	1077.01	83.02	56.51
4	493.67	55.57	42.79	20	203.94	35.84	32.92
5	415.48	50.95	40.48	21	485.60	55.11	42.56
6	269.16	41.06	35.53	22	318.04	44.59	37.30
7	1049.09	81.88	55.94	23	455.45	53.36	41.68
8	307.62	43.86	36.93	24	652.90	64.06	47.03
9	221.35	37.30	33.65	25	552.64	58.84	44.42
10	216.16	36.87	33.43	26	749.76	68.77	49.39
11	783.62	70.36	50.18	27	532.89	57.77	43.88
12	442.63	52.60	41.30	28	187.30	34.38	32.19
13	172.71	33.05	31.53	29	287.10	42.39	36.19
14	406.24	50.38	40.19	30	428.22	51.73	40.87
15	318.13	44.60	37.30	31	313.53	44.28	37.14
16	262.14	40.53	35.26	32	693.16	66.05	48.03
17	179.45	33.67	31.84	33	493.75	55.58	42.79

The presented optimal WT design results corresponded to the ANN predicted Weibull parameters, which showed the stability of the wind potential in Essaouira compared to the observed one [1]. Specific WT design was proposed for each bus node evaluated. The most suitable bus locations for wind energy generation were identified based on the maximum

net present value economic benefits NPV_g^l registered. The suitable bus locations identified in the tested RDNs IEEE 9 and IEEE 33 are illustrated in their associated schemes [4], [95] given in **Figure 5. 10** and **Figure 5. 11** [1].

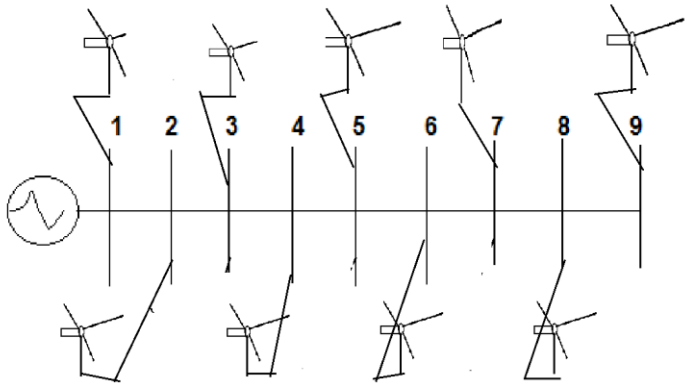

Figure 5. 10 IEEE 9 Bus radial distribution network system scheme with adequate wind turbine locations [1]

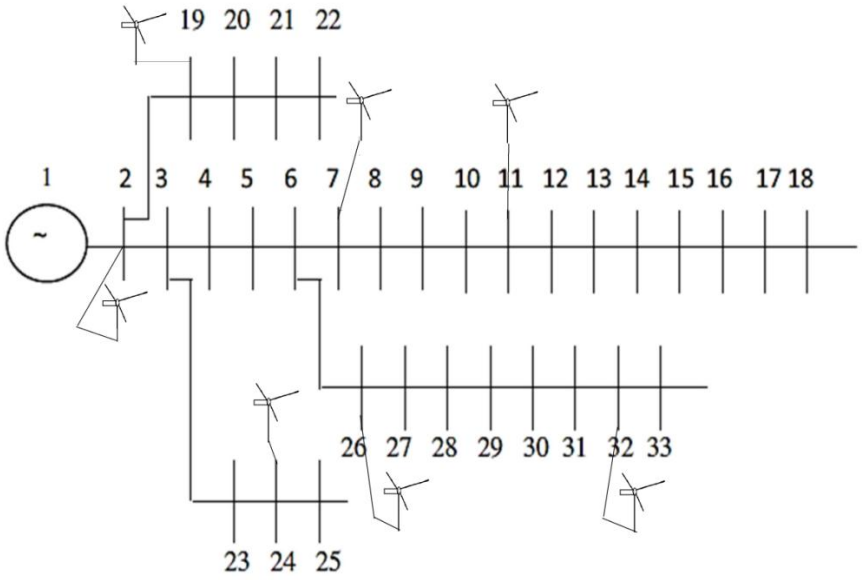

Figure 5. 11 IEEE 33 Bus radial distribution network system scheme with adequate wind turbine locations [1]

Results of the tested IEEE 9 bus system presented good economic benefits with a minimum and maximum NPV_g^l of 3.87 M$ and 18.62 M$ respectively, demonstrating the eligibility of all IEEE 9 buses for Wind energy generation, as describes in **Figure 5. 12** [1].

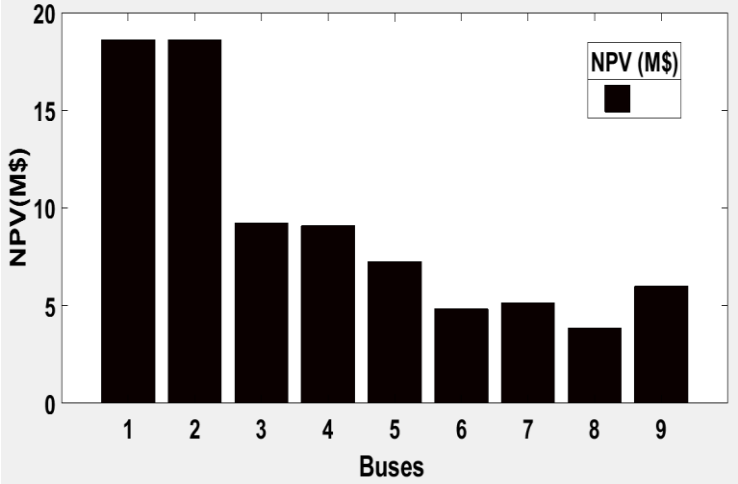

Figure 5. 12 NPV results of the IEEE 9 Bus radial distribution network system [1]

However, the obtained NPV_g^l for the proposed WT design parameters for the IEEE 33 tested system demonstrates that there are only seven most candidate buses in this system for WT installation [1]. The numbers of these buses are: 2, 7, 11, 19, 24, 26, and 32 with an NPV_g^l of 5.95, 3.22, 2.29, 3.32, 1.85, 2.18, and 1.98 M$ respectively, as described in **Figure 5. 13** [1].

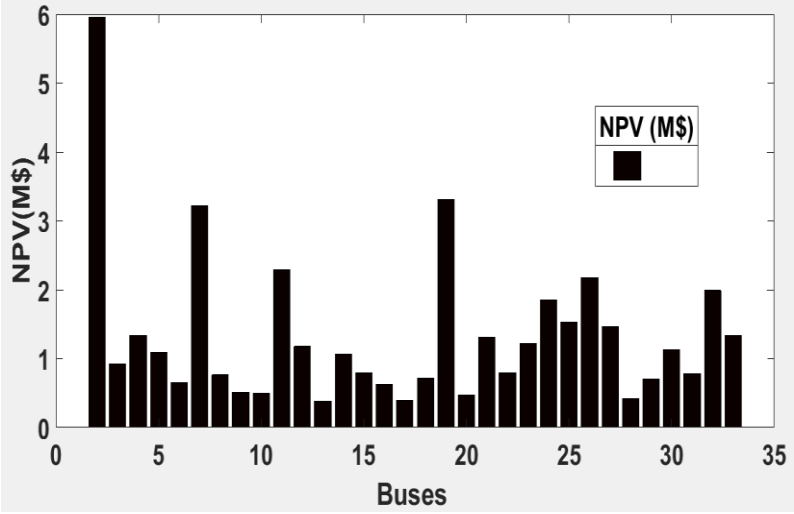

Figure 5. 13 NPV results of the IEEE 33 Bus radial distribution network [1]

From the achieved WT design parameters results in the IEEE 33 bus system; we can observe that the maximum WT power capacity determined for this RDN was approximately 1 MW [1]. However, a larger scale WT power capacity of 5 MW was

determined for the tested IEEE 9 bus system. Therefore, we can conclude that we have a good wind profile at the evaluated site (Essaouira), which offered the opportunity for the installation of more powerful WT technologies with large power capacity in IEEE 9 than IEEE 33 bus system [1]. This difference can be explained by the grid limitations evaluated; because each tested RDN has its own electrical wire characteristics with different values. The IEEE 9 bus system is more powerful than the IEEE 33 bus system with an important active power load demand. This explains the results obtained in this study. Thus, the proposed WTs design by the present techno-economic decision support model follows the available wind potential and grid constraints, demonstrating that the optimal design for a WT technology is not limited to available wind potential in a site but mostly to the grid capability.

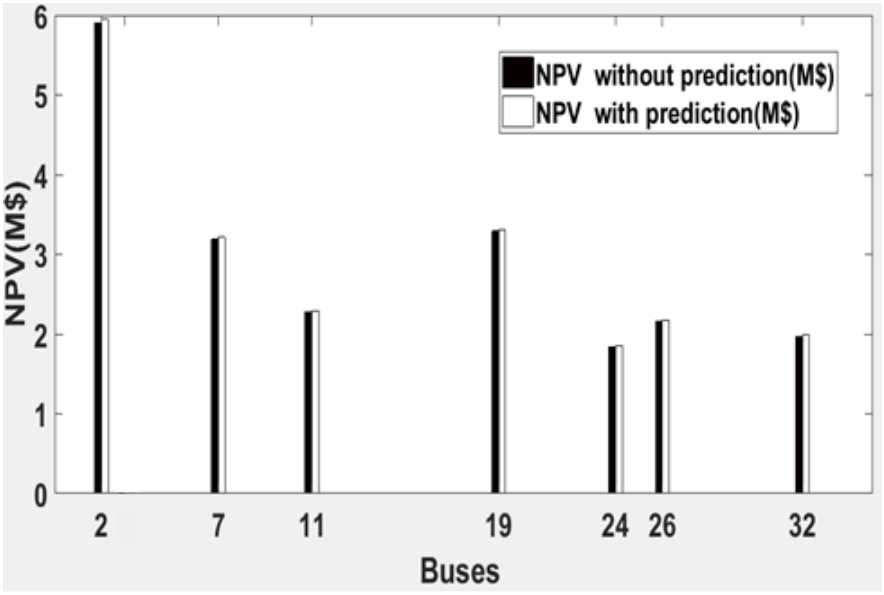

Figure 5. 14 Achieved NPV results with and without ANN prediction of the IEEE 33 Bus radial distribution network system system in the profitable bus locations [1]

A comparison with an optimization study using the initial measured Weibull parameters was realized. The decision support model provided the same WT design parameters for the both evaluated RDNs systems with nearly the same NPV_g^l economic benefits value, using the wind speed potential with and without prediction, as presented in **Figure 5. 14** and **Figure 5. 15** [1].

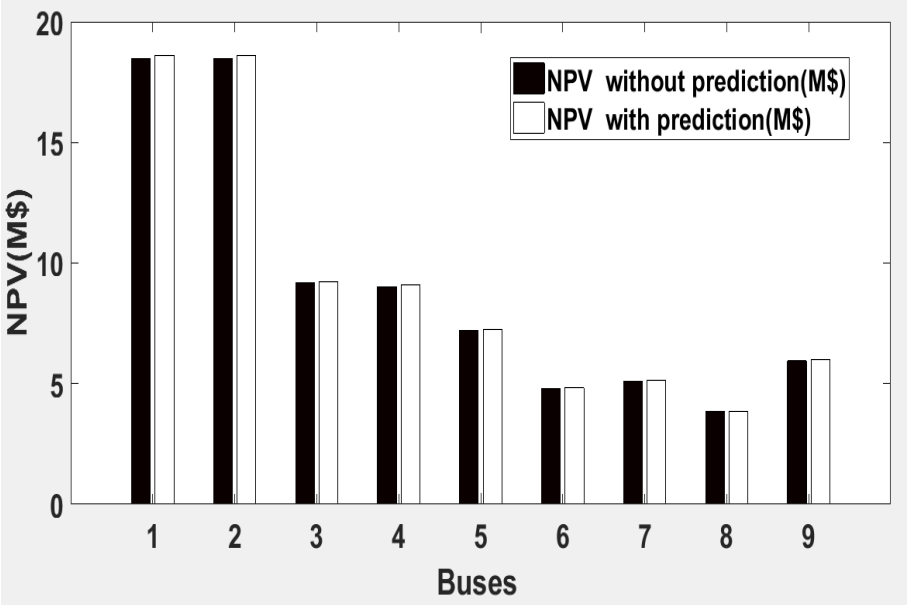

Figure 5. 15 Achieved NPV results with and without ANN prediction of the IEEE 9 Bus radial distribution network system [1]

We can also observe that the use of ANN wind speed prediction results increase slightly the economic benefits of the proposed WTs design owing to the accuracy of forecast wind potential, enhancing the generated energy, and automatically the value of NPV is enhanced in parallel. We note that these designs are not available or commercialized in the market, as suggested by this study [1].

5.4.5 Evaluation of Wind Variation Impact on the Techno-economic Decision Support Model

The previous results demonstrated that the optimal WT design is not determined according to the available wind potential, but mostly according to the grid capability at the Essaouira site. Furthermore, the accuracy of the wind potential predicted by the ANN improved the NPV economic benefits of the proposed WT designs, demonstrating the effect of wind potential on our proposed decision support model. Thus, a supplementary optimization study was performed to show more the effect of wind potential variation on the proposed decision support model with RDN constraints evaluation. To this end, the eligible sites for wind energy projects determined according to the first optimization scenario of this thesis were selected, mainly Dakhla and Tanger. Compared with the Essaouira site, Tanger and

Dakhla have low and high wind potentials, respectively. This study follows the same details as the second optimization scenario presented previously, using the Weibull parameters of the newly evaluated sites measured at H_0= 10 m for the Dakhla and Tanger sites and at H_0= 50 m for Essaouira, as presented in **Table 5. 4**.

Table 5. 4 Dakhla, Tanger, and Essaouira Weibull Parameters

Site l	k^l	C^l (m/s)	$v_{average}$ (m/s)
Tanger	1.62	6.012	5.38
Essaouira	2.56	8.63	7.17
Dakhla	2.38	10.58	9.38

The decision support model provided the same WT design parameters for all evaluated RDN systems in Dakhla and Tanger, similar to the Essaouira site as presented in **Tables 5. 5 and 5. 6**. This proves our previous remark, which demonstrated that the WT design is determined according to the grid capability rather than the available wind potential. Furthermore, for the same WT design, the generated NPV was lower in Tanger and higher in Dakhla because of the difference in the wind potential at each site. Therefore, the most candidate buses for WT installation selected previously based on the registered NPV in Essaouira were found to be more profitable in Dakhla and less profitable in Tanger. Thus, the economic profitability (NPV) is affected more by the wind potential in this case.

Table 5. 5 Optimal Wind Turbine design parameters for IEEE 9 Bus System in Dakhla, Tanger, and Essaouira

Bus node	$P^l_{WT,g}$ (kW)	D_g (m)	H_g (m)	$I^l_{t,g}$ (M$)	NPV^l_g Dakhla (M$)	NPV^l_g Essaouira (M$)	NPV^l_g Tanger (M$)
1	5128.75	200.00	115.00	7.78	24.689	18.217	6.687
2	5128.75	200.00	115.00	7.78	24.689	18.217	6.687
3	2654.17	135.39	82.70	3.75	12.533	9.044	3.317
4	2613.72	134.23	82.11	3.7	12.329	8.891	3.256
5	2140.58	120.08	75.04	3.09	9.951	7.108	2.549
6	1494.87	98.79	64.39	2.28	6.741	4.726	1.609
7	1575.97	101.63	65.82	2.39	7.141	5.021	1.724
8	1230.57	89.06	59.53	1.95	5.450	3.780	1.243
9	1804.29	109.35	69.68	2.67	8.272	5.858	2.053

Table 5. 6 Optimal Wind Turbine design parameters for IEEE 33 Bus System in Dakhla, Tanger, and Essaouira

Bus node	$P_{WT,g}^{l}$ **(kW)**	D_g **(m)**	H_g **(m)**	$I_{t,g}^{l}$ **(M$)**	NPV_g^l **Dakhla (M$)**	NPV_g^l **Essaouira (M$)**	NPV_g^l **Tanger (M$)**
2	1794.33	109.02	69.51	2.66	8.222	5.821	2.039
7	1049.09	81.88	55.94	1.71	4.575	3.145	1.001
11	783.62	70.36	50.18	1.35	3.319	2.242	0.666
19	1077.01	83.02	56.51	1.75	4.709	3.242	1.038
24	652.90	64.06	47.03	1.16	2.713	1.812	0.512
26	749.76	68.77	49.39	1.3	3.161	2.129	0.626
32	693.16	66.05	48.03	1.22	2.898	1.943	0.559

In contrast to the results of our first optimization scenario where the investment cost $I_{t,g}^{l}$was affected by the change in site because of the different rotor diameter and tower height parameters proposed for each evaluated site, the proposed decision support model did not scale up or scale down these WT design parameters in Dakhla and Tanger, respectively, as a function of wind potential in the case of RDN constraints evaluation. Therefore, whatever the wind potential available, a unique WT design parameters is permitted by each bus node of the connected RDN. Therefore, as the proposed investment cost model $I_{t,g}^{l}$ depends on the studied WT design parameters, the resulting cost of $I_{t,g}^{l}$was closed in each bus of the RDN systems for all evaluated sites (see **Tables 5. 5 and 5. 6**). So, the effect of site variation is only observed in the level of generated energy $AEP_{t,g,real}^{l}$, which in turn affects the estimated NPV, as shown in **Figures 5. 16 and 5. 17**.

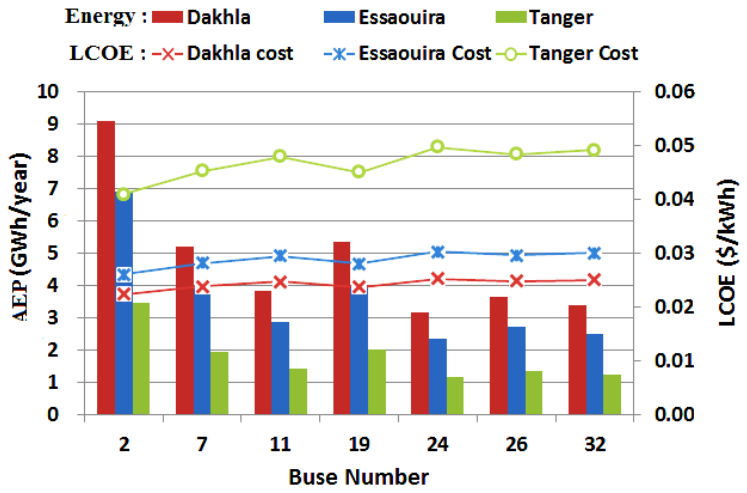

Figure 5. 16 Analysis of generated wind energy $AEP_{t,g,real}^{l}$ and LCOE in IEEE 33 Bus system

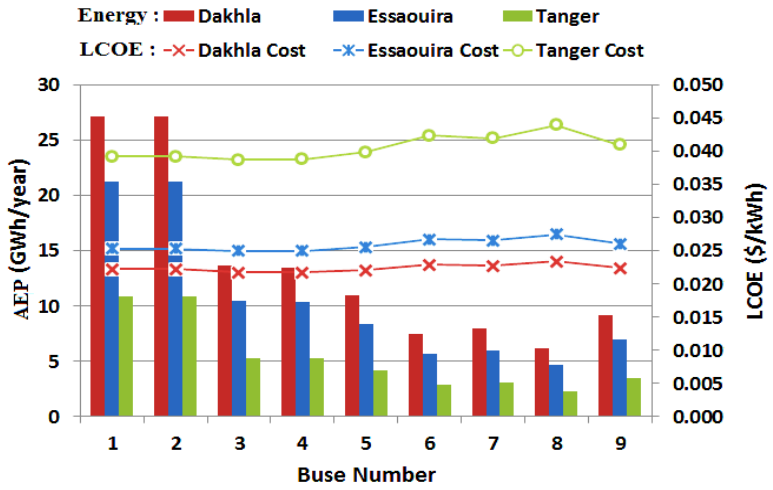

Figure 5. 17 Analysis of generated wind energy $AEP_{t,g,real}^{l}$ and LCOE in IEEE 9 Bus system

An analysis of the LCOE for the proposed WT designs in all the evaluated sites and most candidate buses of the tested RDN systems for WT installation was performed, and the results are presented in **Figures 5. 16 and 5. 17**. We can observe that the more the design of the WT and the available wind potential are important, the more the generated electrical energy increases and its associated cost decreases. Thus, the cost of energy generated in Tanger was greater than that in Essaouira and Dakhla. Dakhla presented the cheapest energy cost, as it has the most powerful wind potential.

5.5 Conclusion

The proposed techno-economic decision support model for optimal WT design based on the wind potential of the site of interest and RDN constraints is evaluated in this chapter, providing significant results. The presented decision support model consists of a constrained optimization problem resolution, having as objective the maximization of the *NPV* economic benefit. The optimal WT technical parameters, including the rotor diameter D_g, tower height H_g, and WT nominal power, were determined for all studied RDNs bus nodes [1]. Wind speed variation has a significant effect on WT-generated energy. Therefore, an ANN model was used to validate the wind profile at the studied site (Essaouira). Based on previously measured wind data, the ANN effectively forecasted future wind speed potential at the Essaouira site, demonstrating its stability. Using the electrical characteristics of two different RDN bus systems, namely IEEE 9 and IEEE 33 buses, the proposed techno-economic decision support model was validated and tested. Based on the maximum value of the resulting NPV, the most candidate bus nodes for WT installation in the tested RDN systems were selected. The results showed that all nine buses of the IEEE 9 system were candidates for WT installation; however, only seven candidate buses in the IEEE 33 system presented good *NPV* economic benefits. Different WTs power capacities were proposed using the decision support model for the evaluated RDN systems, demonstrating that the WT design depends more on the capability of the connected RDN than on the available wind potential. To this end, the decision support model was evaluated for different wind sites, confirming this observation. The variation in wind generally affected the generated energy and economic benefits value. Moreover, the ANN model proved not only the stability of the future wind potential in Essaouira but also supported the validity of the obtained WT designs in the future. The provided WTs design parameters are not available in the market but are suggested in this study.

General conclusion

Green energy sources, such as wind and solar energy, constitute the best solution for energy, water, and climate change issues. Therefore, the development of their associated technologies, mainly solar panels and wind turbines (WTs), plays a significant role in improving their competitiveness and encouraging and facilitating their deployment. This constituted the objective of this thesis, which focused on the development of WT technology design by providing a decision support model based on a techno-economic optimization approach. This model provides the optimal design parameters for future WTs based on the available wind potential and connected radial distribution network (RDN) characteristics, following two optimization case studies performed through two different scenarios. The objective of the techno-economic optimization approach is to maximize the Net Present Value (*NPV*) of wind energy economic revenues when determining the optimal design parameters for the WT. Three principal WT technical design parameters were determined using the proposed decision support model: rotor diameter D_g, tower height H_g, and its nominal power.

As a first step, this thesis provided a state-of-the-art of WT development starting from windmill apparition to WTs inspiration and improvement. Furthermore, the challenges related to the integration of WTs into power system networks are presented. In addition, a bibliographic study of different studies conducted on the optimization of WTs design was presented, showing the originality of our work. No study was found that treated the same objectives of this thesis, providing an optimal design for the WT technology based on the available wind potential at the site of interest and the connected RDN characteristics, giving an idea about the economic revenues associated with the proposed design.

Second, this thesis presents an overview of the origin of wind, its quantification methods, and its exploitation process for electricity production, giving a presentation of different WT components. Moreover, an artificial neural network (ANN) that permits the prediction of the future stochastic behavior of wind speed at the selected site was presented. The use of the ANN helped to address the wind energy generation uncertainty challenge for the grid operator.

As a third step, the modeling of the proposed techno-economic decision support model is presented in detail, starting from a deep WT energy production model to the construction of the optimization problem. This is the main element used in the development of the WT technology design that provides the optimal design parameters for the studied issue.

As a fourth step, the proposed decision support model was verified and validated in comparison with a previous existing model, demonstrating its performance. Then, it was applied to the first case study presented as the first optimization scenario. This scenario consisted of evaluating the decision support model to provide the best optimal WT design parameters based on the available wind potential at the three tested sites. Dakhla, Tanger, and Casablanca were selected as sites characterized by high, medium, and low wind potential, respectively. This selection allows visualization of the wind effect on the final results, that is, the objective function evaluated (NPV). The results showed that Tanger and Dakhla were the most profitable sites for wind project investment, providing the best design parameters for those sites with maximum NPV. However, Casablanca was found to be a not profitable site for wind projects because of its low wind potential. Furthermore, this study demonstrated that every location can have its own WT investment cost for the same installed power capacity, which can be related to different factors such as the costs of transportation, foundation, and assembly and installation of the WT, which vary by changing the location. Therefore, the variation in investment cost has an important impact on the registered NPV, which also affects the wind project decision-making in this case.

The final step of this thesis is to consider the RDN constraints in the proposed techno-economic decision support model as a second case study presented in a second optimization scenario. Thus, the novel proposed WT design parameters were based not only on the wind characteristics, but also on the connected RDN grid capability. The Essaouira wind site and the data of two different RDN systems, IEEE 33 and IEEE 9 RDN bus systems, were used in the evaluation of this study. The tested RDN systems were assumed to have the same wind potential, and all RDN bus nodes were candidates for WT installation. Furthermore, to address the wind energy generation uncertainty challenge that affects the stability of the grid, an ANN was used to effectively forecast the future wind potential at the selected site. The results demonstrated that the optimal WT design parameters were limited to the RDN grid capability and not the strength of the available

wind. This was also confirmed by testing different wind sites, particulary, Dakhla and Tanger. Based on the analysis of the achieved NPV, the most suitable and profitable RDN bus nodes for the installation of WT technology were selected. Finally, an assessment of the LCOE was carried out, which showed a decrease when the WT design and available wind potential were important.

In conclusion, the optimal WT design parameters can be determined using the proposed techno-economic decision support model based on the available wind potential and connected RDN constraints. Furthermore, the optimal site and RDN bus node for wind energy exploitation can also be determined. The WTs design parameters proposed in this thesis are not available in the market, as suggested by this study. The presented techno-economic decision support model supports decision makers in determining the optimal WT design parameters (rotor diameter D_g, tower height H_g, and nominal power), eligible sites, and suitable RDN bus node locations for WT installation at the site of interest. In this thesis, aerodynamic effects, material optimization, and grid power loss reduction were not considered in the evaluated optimization problem and could constitute a recommendation for future work.

Appendix

The distribution network can be represented as the equivalent of two bus system as shown in the following figure [4]:

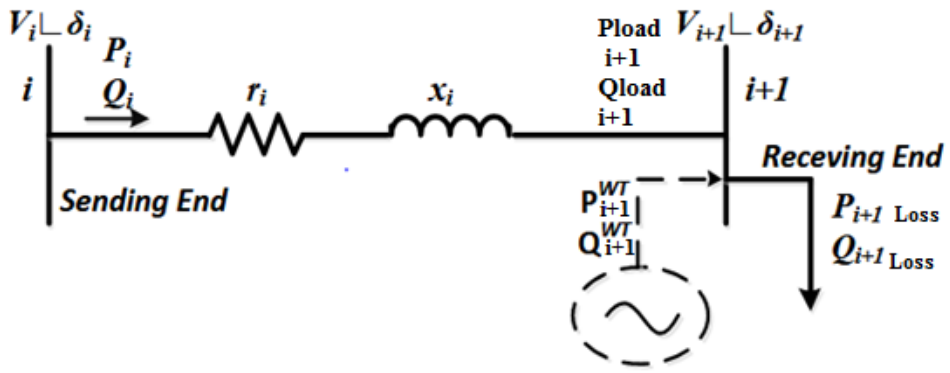

1) IEEE 33 Radial Distribution Network data is as follows [94]:

Branch Number	Send node	Receiv node	Pload reciev node(kW)	Qload reciev node(kVAr)	Resistance (ohm)	Reactance (ohm)
1	1	2	100	60	0.0922	0.047
2	2	3	90	40	0.493	0.2511
3	3	4	120	80	0.366	0.1864
4	4	5	60	30	0.3811	0.1941
5	5	6	60	20	0.819	0.707
6	6	7	200	100	0.1872	0.6188
7	7	8	200	100	1.7114	1.2351
8	8	9	60	20	1.03	0.74
9	9	10	60	20	1.04	0.74
10	10	11	45	30	0.1966	0.065
11	11	12	60	35	0.3744	0.1238
12	12	13	60	35	1.468	1.155
13	13	14	120	80	0.5416	0.7129
14	14	15	60	10	0.591	0.526
15	15	16	60	20	0.7463	0.545
16	16	17	60	20	1.289	1.721
17	17	18	90	40	0.732	0.574
18	2	19	90	40	0.164	0.1565
19	19	20	90	40	1.5042	1.3554
20	20	21	90	40	0.4095	0.4784
21	21	22	90	40	0.7089	0.9373

22	3	23	90	50	0.4512	0.3083
23	23	24	420	200	0.898	0.7091
24	24	25	420	200	0.896	0.7011
25	6	26	60	25	0.203	0.1034
26	26	27	60	25	0.2842	0.1447
27	27	28	60	20	1.059	0.9337
28	28	29	120	70	0.8042	0.7006
29	29	30	200	600	0.5075	0.2585
30	30	31	150	70	0.9744	0.963
31	31	32	210	100	0.3105	0.3619
32	32	33	60	40	0.341	0.5302

Bus node	**V(p.u)**	**δ(deg)**
1	1	0
2	0.99703	0.01369
3	0.98289	0.09637
4	0.97538	0.16301
5	0.96796	0.23056
6	0.94948	0.13820
7	0.94595	-0.09626
8	0.9323	-0.26357
9	0.92597	-0.34550
10	0.92009	-0.41597
11	0.91922	-0.41024
12	0.91771	-0.40050
13	0.91153	-0.50192
14	0.90924	-0.58500
15	0.90782	-0.62568
16	0.90643	-0.65146
17	0.90439	-0.73397
18	0.90377	-0.74486
19	0.9965	0.00286
20	0.99292	-0.06475
21	0.99221	-0.08423
22	0.99158	-0.10485
23	0.97931	0.06515
24	0.97264	-0.24065
25	0.96931	-0.06818

26	0.94755	0.17934
27	0.94499	0.23790
28	0.93354	0.33198
29	0.92532	0.41815
30	0.92177	0.52707
31	0.9176	0.44657
32	0.91669	0.42440
33	0.9164	0.41689

Base voltage= 12.66 kV

2) IEEE 9 Radial Distribution Network data is as follows [4]:

Branche Number	**Send node**	**Receiv node**	**Pload reciev node(kW)**	**Qload reciev node(kVAr)**	**Resistance (ohm)**	**Reactance (ohm)**
1	0	1	1840	460	0.1233	0.4127
2	1	2	980	340	0.014	0.6057
3	2	3	1790	446	0.7463	1.205
4	3	4	1598	1840	0.6984	0.6084
5	4	5	1610	600	1.9831	1.7276
6	5	6	780	110	0.9053	0.7886
7	6	7	1150	60	2.0552	1.164
8	7	8	980	130	4.7953	2.716
9	8	9	1640	200	5.3434	3.0264

Bus node	**V(p.u)**	**δ(deg)**
0	1	0
1	0.9929014	-0.522
2	0.9873783	-1.268
3	0.9634085	-2.331
4	0.9480165	-2.652
5	0.917171	-3.721
6	0.9071685	-4.137
7	0.8890	-4.618
8	0.8586946	-5.404
9	0.8375037	-5.99

Base voltage= 23 kV

Bibliography

[1] F.-A. Bourhim, A. Ouammi, R. Benchrifa, and M. Chaouch, "Optimal Wind Turbine Design Based Wind Potential and Radial Distribution Network Characteristics," *IEEE Access*, vol. 11, pp. 116594–116607, 2023, doi: 10.1109/ACCESS.2023.3324884.

[2] IRENA (2023), "Renewable capacity statistics 2023," International Renewable Energy Agency, Abu Dhabi, ISBN: 978-92-9260-525-4, Mar. 2023.

[3] A. Ouammi, H. Dagdougui, and R. Sacile, "Optimal Planning With Technology Selection for Wind Power Plants in Power Distribution Networks," *IEEE Systems Journal*, vol. 13, no. 3, pp. 3059–3069, Sep. 2019, doi: 10.1109/JSYST.2019.2903555.

[4] G. A. E.-A. Mahmoud and E. S. S. Oda, "Investigation of Connecting Wind Turbine to Radial Distribution System on Voltage Stability Using SI Index and λ - V Curves," *Smart Grid and Renewable Energy*, vol. 7, no. 1, Art. no. 1, Jan. 2016, doi: 10.4236/sgre.2016.71002.

[5] A. Boliev, U. Jalilov, A. Suyarov, A. Jumanov, and A. Kurbanov, "Optimal Integration of Wind Turbine Based Dg Units in Distribution System Considering Uncertainties," *International Journal of Academic and Applied Research*, vol. 5, no. 4, pp. 183–187, Apr. 2021.

[6] F.-A. Bourhim, S. Berrhazi, A. Ouammi, and R. Benchrifa, "Decision Support Model for Optimal Design of Wind Technologies Based Techno–Economic Approach," *IEEE Access*, vol. 9, pp. 148264–148276, 2021, doi: 10.1109/ACCESS.2021.3123561.

[7] D. G. Shepherd, "Historical development of the windmill," Cornell Univ., Ithaca, NY (USA). Dept. of Mechanical and Aerospace Engineering, DOE/NASA-5266-2; NASA-CR-4337, Dec. 1990. doi: 10.2172/6342767.

[8] J. Needham, *Science and Civilisation in China*. Cambridge University Press, 1965.

[9] J. I. Rojas Sola and J. Amezcua-Ogáyar, "Origen y expansion de los molinos de viento en España," *Interciencia*, vol. 30, pp. 316–325, Jun. 2005.

[10] J. K. Kaldellis and D. Zafirakis, "The wind energy (r)evolution: A short review of a long history," *Renewable Energy*, vol. 36, no. 7, pp. 1887–1901, Jul. 2011, doi: 10.1016/j.renene.2011.01.002.

[11] P. Gipe and E. Möllerström, "An overview of the history of wind turbine development: Part I—The early wind turbines until the 1960s," *Wind Engineering*, vol. 46, p. 0309524X2211178, Aug. 2022, doi: 10.1177/0309524X221117825.

[12] P. Gipe and E. Möllerström, "An overview of the history of wind turbine development: Part II–The 1970s onward," *Wind Engineering*, vol. 47, p. 0309524X2211225, Sep. 2022, doi: 10.1177/0309524X221122594.

[13] ONEE, "Site web officiel de l'ONEE - Branche Electricité." Accessed: Oct. 25, 2020. [Online]. Available: http://www.one.org.ma/FR/pages/interne.asp?esp=1&id1=14&id2=114&t2=1

[14] L. Bauer, "Base de données sur les éoliennes." Accessed: Apr. 29, 2023. [Online]. Available: https://fr.wind-turbine-models.com/turbines

[15] D. Y. Goswami and F. Kreith, Eds., *Handbook of Energy Efficiency and Renewable Energy*. Boca Raton: CRC Press, 2007. doi: 10.1201/9781420003482.

[16] S. D. AHMED, F. S. M. Al-Ismail, M. Shafiullah, F. A. Al-Sulaiman, and I. M. El-Amin, "Grid Integration Challenges of Wind Energy: A Review," *IEEE Access*, vol. 8, pp. 10857–10878, 2020, doi: 10.1109/ACCESS.2020.2964896.

[17] IRENA, “Wind energy.” Accessed: Feb. 28, 2024. [Online]. Available: https://www.irena.org/Energy-Transition/Technology/Wind-energy
[18] A. Aoun, A. Ilinca, H. Ibrahim, and M. Ghandour, “Chapter 13: Demand Side Management,” in *Hybrid Renewable Energy Systems and Microgrids*, Academic Press - Elsevier, 2020, pp. 463–490. doi: 10.1016/B978-0-12-821724-5.00001-5.
[19] M. Mohseni, “Enhanced reactive power support capability of fully rated converter-based wind generators,” in *IECON 2011 - 37th Annual Conference of the IEEE Industrial Electronics Society*, Nov. 2011, pp. 2486–2491. doi: 10.1109/IECON.2011.6119700.
[20] L. Wang, M. E. Cholette, Y. Zhou, J. Yuan, A. C. C. Tan, and Y. Gu, “Effectiveness of optimized control strategy and different hub height turbines on a real wind farm optimization,” *Renewable Energy*, vol. 126, pp. 819–829, Oct. 2018, doi: 10.1016/j.renene.2018.04.004.
[21] M. Abdulrahman and D. Wood, “Investigating the Power-COE trade-off for wind farm layout optimization considering commercial turbine selection and hub height variation,” *Renewable Energy*, vol. 102, pp. 267–278, 2016, doi: 10.1016/j.renene.2016.10.038.
[22] E. G. A. Antonini, D. A. Romero, and C. H. Amon, “Optimal design of wind farms in complex terrains using computational fluid dynamics and adjoint methods,” *Applied Energy*, vol. 261, p. 114426, Mar. 2020, doi: 10.1016/j.apenergy.2019.114426.
[23] N. Charhouni, M. Sallaou, and K. Mansouri, “Realistic wind farm design layout optimization with different wind turbines types,” *Int J Energy Environ Eng*, vol. 10, no. 3, pp. 307–318, Sep. 2019, doi: 10.1007/s40095-019-0303-2.
[24] M. Tahani,T. Maeda, N. Babayan, S. Mehrnia, M. Shadmehri, Q. Li, R. Fahimi, and M. Masdari, “Investigating the effect of geometrical parameters of an optimized wind turbine blade in turbulent flow,” *Energy Conversion and Management*, vol. 153, pp. 71–82, Dec. 2017, doi: 10.1016/j.enconman.2017.09.073.
[25] R. Balijepalli, V. P. Chandramohan, and K. Kirankumar, “Optimized design and performance parameters for wind turbine blades of a solar updraft tower (SUT) plant using theories of Schmitz and aerodynamics forces,” *Sustainable Energy Technologies and Assessments*, vol. 30, pp. 192–200, Dec. 2018, doi: 10.1016/j.seta.2018.10.001.
[26] M. Sessarego, J. Feng, N. Ramos-García, and S. G. Horcas, “Design optimization of a curved wind turbine blade using neural networks and an aero-elastic vortex method under turbulent inflow,” *Renewable Energy*, vol. 146, pp. 1524–1535, Feb. 2020, doi: 10.1016/j.renene.2019.07.046.
[27] V. Cognet, S. Courrech du Pont, and B. Thiria, “Material optimization of flexible blades for wind turbines,” *Renewable Energy*, vol. 160, pp. 1373–1384, Nov. 2020, doi: 10.1016/j.renene.2020.05.188.
[28] H. Yang, J. Chen, and X. Pang, “Wind Turbine Optimization for Minimum Cost of Energy in Low Wind Speed Areas Considering Blade Length and Hub Height,” *Applied Sciences*, vol. 8, no. 7, p. 1202, Jul. 2018, doi: 10.3390/app8071202.
[29] T. Ashuri, M. B. Zaaijer, J. R. R. A. Martins, G. J. W. van Bussel, and G. A. M. van Kuik, “Multidisciplinary design optimization of offshore wind turbines for minimum levelized cost of energy,” *Renewable Energy*, vol. 68, pp. 893–905, Aug. 2014, doi: 10.1016/j.renene.2014.02.045.

[30] J. Zhu, Z. Zhou, and X. Cai, “Multi-objective aerodynamic and structural integrated optimization design of wind turbines at the system level through a coupled blade-tower model,” *Renewable Energy*, vol. 150, pp. 523–537, May 2020, doi: 10.1016/j.renene.2020.01.013.
[31] R. Wass, “Design of Wind Turbine Tower Height and Blade Length: an Optimization Approach,” *Mechanical Engineering Undergraduate Honors Theses*, p. 76, 2018.
[32] D. Song *et al.*, “Optimal design of wind turbines on high-altitude sites based on improved Yin-Yang pair optimization,” *Energy*, vol. 193, p. 116794, Feb. 2020, doi: 10.1016/j.energy.2019.116794.
[33] M. A. Mellal and M. Pecht, “A multi-objective design optimization framework for wind turbines under altitude consideration,” *Energy Conversion and Management*, vol. 222, p. 113212, Oct. 2020, doi: 10.1016/j.enconman.2020.113212.
[34] T. Ashuri, M. B. Zaaijer, J. R. R. A. Martins, and J. Zhang, “Multidisciplinary design optimization of large wind turbines—Technical, economic, and design challenges,” *Energy Conversion and Management*, vol. 123, pp. 56–70, Sep. 2016, doi: 10.1016/j.enconman.2016.06.004.
[35] A. W. Ciavarra, R. V. Rodrigues, K. Dykes, and P.-E. Réthoré, “Wind farm optimization with multiple hub heights using gradient-based methods,” *J. Phys.: Conf. Ser.*, vol. 2265, no. 2, p. 022012, May 2022, doi: 10.1088/1742-6596/2265/2/022012.
[36] G. Kütükcü and O. Uzol, “Monte-Carlo simulations based hub height optimization using FLORIS for two interacting onshore wind farms,” *Journal of Renewable and Sustainable Energy*, vol. 14, no. 6, Nov. 2022, doi: 10.1063/5.0107244.
[37] D. Li, H. Bao, and N. Zhao, “Research of Turbine Tower Optimization Based on Criterion Method,” *Energies*, vol. 16, no. 2, Art. no. 2, Jan. 2023, doi: 10.3390/en16020906.
[38] N. J. Abbas, P. Bortolotti, C. Kelley, J. Paquette, L. Pao, and N. Johnson, “Aero-servo-elastic co-optimization of large wind turbine blades with distributed aerodynamic control devices,” *Wind Energy*, vol. 26, no. 8, pp. 763–785, 2023, doi: 10.1002/we.2840.
[39] R. Özkan and M. S. Genç, “Aerodynamic design and optimization of a small-scale wind turbine blade using a novel artificial bee colony algorithm based on blade element momentum (ABC-BEM) theory,” *Energy Conversion and Management*, vol. 283, p. 116937, May 2023, doi: 10.1016/j.enconman.2023.116937.
[40] S. R. Reddy, “Wind Farm Layout Optimization (WindFLO): An advanced framework for fast wind farm analysis and optimization,” *Applied Energy*, vol. 269, p. 115090, Jul. 2020, doi: 10.1016/j.apenergy.2020.115090.
[41] M. Kim and J. Kim, “An integrated decision support model for design and operation of a wind-based hydrogen supply system,” *International Journal of Hydrogen Energy*, vol. 42, no. 7, 2016, doi: 10.1016/j.ijhydene.2016.10.129.
[42] A. P. J. Stanley and A. Ning, “Coupled wind turbine design and layout optimization with nonhomogeneous wind turbines,” *Wind Energ. Sci.*, vol. 4, no. 1, pp. 99–114, Jan. 2019, doi: 10.5194/wes-4-99-2019.
[43] A. Ouammi, V. Ghigliotti, M. Robba, A. Mimet, and R. Sacile, “A decision support system for the optimal exploitation of wind energy on regional scale,” *Renewable Energy*, vol. 37, no. 1, pp. 299–309, Jan. 2012, doi: 10.1016/j.renene.2011.06.027.

[44] G. Aquila, L. C. Souza Rocha, P. Rotela Junior, J. Y. Saab Junior, J. de Sá Brasil Lima, and P. P. Balestrassi, "Economic planning of wind farms from a NBI-RSM-DEA multiobjective programming," *Renewable Energy*, vol. 158, pp. 628–641, Oct. 2020, doi: 10.1016/j.renene.2020.05.179.

[45] H. Qu, F. Yang, Q. Lin, and Y. Jia, "Active and Reactive Power Coordinated Optimal Dispatch in Active Distribution Network Considering Spatial-temporal Correlation of Wind Power," *IOP Conf. Ser.: Earth Environ. Sci.*, vol. 687, no. 1, Mar. 2021, doi: 10.1088/1755-1315/687/1/012093.

[46] A. K. Khamees, A. Y. Abdelaziz, M. R. Eskaros, A. El-Shahat, and M. A. Attia, "Optimal Power Flow Solution of Wind-Integrated Power System Using Novel Metaheuristic Method," *Energies*, vol. 14, no. 19, Art. no. 19, 2021, doi: 10.3390/en14196117.

[47] W. Gil-González, O. D. Montoya, L. F. Grisales-Noreña, A.-J. Perea-Moreno, and Q. Hernandez-Escobedo, "Optimal Placement and Sizing of Wind Generators in AC Grids Considering Reactive Power Capability and Wind Speed Curves," *Sustainability*, vol. 12, no. 7, Art. no. 7, 2020, doi: 10.3390/su12072983.

[48] P. Siano and G. Mokryani, "Evaluating the Benefits of Optimal Allocation of Wind Turbines for Distribution Network Operators," *IEEE Systems Journal*, vol. 9, no. 2, pp. 629–638, Jun. 2015, doi: 10.1109/JSYST.2013.2279733.

[49] T. Corke and R. Nelson, *Wind Energy Design*. Boca Raton: CRC Press, 2018. doi: 10.1201/b22301.

[50] P. Webb, *Introduction to Oceanography*. Roger Williams University: Pressbooks, 2019. [Online]. Available: https://rwu.pressbooks.pub/webboceanography/

[51] N. Schlager and J. Weisblatt, *Alternative Energy*, vol. 3. in Gale eBooks, vol. 3. 2006.

[52] NCERT, *Fundamentals of Physical Geography - Textbook for Class - 11*. National Council Of Educational Research And Training, 2019.

[53] J. Park, *The Wind Power Book*. Palo Alto, California: Chesire Books, 1981.

[54] R. W. Christopherson, *Geosystems: An Introduction to Physical Geography*. Macmillan Publishing Company, 1992.

[55] A. Zakariazadeh, S. Jadid, and P. Siano, "Smart microgrid energy and reserve scheduling with demand response using stochastic optimization," *International Journal of Electrical Power & Energy Systems*, vol. 63, pp. 523–533, Dec. 2014, doi: 10.1016/j.ijepes.2014.06.037.

[56] A. Ouammi, R. Sacile, D. Zejli, A. Mimet, and R. Benchrifa, "Sustainability of a wind power plant: Application to different Moroccan sites," *Energy*, vol. 35, no. 10, pp. 4226–4236, Oct. 2010, doi: 10.1016/j.energy.2010.07.010.

[57] Y. El Khchine, M. Sriti, and N. E. El Kadri Elyamani, "Evaluation of wind energy potential and trends in Morocco," *Heliyon*, vol. 5, no. 6, Jun. 2019, doi: 10.1016/j.heliyon.2019.e01830.

[58] M. H. Ouahabi, H. Elkhachine, F. Benabdelouahab, and A. Khamlichi, "Comparative study of five different methods of adjustment by the Weibull model to determine the most accurate method of analyzing annual variations of wind energy in Tetouan - Morocco.," *Procedia Manufacturing*, vol. 46, pp. 698–707, 2020, doi: 10.1016/j.promfg.2020.03.099.

[59] T. Brahimi, F. Alhebshi, H. Alnabilsi, A. Bensenouci, and M. Rahman, "Prediction of Wind Speed Distribution Using Artificial Neural Network: The Case of Saudi Arabia," *Procedia Computer Science*, vol. 163, pp. 41–48, Jan. 2019, doi: 10.1016/j.procs.2019.12.084.

[60] C. G. Justus and A. Mikhail, "Height variation of wind speed and wind distributions statistics," *Geophysical Research Letters*, vol. 3, no. 5, pp. 261–264, 1976, doi: 10.1029/GL003i005p00261.

[61] A. Spera and T. R. Richards, "MODIFIED POWER LAW EQUATIONS FOR VERTICAL WIND PROFILES," Dept. Energy,Lewis Res. Center, NASA, Washington, DC, USA, Tech. Rep DOE/NASA/1059-79/4, Jun. 1979.

[62] Y. P. Faniband and S. M. Shaahid, "Forecasting Wind Speed using Artificial Neural Networks – A Case Study of a Potential Location of Saudi Arabia," *E3S Web Conf.*, vol. 173, p. 01004, 2020, doi: 10.1051/e3sconf/202017301004.

[63] S. Scher, "Artificial intelligence in weather and climate prediction : Learning atmospheric dynamics," Stockholm University, Sweden, 2020. [Online]. Available: http://urn.kb.se/resolve?urn=urn:nbn:se:su:diva-180877

[64] A. Arzu, M. R. Ahmed, and M. G. M. Khan, "Wind Speed Forecasting using Regression, Time Series and Neural Network Models: A Case Study of Suva," 22nd Australasian Fluid Mechanics Conference AFMC2020, Dec. 2020. doi: 10.14264/ccee311.

[65] E. Hau, *Wind Turbines : Fundamentals, Technologies, Application, Economics*. Verlag Berlin and Heidelberg New York: Springer, 2005.

[66] H. Allamehzadeh, "Wind energy history, technology and control," in *2016 IEEE Conference on Technologies for Sustainability (SusTech)*, Oct. 2016, pp. 119–126. doi: 10.1109/SusTech.2016.7897153.

[67] R. N. Clark, *Small Wind*. Elsevier Inc., 2014. doi: 10.1016/C2010-0-67034-9.

[68] S. Mathew, *Wind Energy Fundamentals, Resource Analysis and Economics*. Springer, 2006. doi: 10.5860/CHOICE.44-0337.

[69] W. Teng, R. Jiang, X. Ding, Y. Liu, and Z. Ma, "Detection and Quantization of Bearing Fault in Direct Drive Wind Turbine via Comparative Analysis," *Shock and Vibration*, 2016, doi: 10.1155/2016/2378435.

[70] M. Ragheb and A. M. Ragheb, "Wind Turbines Theory - The Betz Equation and Optimal Rotor Tip Speed Ratio," in *Fundamental and Advanced Topics in Wind Power*, R. Carriveau, Ed., InTech, 2011. doi: 10.5772/21398.

[71] M. Ragheb, "Economics of Wind Power Generation," in *Wind Energy Engineering*, Elsevier, 2017, pp. 537–555. doi: 10.1016/B978-0-12-809451-8.00025-4.

[72] L. Fingersh, M. Hand, and A. Laxson, "Wind Turbine Design Cost and Scaling Model," Tech. Rep NREL/TP-500-40566, Dec. 2006. doi: 10.2172/897434.

[73] H. S. Dhiman, D. Deb, S. M. Muyeen, and I. Kamwa, "Wind Turbine Gearbox Anomaly Detection based on Adaptive Threshold and Twin Support Vector Machines," *IEEE Transactions on Energy Conversion*, vol. 36, no. 4, Apr. 2021, doi: 10.1109/TEC.2021.3075897.

[74] Nations Unies, "Les mécanismes innovants de financement des projets d'énergies renouvelables en Afrique du Nord," Commission Economique pour l'Afrique, 2014. [Online]. Available: https://repository.uneca.org/handle/10855/22373

[75] M. Bruck, P. Sandborn, and N. Goudarzi, "A Levelized Cost of Energy (LCOE) model for wind farms that include Power Purchase Agreements (PPAs)," *Renewable Energy*, vol. 122, pp. 131–139, Jul. 2018, doi: 10.1016/j.renene.2017.12.100.
[76] I. Staffell and R. Green, "How does wind farm performance decline with age?," *Renewable Energy*, vol. 66, pp. 775–786, Jun. 2014, doi: 10.1016/j.renene.2013.10.041.
[77] S. Cox, Tegen. S, Baring-Gould. I, Oteri. F.A; Esterly. S, Forsyth. T, Baranowski. R, "Policies to Support Wind Power Deployment: Key Considerations and Good Practices," National Renewable Energy Lab. (NREL), Golden, CO (United States), Tech. Rep NREL/TP-6A20-64177, May 2015. doi: 10.2172/1215245.
[78] A. Chehouri, R. Younes, A. Ilinca, and J. Perron, "Wind Turbine Design: Multi-Objective Optimization," in *Wind Turbines - Design, Control and Applications*, InTech, 2016. doi: 10.5772/63481.
[79] C. T. Kiranoudis and Z. B. Maroulis, "Effective short-cut modelling of wind park efficiency," *Renewable Energy*, vol. 11, no. 4, pp. 439–457, Aug. 1997, doi: 10.1016/S0960-1481(97)00011-6.
[80] A. Chehouri, "OPTIMISATION OF WIND TURBINE BLADE STRUCTURES USING A GENETIC ALGORITHM," Chicoutimi, Québec, Canada, Tech. Rep, Dec. 2018. doi: 10.13140/RG.2.2.25415.34723.
[81] I. Khan, Z. Li, Y. Xu, and W. Gu, "Distributed control algorithm for optimal reactive power control in power grids," *International Journal of Electrical Power & Energy Systems*, vol. 83, pp. 505–513, Dec. 2016, doi: 10.1016/j.ijepes.2016.04.004.
[82] M. Gölçek, H. H. Erdem, and A. Bayülken, "A Techno-Economical Evaluation for Installation of Suitable Wind Energy Plants in Western Marmara, Turkey," *Energy Exploration & Exploitation*, vol. 25, no. 6, pp. 407–427, Dec. 2007, doi: 10.1260/014459807783791791.
[83] R. H. Wiser and M. Bolinger, "2017 Wind Technologies Market Report," Lawrence Berkeley National Lab. (LBNL), Berkeley, CA (United States), Tech. Rep, Aug. 2018. doi: 10.2172/1471044.
[84] C. Mone, M. Hand, M. Bolinger, J. Rand, D. Heimiller, and J. Ho, "2015 Cost of Wind Energy Review," National Renewable Energy Lab. (NREL), Golden, CO (United States), Tech. Rep NREL/TP-6A20-66861, Apr. 2017. doi: 10.2172/1351062.
[85] R. Wiser and M. Bolinger, "2016 Wind Technologies Market Report," Lawrence Berkeley National Lab. (LBNL), Berkeley, CA (United States), Tech. Rep DOE/GO-102917-5033, Aug. 2017. doi: 10.2172/1375677.
[86] R. H. Wiser and M. Bolinger, "2018 Wind Technologies Market Report," EERE Publication and Product Library, Washington, D.C. (United States), Tech. Rep DOE/GO-102019-5191, Aug. 2019. doi: 10.2172/1559881.
[87] M. S. Adaramola, S. S. Paul, and S. O. Oyedepo, "Assessment of electricity generation and energy cost of wind energy conversion systems in north-central Nigeria," *Energy Conversion and Management*, vol. 52, no. 12, pp. 3363–3368, Nov. 2011, doi: 10.1016/j.enconman.2011.07.007.
[88] O. S. Ohunakin, O. M. Oyewola, and M. S. Adaramola, "Economic analysis of wind energy conversion systems using levelized cost of electricity and present value cost methods in Nigeria," *Int J Energy Environ Eng*, vol. 4, no. 1, p. 2, 2013, doi: 10.1186/2251-6832-4-2.

[89] M. Gökçek and M. S. Genç, "Evaluation of electricity generation and energy cost of wind energy conversion systems (WECSs) in Central Turkey," *Applied Energy*, vol. 86, no. 12, pp. 2731–2739, Dec. 2009, doi: 10.1016/j.apenergy.2009.03.025.

[90] IRENA, "Renewable Energy Cost Analysis - Wind Power," International Renewable Energy Agency, Tech. Rep, Jun. 2012. [Online]. Available: https://www.irena.org/publications/2012/Jun/Renewable-Energy-Cost-Analysis---Wind-Power

[91] O. Charrouf, A. Betka, M. Becherif, and A. Tabanjat, "Techno-economic Analysis of Wind Turbines in Algeria," *International Journal of Emerging Electric Power Systems*, vol. 19, no. 1, Feb. 2018, doi: 10.1515/ijeeps-2017-0178.

[92] F. Knidiri, A. Laaouina, M. Fabre, and A. Wyatt, "L'Énergie Éolienne au Maroc : Gisement - Dimensionnement," Renew. Energy Develop. Center, Ministry Energy Mines, Morocco, Tech. Rep 86–0109, 1986.

[93] D. Zejli, R. Benchrifa, A. Bennouna, and K. Zazi, "Economic analysis of wind-powered desalination in the south of Morocco," *Desalination*, vol. 165, pp. 219–230, Aug. 2004, doi: 10.1016/j.desal.2004.06.025.

[94] R. RANJAN and DAS, "Simple and Efficient Computer Algorithm to Solve Radial Distribution Networks," *Electric Power Components and Systems*, vol. 31, no. 1, pp. 95–107, Jan. 2003, doi: 10.1080/15325000390112099.

[95] M. A. Tolba, H. Rezk, V. Tulsky, A. A. Z. Diab, A. Y. Abdelaziz, and A. Vanin, "Impact of Optimum Allocation of Renewable Distributed Generations on Distribution Networks Based on Different Optimization Algorithms," *Energies*, vol. 11, no. 1, Art. no. 1, Jan. 2018, doi: 10.3390/en11010245.